Syntheses and Structures of new P/S and P/Se Metal Complexes

(Synthese und Strukturaufklärung neuer P/S- und P/Se- Metallkomplexe)

Zur Erlangung des akademischen Grades eines

Doktors der Naturwissenschaften
(Dr. rer. nat.)

der Fakultät für Chemie und Biowissenschaften
der Universität Fridericiana zu Karlsruhe (TH)
vorgelegte

Dissertation

von
Weifeng Shi(施卫峰)
aus Jiangsu/China(江苏/中国)

Dekan: Prof. Dr. H. Puchta
Referent: Prof. Dr. D. Fenske
Korreferent: Priv.-Doz. Dr. A. Schnepf
Tag der mündlichen Prüfung: 12.02.2007, 14.02.2007 und 15.02.2007

I. Abbreviation

1. For Chemicals

Me	Methyl	$-CH_3$
Et	Ethyl	$-C_2H_5$
^{i}Pr	*iso*-Propyl	$-CH(CH_3)_2$
^{S}Bu	*sec*-Butyl	$-CH_2CH(CH_3)_2$
^{t}Bu	*tert*-Butyl	$-C(CH_3)_3$
-O^{t}Bu	*tert*-Butoxy	$-OC_4H_9$
-OMe	Methoxy	$-OCH_3$
-OAc	Acetoxy	$-OCOCH_3$
THF	Tetrahydrofuran	C_4H_8O
Et_2O	Diethylether	$C_4H_{10}O$
DME	Dimethoxyethane	$C_4H_{10}O_2$
DCM	Dichloromethane	CH_2Cl_2
DMSO	Dimethylsulfoxide	$(CH_3)_2SO$
PPh_3	Triphenylphosphine	$(C_6H_5)_3P$

2. Spectrum

NMR	Nuclear Magnetic Resonance
δ	Chemical Shift
s	Singlet
d	Doublet
t	Triplet
q	Quadruplet
m	Multiplet
IR	Infra-red
GC-MS	Gas Chromatography-Mass Spectrum

II. List of New Complexes

1 $[Cu_2(o\text{-}CO_2C_6H_4SO_3)(dppm)_2]\cdot 3CH_2Cl_2$ **(1)**

2 $[Cu_2(\mu_2\text{-}ArS_2P\text{-}O\text{-}PS_2Ar)(PPh_3)_4]\cdot CH_2Cl_2$ (Ar = 4-anisyl) **(2)**

3 $[Cu_4\{Ar(\mu_2\text{-}S)_2P\text{-}O\text{-}P(\mu_2\text{-}S)_2Ar\}_2(dppa)_2]\cdot 3CH_2Cl_2$ (Ar = 4-anisyl) **(3)**

4 $[Cu_2(\mu_4\text{-}ArPS_3)(PPh_3)_2]_2\cdot 2CH_2Cl_2$ (Ar = 4-anisyl) **(4)**

5 $[Cu(ArP(S^tBu)S_2)(PPh_3)_2]$ (Ar = 4-anisyl) **(5)**

6 $1/\infty[Na\{ArP(O^tBu)S_2\}(thf)]_\infty$ (Ar = 4-anisyl) **(6)**

7 $[Na_2\{ArP(O^tBu)(\mu\text{-}S)S\}_2(dme)_2]$ (Ar = 4-anisyl) **(7)**

8 $1/\infty[K_2\{ArP(O^tBu)(\mu\text{-}S)S\}_2(thf)_2]_\infty$ (Ar = 4-anisyl) **(8)**

9 $1/\infty[K_2\{ArP(O^tBu)(\mu\text{-}S)S\}_2(dme)_2]_\infty$ (Ar = 4-anisyl) **(9)**

10 $1/\infty[K_4\{ArP(S^tBu)(\mu\text{-}S)S\}_4(thf)_4]_\infty$ (Ar = 4-anisyl) **(10)**

11 $[Cu_{14}(\mu_6\text{-}ArP(O)S_2)_6(\mu_3\text{-}ArP(O)(OAc)S)_2(PPh_3)_6)]\cdot 8THF$ (Ar=4-anisyl) **(11)**

12 $[Ag_4\{\mu_4\text{-}ArP(O)S_2\}_2(dppm)_4]\cdot 2Et_2O\cdot 2THF$ (Ar = 4-anisyl) **(12)**

13 $[Ag_{28}(\mu_6\text{-}S)_2\{ArP(O)S_2\}_{12}(PPh_3)_{12}]\cdot 2Et_2O\cdot 13THF$ (Ar = 4-anisyl) **(13)**

14 $[Fe_2(\mu\text{-}ArPS_3)(thf)_4]$ (Ar = 4-anisyl) **(14)**

15 $[Ni_2\{ArP(O)S_2\}_2(thf)_2(H_2O)_2]_2$ (Ar = 4-anisyl) **(15)**

16 $[Cd_2\{ArP(O^tBu)(\mu\text{-}S)S\}_4]$ (Ar = 4-anisyl) **(16)**

17 $[Fe_2(\mu\text{-}ArPS_3)(thf)_4]$ (Ar = 4-anisyl) **(17)**

18 $[Ni\{ArP(OH)S_2\}_2(thf)_2]$ (Ar = 4-anisyl) **(18)**

19 $1/\infty[K_2\{PhP(O^tBu)Se_2\}_2(thf)]_\infty$ **(19)**

20 $1/\infty[PhPSe_3Na_2(thf)_3]_\infty$ **(20)**

21 $1/\infty[(PhPSe_2Se\text{-}SeSe_2PPh)K_2(thf)_4]_\infty$ **(21)**

22 $1/\infty[(PhPSe_2Se\text{-}SeSe_2PPh)Rb_2(thf)_4]_\infty$ **(22)**

23 $1/\infty[Na_2\{PhSe_2P\text{-}PSe_2Ph\}(thf)_3]_\infty$ **(23)**

24 $1/\infty[K_2(PhPSe_2Se\text{-}SeSe_2PPh)(thf)_4]_\infty$ **(24)**

25 $1/\infty[Na_2(PhPSe_2O)(H_2O)_4(thf)]_\infty$ **(25)**

26 $[Cu_4(PhSeP\text{-}O\text{-}PSePh)_2(PPh_3)_4]$ **(26)**

27 $[\mathrm{Ni}\{\mathrm{PhP(OH)Se_2}\}_2(\mathrm{thf})_2]$ **(27)**

28 $[\mathrm{Mg}\{\mathrm{PhP(Se,O)Se\text{-}Se(O,Se)PPh}\}(\mathrm{thf})_4(\mathrm{H_2O})_2]\cdot[\mathrm{Mg}\{\mathrm{PhP(Se,O)Se\text{-}Se(O,Se)PPh}\}$
$(\mathrm{thf})_3\,(\mathrm{H_2O})]$ **(28)**

29 $[\mathrm{Mg}\{\mathrm{PhP(Se,O)Se\text{-}Se(O,Se)PPh}\}(\mathrm{thf})_3(\mathrm{H_2O})]$ **(29)**

30 $[\mathrm{Mn}\{\mathrm{PhP(Se,O)Se\text{-}Se(O,Se)PPh}\}(\mathrm{thf})_3(\mathrm{H_2O})]$ **(30)**

31 $[\{\mathrm{PhPSe_2}(\mu_2\text{-}\mathrm{Se})\mathrm{Na}(\mathrm{thf})_3\}_2\mathrm{Ni}]$ **(31)**

32 $1/\infty[\mathrm{Ni}\{\mathrm{Na(PhPSe_3)(thf)_2}]_\infty$ **(32)**

33 $[\mathrm{Cu_3}\{\mathrm{PS_2(OPS_2O}^{t}\mathrm{Bu})_2\}(\mathrm{PPh_3})_4]$ **(33)**

34 $[\mathrm{Cu_4}\{\mu_3\text{-}\mathrm{P(O}^{t}\mathrm{Bu)S_3}\}_2(\mathrm{PPh_3})_4]$ **(34a,b)**

35 $1/\infty[\mathrm{Na_2(S_3PS}^{t}\mathrm{Bu)(dme)}]_\infty$ **(35)**

36 $[\mathrm{Ni}\{\mathrm{P(OH)_2S_2}\}_2(\mathrm{thf})_2]$ **(36)**

37 $[\mathrm{ArPS}(\mu\text{-}\mathrm{S})(\mu\text{-}\mathrm{NPh})\mathrm{SPAr}]$ (Ar = 4-anisyl) **(37)**

Contents

1 Introduction 1

1.1 P/S ligands and their compounds 1

1.2 P/Se ligands and their compounds 9

2 Aims and Objections 13

3 Results and Discussions 15

4 Experimental Section 68

4.1 Synthesis of starting materials 68

4.1.1 Synthesis of $CuO^{t}Bu$ 68

4.1.2 Synthesis of CuSR (R = ^{t}Bu, Et and Cyclohexyl) 69

4.1.3 Synthesis of dppa 69

4.1.4 Synthesis of Woollins' reagent 70

4.1.5 Synthesis of $PhP(S^{t}Bu)_2$ 70

4.1.6 Synthesis of $PhP(Se)(S^{t}Bu)_2$ 70

4.2 Synthesis of new complexes 71

4.2.1 Synthesis of $[Cu_2(o\text{-}CO_2C_6H_4SO_3)(dppm)_2]\bullet 3CH_2Cl_2$ (1) 71

4.2.2 Synthesis of $[Cu_2(\mu_2\text{-}ArS_2P\text{-}O\text{-}PS_2Ar)(PPh_3)_4]\bullet CH_2Cl_2$ (Ar = 4-anisyl) (2) 71

4.2.3 Synthesis of $[Cu_4\{Ar(\mu_2\text{-}S)_2P\text{-}O\text{-}P(\mu_2\text{-}S)_2Ar\}_2(dppa)_2]\bullet 3CH_2Cl_2$ (Ar = 4-anisyl) (3) 72

4.2.4 Synthesis of $[Cu_2(\mu_4\text{-}ArPS_3)(PPh_3)_2]_2\bullet 2CH_2Cl_2$ (Ar = 4-anisyl) (4) 72

4.2.5 Synthesis of $[Cu(ArP(S^{t}Bu)S_2)(PPh_3)_2]$ (Ar = 4-anisyl) (5) 73

4.2.6 Synthesis of $1/\infty[Na\{ArP(O^{t}Bu)S_2\}(thf)]_{\infty}$ (Ar = 4-anisyl) (6) 73

4.2.7 Synthesis of $[Na_2\{ArP(O^{t}Bu)(\mu\text{-}S)S\}_2(dme)_2]$ (Ar = 4-anisyl) (7) 74

4.2.8 Synthesis of $1/\infty[K_2\{ArP(O^{t}Bu)(\mu\text{-}S)S\}_2(thf)_2]_{\infty}$ (Ar = 4-anisyl) (8) 74

4.2.9 Synthesis of $1/\infty[K_2\{ArP(O^{t}Bu)(\mu\text{-}S)S\}_2(dme)_2]_{\infty}$ (Ar = 4-anisyl) (9) 74

4.2.10 Synthesis of $1/\infty[K_4\{ArP(S^{t}Bu)(\mu\text{-}S)S\}_4(thf)_4]_{\infty}$ (Ar = 4-anisyl) (10) 75

4.2.11 Synthesis of $[Cu_{14}(\mu_6\text{-}ArP(O)S_2)_6(\mu_3\text{-}ArP(O)(OAc)S)_2(PPh_3)_6)]\bullet 8THF$ (Ar=4-anisyl) (11) 75

4.2.12 Synthesis of $[Ag_4\{\mu_4\text{-}ArP(O)S_2\}_2(dppm)_4]\bullet 2Et_2O\bullet 2THF$ (Ar = 4-anisyl) (12) 75

4.2.13 Synthesis of $[Ag_{28}(\mu_6\text{-}S)_2\{ArP(O)S_2\}_{12}(PPh_3)_{12}]\bullet 2Et_2O\bullet 13THF$ (Ar = 4-anisyl) (13) 76

4.2.14 Synthesis of $[Fe_2(\mu\text{-}ArPS_3)(thf)_4]$ (Ar = 4-anisyl) (14) 76

4.2.15 Synthesis of $[Ni_2\{ArP(O)S_2\}_2(thf)_2(H_2O)_2]_2$ (Ar = 4-anisyl) (15) 76

4.2.16 Synthesis of $[Cd_2\{ArP(O^{t}Bu)(\mu\text{-}S)S\}_4]$ (Ar = 4-anisyl) (16) 77

4.2.17 Synthesis of $[Fe_2(\mu\text{-}ArPS_3)(thf)_4]$ (Ar = 4-anisyl) (17) 77

4.2.18 Synthesis of $[Ni\{ArP(OH)S_2\}_2(thf)_2]$ (Ar = 4-anisyl) (18) 77

4.2.19 Synthesis of $1/\infty[K_2\{PhP(O^tBu)Se_2\}_2(thf)]_\infty$ (19) 78

4.2.20 Synthesis of $1/\infty[PhPSe_3Na_2(thf)_3]_\infty$ (20) 78

4.2.21 Synthesis of $1/\infty[(PhPSe_2Se\text{-}SeSe_2PPh)K_2(thf)_4]_\infty$ (21) 79

4.2.22 Synthesis of $1/\infty[(PhPSe_2Se\text{-}SeSe_2PPh)Rb_2(thf)_4]_\infty$ (22) 79

4.2.23 Synthesis of $1/\infty[Na_2\{PhSe_2P\text{-}PSe_2Ph\}(thf)_3]_\infty$ (23) 80

4.2.24 Synthesis of $1/\infty[K_2(PhPSe_2Se\text{-}SeSe_2PPh)(thf)_4]_\infty$ (24) 80

4.2.25 Synthesis of $1/\infty[Na_2(PhPSe_2O)(H_2O)_4(thf)]_\infty$ (25) 80

4.2.26 Synthesis of $[Cu_4(PhSeP\text{-}O\text{-}PSePh)_2(PPh_3)_4]$ (26) 81

4.2.27 Synthesis of $[Ni\{PhP(OH)Se_2\}_2(thf)_2]$ (27) 81

4.2.28 Synthesis of $[Mg\{PhP(Se,O)Se\text{-}Se(O,Se)PPh\}(thf)_4(H_2O)_2]\cdot[Mg\{PhP(Se,O)Se\text{-}Se(O,Se)PPh\}(thf)_3(H_2O)]$ (28) 81

4.2.29 Synthesis of $[Mg\{PhP(Se,O)Se\text{-}Se(O,Se)PPh\}(thf)_3(H_2O)]$ (29) 82

4.2.30 Synthesis of $[Mn\{PhP(Se,O)Se\text{-}Se(O,Se)PPh\}(thf)_3(H_2O)]$ (30) 82

4.2.31 Synthesis of $[\{PhPSe_2(\mu_2\text{-}Se)Na(thf)_3\}_2Ni]$ (31) 83

4.2.32 Synthesis of $1/\infty[Ni\{Na(PhPSe_3)(thf)_2\}_2]_\infty$ (32) 83

4.2.33 Synthesis of $[Cu_3\{PS_2(OPS_2O^tBu)_2\}(PPh_3)_4]$ (33) 83

4.2.34 Synthesis of $[Cu_4\{\mu_3\text{-}P(O^tBu)S_3\}_2(PPh_3)_4]$ (34a,b) 84

4.2.35 Synthesis of $1/\infty[Na_2(S_3PS^tBu)(dme)]_\infty$ (35) 84

4.2.36 Synthesis of $[Ni\{P(OH)_2S_2\}_2(thf)_2]$ (36) 84

4.2.37 Synthesis of $[ArPS(\mu\text{-}S)(\mu\text{-}NPh)SPAr]$ (Ar = 4-anisyl) (37) 85

5 Crystallographic Data 86

5.1 General information 86

5.2 Crystallographic data 87

5.2.1 Data for $[Cu_2(o\text{-}CO_2C_6H_4SO_3)(dppm)_2]\text{•}3CH_2Cl_2$ (1) 87

5.2.2 Data for $[Cu_2(\mu_2\text{-}ArS_2P\text{-}O\text{-}PS_2Ar)(PPh_3)_4]\text{•}CH_2Cl_2$ (Ar = 4-anisyl) (2) 90

5.2.3 Data for $[Cu_4\{Ar(\mu_2\text{-}S)_2P\text{-}O\text{-}P(\mu_2\text{-}S)_2Ar\}_2(dppa)_2]\text{•}3CH_2Cl_2$ (Ar = 4-anisyl) (3) 91

5,2.4 Data for $[Cu_2(\mu_4\text{-}ArPS_3)(PPh_3)_2]_2\text{•}2CH_2Cl_2$ (Ar = 4-anisyl) (4) 92

5.2.5 Data for $[Cu(ArP(S^tBu)S_2)(PPh_3)_2]$ (Ar = 4-anisyl) (5) 93

5.2.6 Data for $1/\infty[Na\{ArP(O^tBu)S_2\}(thf)]_\infty$ (Ar = 4-anisyl) (6) 94

5.2.7 Data for $[Na_2\{ArP(O^tBu)(\mu\text{-}S)S\}_2(dme)_2]$ (Ar = 4-anisyl) (7) 95

5.2.8 Data for $1/\infty[K_2\{ArP(O^tBu)(\mu\text{-}S)S\}_2(thf)_2]_\infty$ (Ar = 4-anisyl) (8) 96

5.2.9 Data for $1/\infty[K_2\{ArP(O^tBu)(\mu\text{-}S)S\}_2(dme)_2]_\infty$ (Ar = 4-anisyl) (9) 97

5.2.10 Data for $1/\infty[K_4\{ArP(S^tBu)(\mu\text{-}S)S\}_4(thf)_4]_\infty$ (Ar = 4-anisyl) (10) 98

5.2.11 Data for $[Cu_{14}(\mu_6\text{-}ArP(O)S_2)_6(\mu_3\text{-}ArP(O)(OAc)S)_2(PPh_3)_6)]\text{•}8THF$ (Ar=4-anisyl) (11) 99

5.2.12 Data for $[Ag_4\{\mu_4\text{-}ArP(O)S_2\}_2(dppm)_4]\cdot 2Et_2O\cdot 2THF$ (Ar = 4-anisyl) (12) 100

5.2.13 Data for $[Ag_{28}(\mu_6\text{-}S)_2\{ArP(O)S_2\}_{12}(PPh_3)_{12}]\cdot 2Et_2O\cdot 13THF$ (Ar = 4-anisyl) (13) 101

5.2.14 Data for $[Fe_2(\mu\text{-}ArPS_3)(thf)_4]$ (Ar = 4-anisyl) (14) 102

5.2.15 Data for $[Ni_2\{ArP(O)S_2\}_2(thf)_2(H_2O)_2]_2$ (Ar = 4-anisyl) (15) 103

5.2.16 Data for $[Cd_2\{ArP(O^tBu)(\mu\text{-}S)S\}_4]$ (Ar = 4-anisyl) (16) 104

5.2.17 Data for $[Fe_2(\mu\text{-}ArPS_3)(thf)_4]$ (Ar = 4-anisyl) (17) 105

5.2.18 Data for $[Ni\{ArP(OH)S_2\}_2(thf)_2]$ (Ar = 4-anisyl) (18) 108

5.2.19 Data for $1/\infty[K_2\{PhP(O^tBu)Se_2\}_2(thf)]_\infty$ (19) 109

5.2.20 Data for $1/\infty[PhPSe_3Na_2(thf)_3]_\infty$ (20) 110

5.2.21 Data for $1/\infty[(PhPSe_2Se\text{-}SeSe_2PPh)K_2(thf)_4]_\infty$ (21) 111

5.2.22 Data for $1/\infty[(PhPSe_2Se\text{-}SeSe_2PPh)Rb_2(thf)_4]_\infty$ (22) 112

5.2.23 Data for $1/\infty[Na_2\{PhSe_2P\text{-}PSe_2Ph\}(thf)_3]_\infty$ (23) 113

5.2.24 Data for $1/\infty[K_2(PhPSe_2Se\text{-}SeSe_2PPh)(thf)_4]_\infty$ (24) 114

5.2.25 Data for $1/\infty[Na_2(PhPSe_2O)(H_2O)_4(thf)]_\infty$ (25) 115

5.2.26 Data for $[Cu_4(PhSeP\text{-}O\text{-}PSePh)_2(PPh_3)_4]$ (26) 116

5.2.27 Data for $[Ni\{PhP(OH)Se_2\}_2(thf)_2]$ (27) 117

5.2.28 Data for $[Mg\{PhP(Se,O)Se\text{-}Se(O,Se)PPh\}(thf)_4(H_2O)_2]\cdot[Mg\{PhP(Se,O)Se\text{-}Se(O,Se)PPh\}(thf)_3(H_2O)]$ (28) 118

5.2.29 Data for $[Mg\{PhP(Se,O)Se\text{-}Se(O,Se)PPh\}(thf)_3(H_2O)]$ (29) 119

5.2.30 Data for $[Mn\{PhP(Se,O)Se\text{-}Se(O,Se)PPh\}(thf)_3(H_2O)]$ (30) 120

5.2.31 Data for $[\{PhPSe_2(\mu_2\text{-}Se)Na(thf)_3\}_2Ni]$ (31) 121

5.2.32 Data for $1/\infty[Ni\{Na(PhPSe_3)(thf)_2]_\infty$ (32) 122

5.2.33 Data for $[Cu_3\{PS_2(OPS_2O^tBu)_2\}(PPh_3)_4]$ (33) 123

5.2.34a Data for $[Cu_4\{\mu_3\text{-}P(O^tBu)S_3\}_2(PPh_3)_4]$ (34a) 124

5.2.34b Data for $[Cu_4\{\mu_3\text{-}P(O^tBu)S_3\}_2(PPh_3)_4]$ (34b) 125

5.2.35 Data for $1/\infty[Na_2(S_3PS^tBu)(dme)]_\infty$ (35) 126

5.2.36 Data for $[Ni\{P(OH)_2S_2\}_2(thf)_2]$ (36) 127

5.2.37 Data for $[ArPS(\mu\text{-}S)(\mu\text{-}NPh)SPAr]$ (Ar = 4-anisyl) (37) 128

6 Conclusion 129

7 Literature 132

8 Publication List 141

1. Introduction

The generation of metal complexes with phosphorus- and sulfur- or selenium-containing ligands is a very active area of research. It is hoped that as a result of these efforts, materials with novel features will emerge.[1,2] Motivated by the enormous progress made on the synthesis and application of metal phosphonates,[3-6] a wide variety of complexes has been reported, where oxygen atoms of $[RPO_3]^{2-}$ anions were formally replaced with other functional groups, *e.g.*, RO, RS, S, etc. The coordination chemistry of resulting sulfur-analogs to known [P/O]-anions has been investigated intensively and some recent work is now directed towards the development of metal complexes containing [P/Se]-anions.[7-15]

1.1 P/S ligands and their compounds

Thiophophorus ligands, including dithiophosphates, dithiophosphinates, and mixed thio-oxo analogues, have been in the center of interest in many labs.[2,7,16-34] The mono-thiophosphinato groups are ambident ligands, able to form primary bonds either through sulfur or oxygen (**1a** and **1b**) (Scheme 1.1.1). Primary bonding through sulfur was observed in the 'soft' metal derivatives, *e.g.* mercury, thallium, lead, whereas germanium and tin are bonded to oxygen.

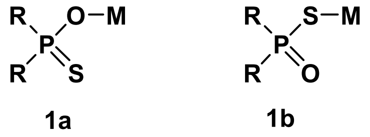

Scheme 1.1.1 Coordination modes of monothiophosphinato groups

As a result, these dithio-compounds can be found in the literature under various names (Scheme 1.1.2). [35]

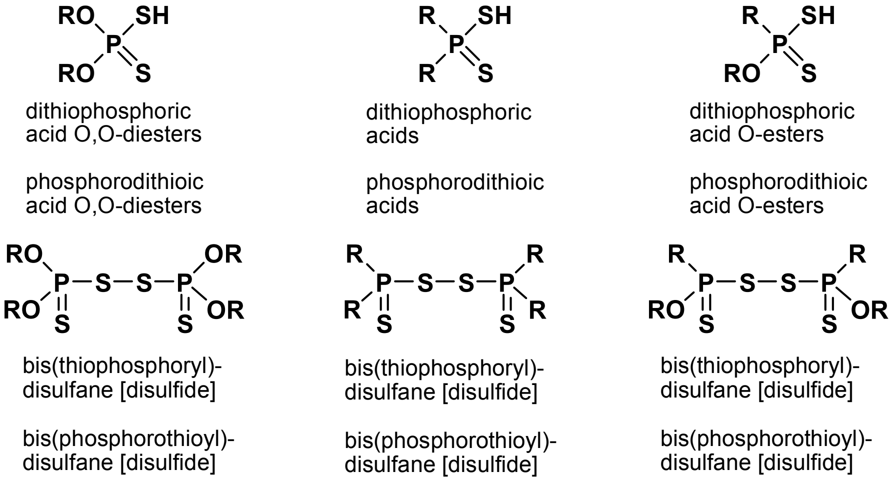

Scheme 1.1.2 Various names of different dithiophosphorus compounds

The dithiophosphorus compounds are versatile ligands, and can exhibit various coordination patterns, mainly monodentate (**2**) (rare), bidentate chelating (**3**) and bridging (**4**). Coordination mode (**3**) and (**4**) can lead to inorganic ring formation (Scheme 1.1.3).

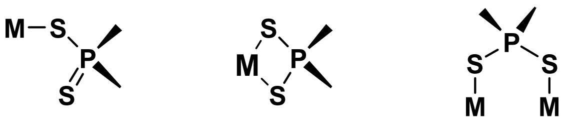

2 **3** **4**

Scheme 1.1.3 Coordination modes of dithiophosphorus compounds

The coordination patterns of dithiophosphorus ligands are diverse, since the S-P-S group can behave as isobidentate (symmetrical) or anisobidentate (asymmetrical), both in chelating and bridging mode (Scheme 1.1.4).[7,24,36-41]

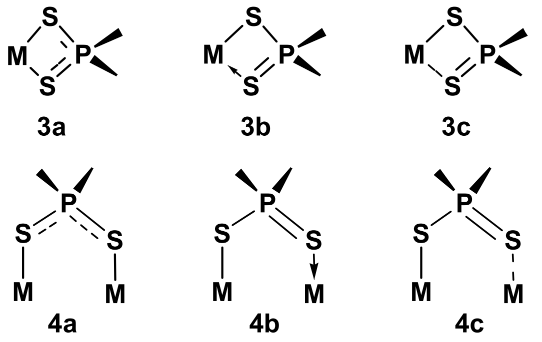

Scheme 1.1.4 Diverse coordination modes of dithiophosphorus ligands

For compounds based upon the =P(S)SSP(S)= skeleton, at least four types of reactions can be expected (Scheme 1.1.5): a. *adduct formation* resulting in ring closure through *chelation*; b. *metal insertion*--involving homolytic cleavage of the S-S bond and oxidative addition of the metal species; c. *redistribution* between M-M and S-S bonds, involving homolytic cleavage of both S-S and M-M bonds and oxidation of the metals; d. *addition* to metal-metal multiple bonds, but this kind of reaction is not well-documented.[35]

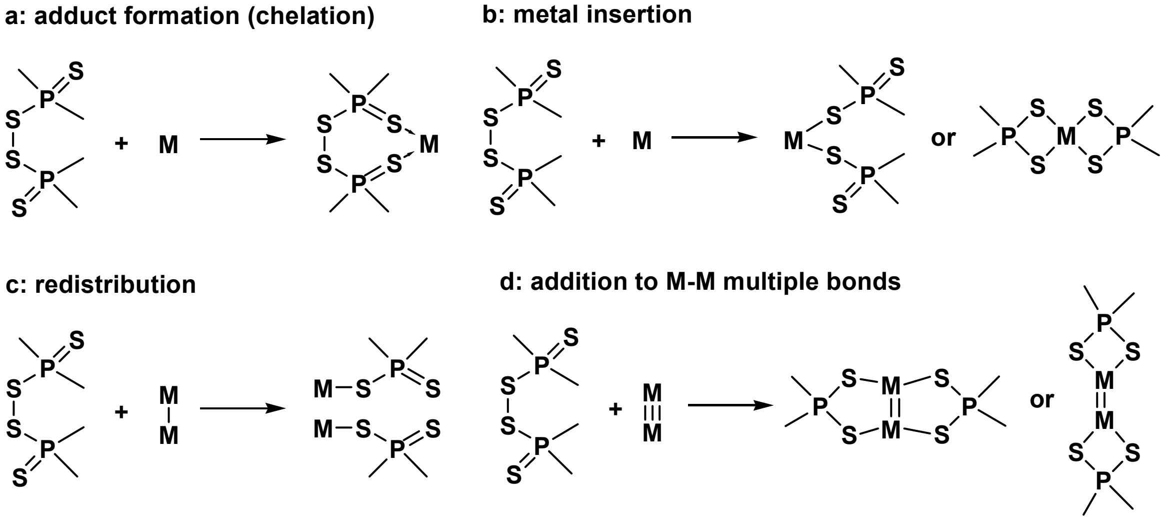

Scheme 1.1.5 Different reaction types of =P(S)SSP(S)= compounds

Organodithio-derivatives of phosphorus are relevant for a number of industrial and agricultural applications, *e.g.*, as antioxidant and antiwear additives in lubricant oils, insecticides and pesticides.[42-61] The most important route to dialkyl dithiophosphoric acids [$(RO)_2PS(SH)$ (R = organic groups)] is the alcoholysis of P_4S_{10} (Scheme 1.1.6).[62-64]

$$\mathbf{4ROH + P_2S_5 \longrightarrow 2(RO)_2PS(SH) + H_2S}$$

Scheme 1.1.6 The alcoholysis of P_4S_{10}

The alkali metal salts $(RO)_2P(S)SM$ (M = Li, Na, K) can react with lots of transition metal salts to afford many new complexes.[2,19,24,26,32,37,41,65-67] For example, $[Ru\{S_2P(OEt)\}_2(PPh_3)_2]$ (**5**) could be obtained from the reaction of $K[S_2P(OEt)_2]$ with $[Ru(PPh_3)_3Cl_2]$ (Figure 1.1.1).[26]

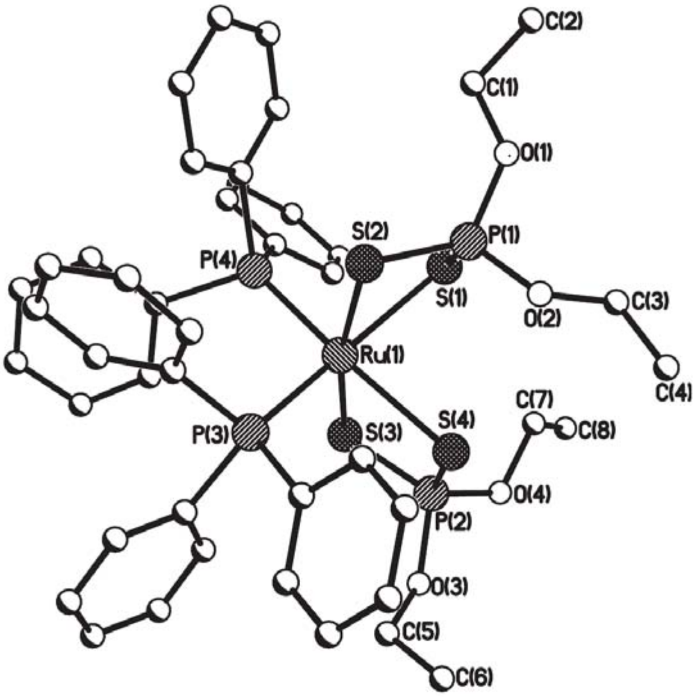

Fgure 1.1.1 Structure of [Ru{$S_2P(OEt)$}$_2$(PPh_3)$_2$]

There are a variety of ways to synthesize bis(thiophosphoryl)-disulfanes,[68-69] among those, the most common method used for the preparation is based upon the oxidation of alkali metal salts of dithiophosphoric acids with iodine dissolved in potassium iodide aqueous solution (Scheme 1.1.7).

$$2MS_2P(OR)_2 + I_2 \longrightarrow (RO)_2P(S)SSP(S)(OR)_2 + 2\ MI$$

Scheme 1.1.7 Synthesis of bis(thiophosphoryl)-disulfanes

The method is very general and used for all common alkyl and aryl derivatives. Thus, $(RO)_2P(S)SSP(S)(OR)_2$ with R = alkyl, aryl and similar mixed disulfanes were prepared in 61-81% yields from $KS_2P(OR)_2$ and iodine. In the reactions of bis(thiophosphoryl)-disulfanes with metal compounds, various metal complexes were obtained (Scheme 1.1.8).[70-72]

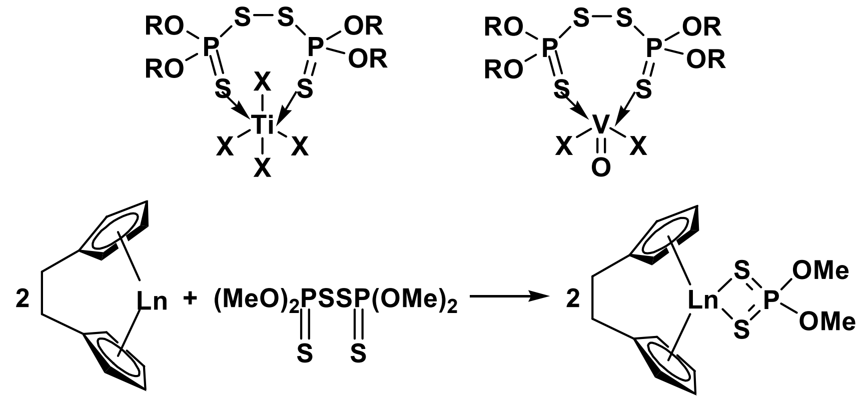

Scheme 1.1.8 Metal complexes from bis(thiophosphoryl)disulfanes

Among the neutral P/S ligands precursors, 2,4-bis(*p*-methoxyphenyl)-1,3-dithiadiphosphetane-2,4-disulfide, also named as Lawesson's reagent (L.R.) (Scheme 1.1.9), was widely used in thionation reactions at first as well as dialkyl dithiophosphoric acids, which are especially applied in organic synthesis (Scheme 1.1.10).[73-82]

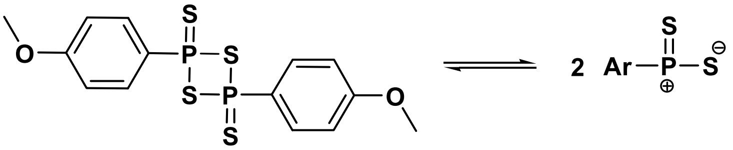

Scheme 1.1.9 Resonant structures of Lawesson's reagent

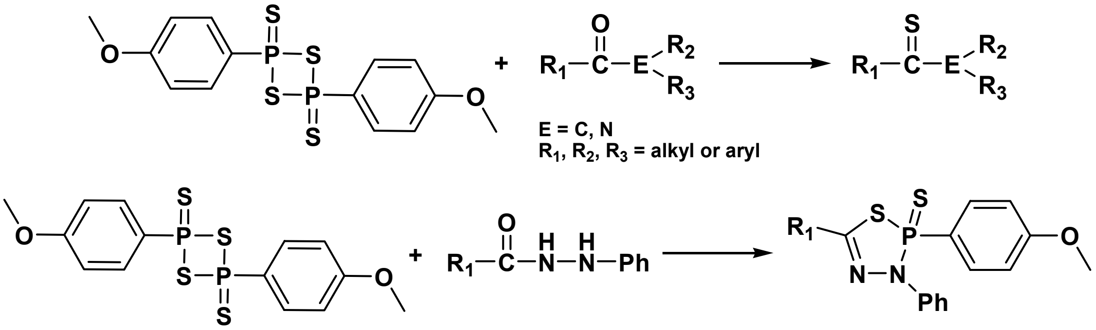

Scheme 1.1.10 Thionation reactions with Lawesson's reagent

In 1952, Fay and Lankelma synthesized the dimeric thioanhydride of Δ^2-cyclohexenetrithio-phosphonic acid—analogue of Lawesson's reagent for the first time,[83] and then Lecher *et al.* prepared L.R. in 1956.[84] After that, a series of alkyl- and arylphosphonotrithioic dianhydrosulfides $(RPS_2)_2$ (R = cyclo, ^{s}Bu, ^{t}Bu, C_5H_{11}, ClC_6H_{10}, C_6H_5) were documented, but because of their poor solubility and high sensitivity to moisture and other solvent impurities, those compounds were only confirmed by element and spectrum analysis.[85,86] The first crystallographic studies for the solvent-free crystals and the toluene solvate crystals were reported in 1992 and 1995 separately (Figure 1.1.2).[87,88]

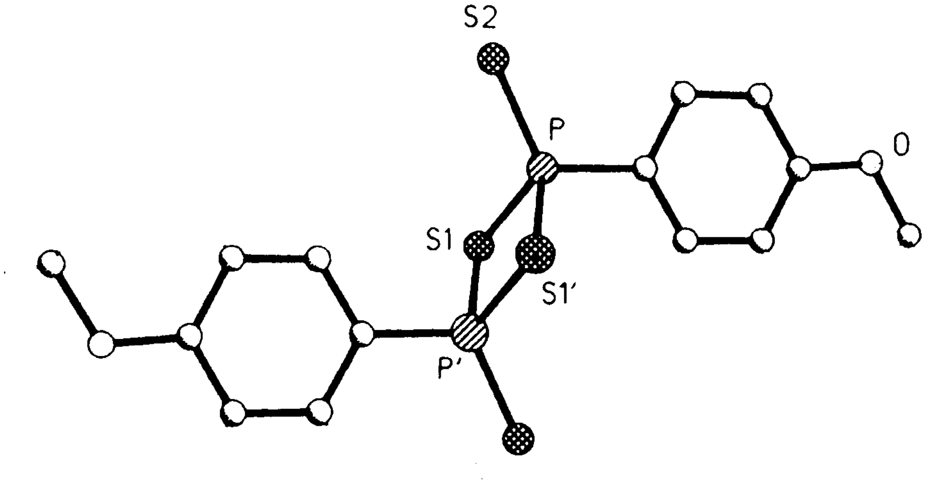

Figure 1.1.2 Structure of Lawesson's reagent

In the past decade, a great deal of work which focused on metal complexes containing P/S-ligands derivated from L.R. has been reported, especially by Woollins' group.[9-11,89-92] In these work, sodium phosphonodithioate salts were generated first from the dimeric ring-cleavage reactions of L.R. and NaOR (R = Me, Et, ^{i}Pr) in the corresponding alcohols, and then reacted with transition metal halides (*e.g.*, $NiCl_2$) or acetates (*e.g.*, $Cd(OAc)_2{\cdot}2H_2O$) to yield the metal complexes (Scheme 1.1.11, Figure 1.1.3).

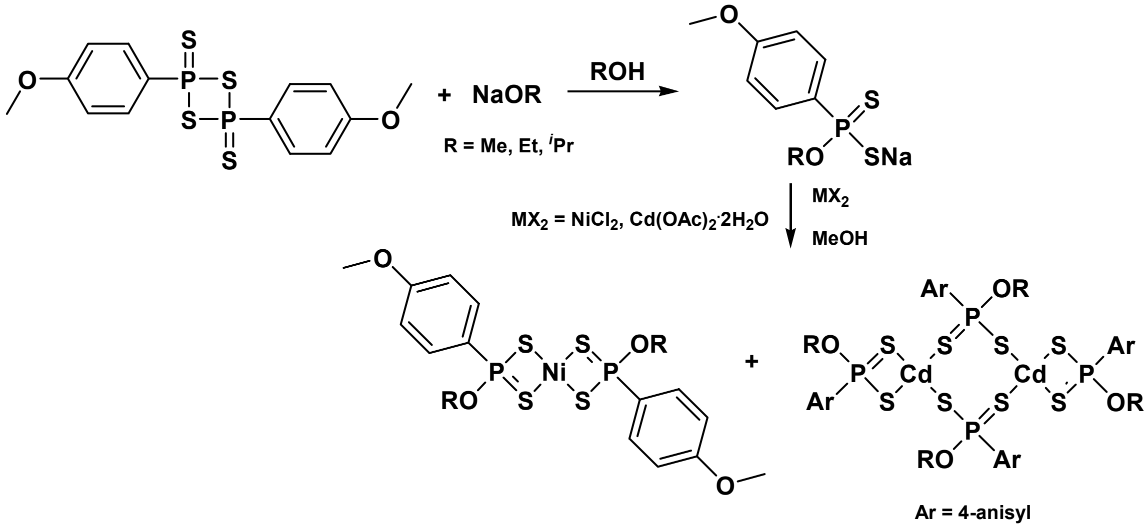

Scheme 1.1.11 Metathesis reactions of Lawesson's reagent (R = Me, Et, ^{i}Pr)

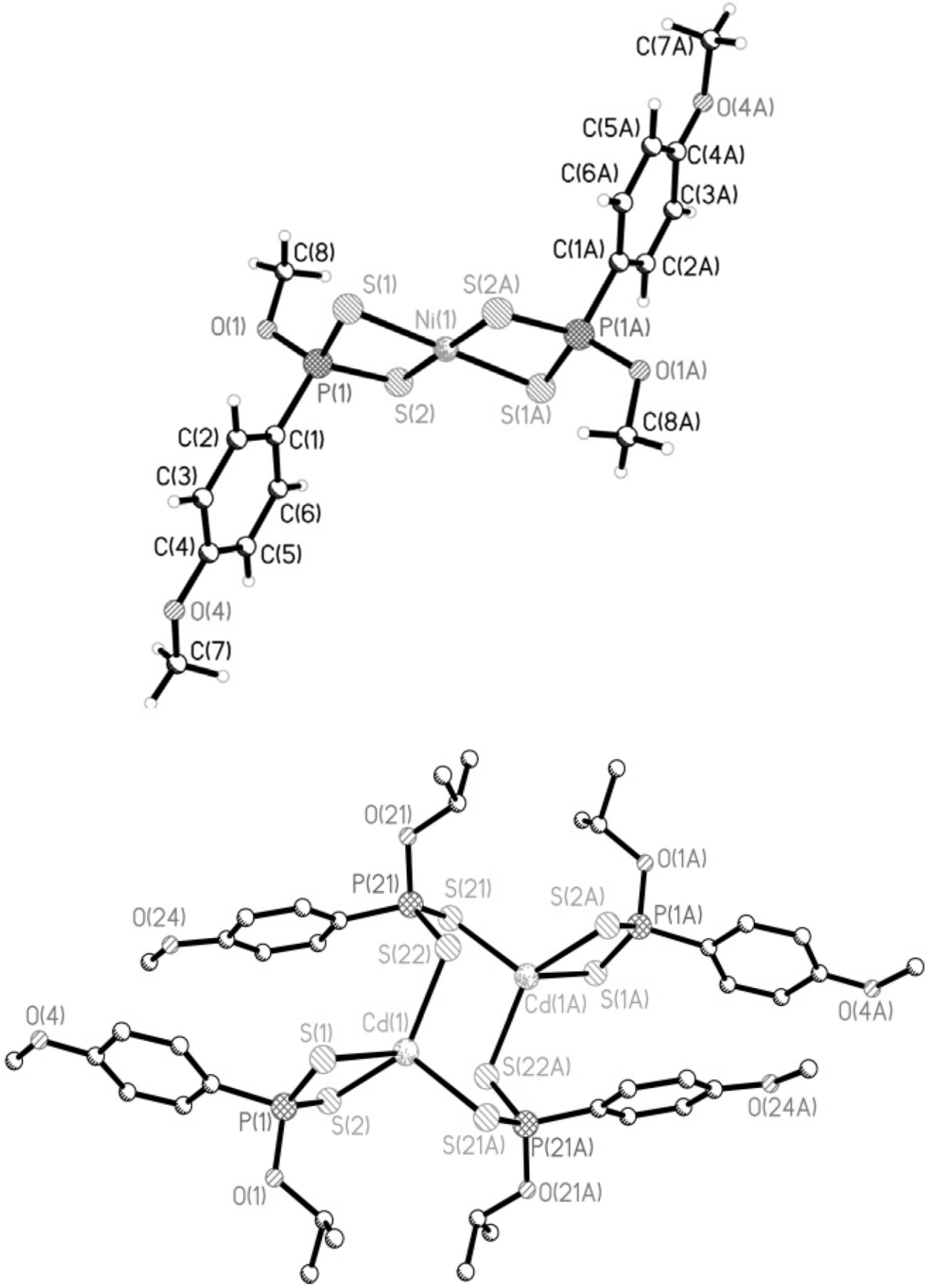

Figure 1.1.3 Top: Structure of [Ni{ArP(OCH$_3$)S$_2$}$_2$]
Bottom: Structure of [Cd$_2${ArP(O^{i}Pr)S$_2$}$_4$] (Ar = anisyl)

Zhang *et al.* also reported the decomposition of L.R. by heating it in alcohol, and the formation of Ni(II) and Co(II) complexes with P/S ligands.[92] The different organic group (2,4-dinitro- phenyl, benzyl and Ferrocenyl) on the phosphorus of P/S ligands were studies by Woollins, and the similar metal complexes to L.R. were obtained.

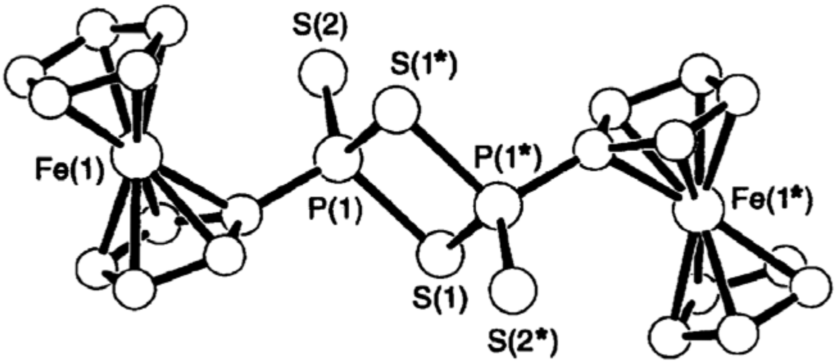

Figure 1.1.4 Structure of Ferrocenyl Lawesson's reagent (FcLR)

Here, Ferrocenyl Lawesson's reagent (FcLR) was received more attention since it was synthesized in 1996 (Figure 1.1.4).[93] The cleavage of the dimeric ring of FcLR gave stable phosphonodithioate salts for ligation to various metals (*e.g.*, Ni and Zn) (Scheme 1.1.12, Figure 1.1.5).[94-98]

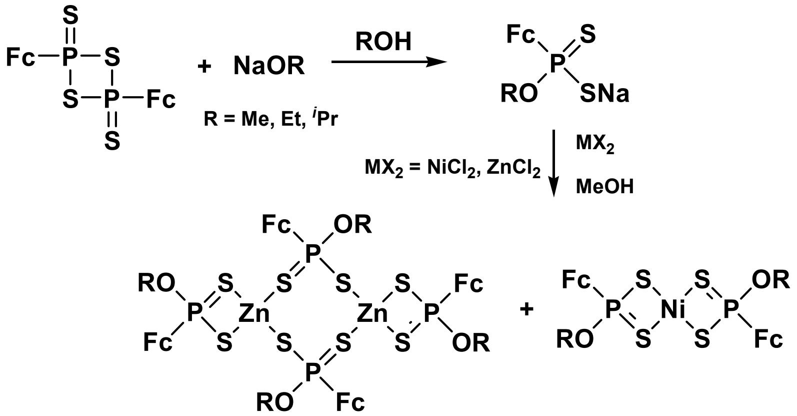

Scheme 1.1.12 Metathesis reactions of Ferrocenyl Lawesson's reagent (R = Me, Et, ⁱPr)

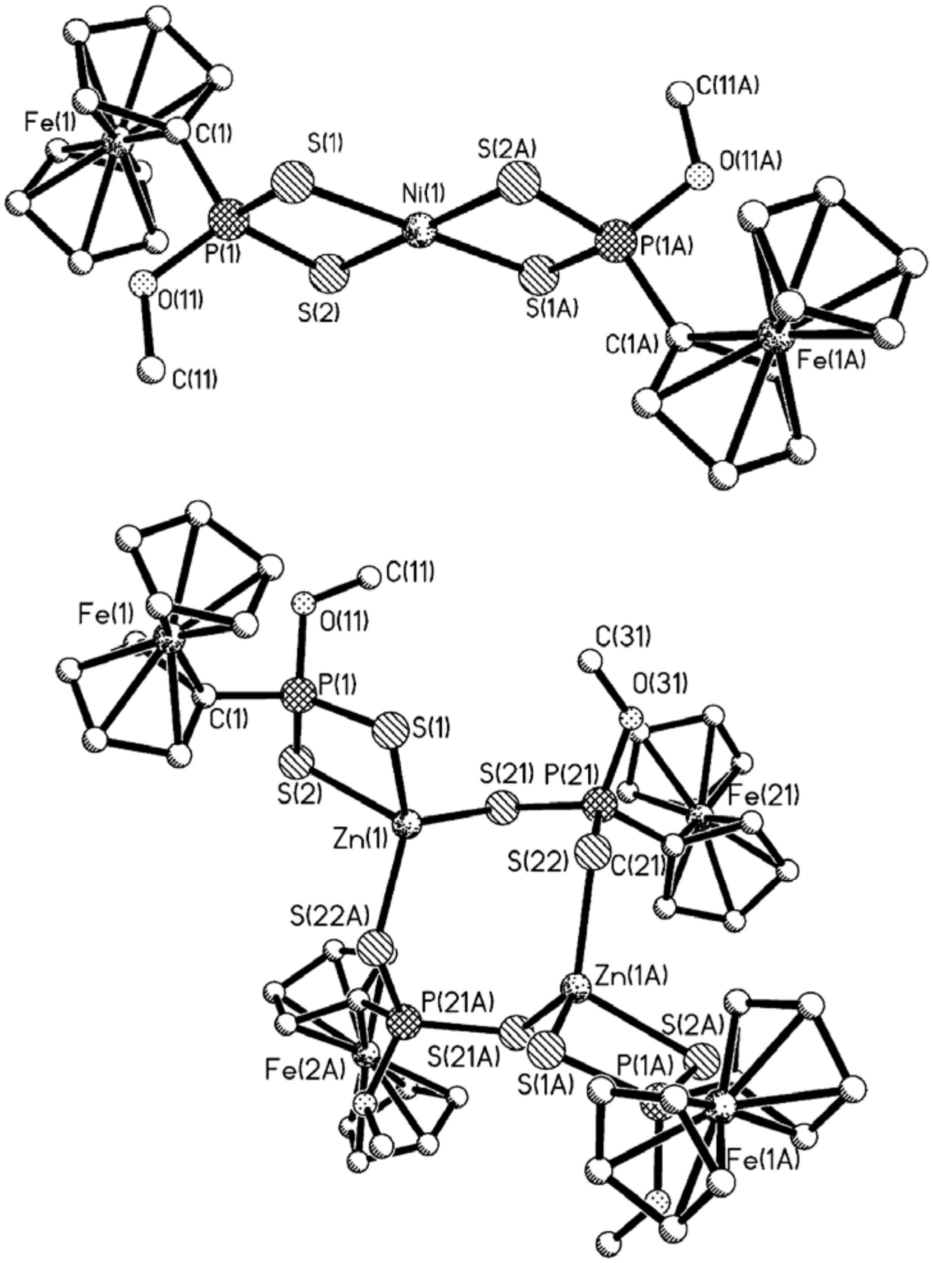

Figure 1.1.5 Top: Structure of [Ni{FcP(OCH$_3$)S$_2$}$_2$]. Bottom: Structure of [Zn$_2${FcP(OCH$_3$)S$_2$}$_4$]

1.2 P/Se ligands and their compounds

In the area of phosphorus-chalcogenide coordination chemistry, L.R. offers an approach to P/S-organometallic complexes, whilst 2,4-bis(phenyl)-1,3-diselenadiphosphetane-2,4-diselenide ([PhP(Se)(μ-Se)]$_2$, also named as Woollins' reagent, W.R.) offers an alternative route to complexes containing P/Se-based anionic ligands.

Woollins' reagent was first synthesized in 1988 by treating $(PhP)_5$ with ten equivalents of elemental selenium,[99-101] and then in 2001, its x-ray structure and NMR spectrum were reported (Figure 1.2.1).[102,103]

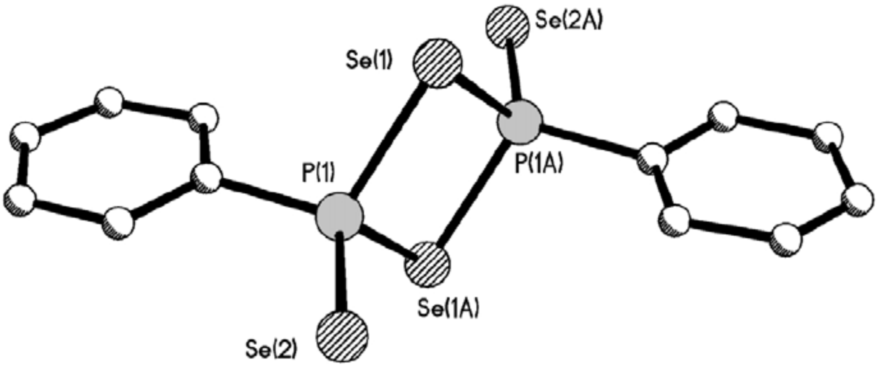

Figure 1.2.1 Structure of Woollins' reagent

After that, the chemistry of W.R. has been the subject of a few reports. Baxter *et al.*,[104] Bhattacharyya *et al.*[105] and Bethke *et al.*[106] have reported the selenation reactions of W.R. in the synthesis of selenoketenyl complexes and a range of selenoamides and selenoaldehydes, and Knapp *et al.* described its use for the selenation of carboxylic acids.[107] Meanwhile, Woollins reported the use of W.R. in the preparation of novel phosphorus-selenium heterocycles by the reaction with several organic substrates containing reactive unsaturated C=C double bonds, C≡C triple bonds and C≡N triple bonds.[102, 108-111]

Just like the preparations involving L.R., the phosphonodiselenoate salts can be prepared by reaction of W.R. with sodium alkoxides in corresponding alcohols, and subsequently reacted with transition metal halides (*e.g.*, $NiCl_2$) or acetates (*e.g.*, $Cd(OAc)_2{\cdot}2H_2O$) to generate metal complexes (Scheme 1.2.1, Figure 1.2.2).[15,112]

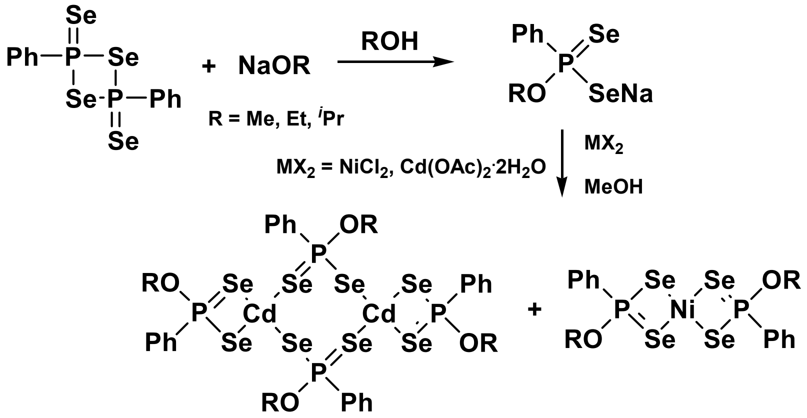

Scheme 1.2.1 Metathesis reactions of Woollins' reagent (R = Me, Et, ^{i}Pr)

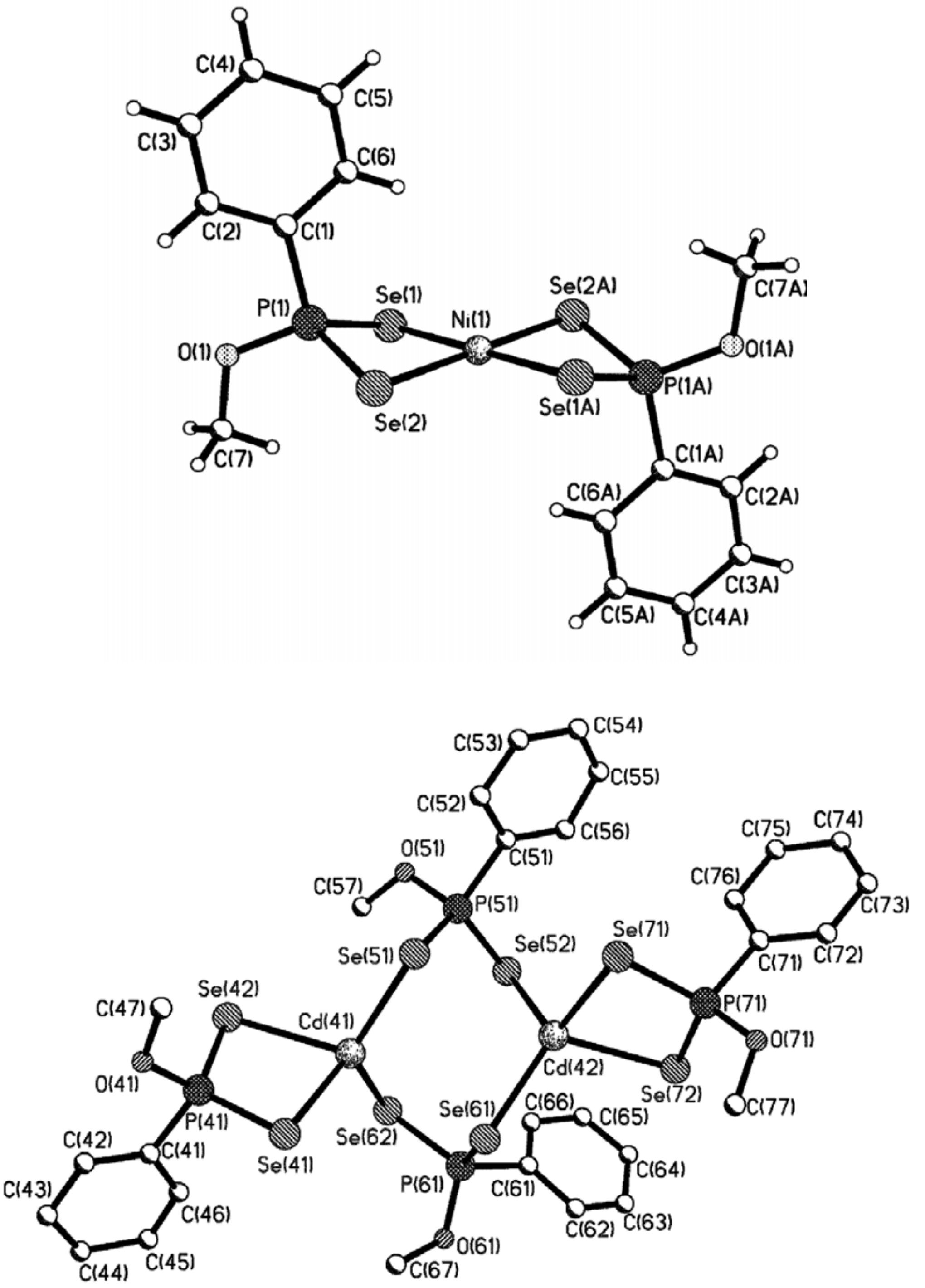

Figure 1.2.2 Top: Structure of [Ni{PhP(OCH$_3$)Se$_2$}$_2$]. Bottom: Structure of [Cd$_2${PhP(OCH$_3$)Se$_2$}$_4$]

Some other methods to create metal complexes containing P/Se ligands were demonstrated by Davies *et al.*[113-114], Liu *et al.*[115] and Kabir *et al.*[116].

Within this thesis routes to generate new P/S and P/Se (together with their derivatives--As and Te) ligands for metal coordination chemistry from available readily starting material (*e.g.* L.R. and W.R.) is further explored.

2. Aims and Objectives

Copper(I)-*tert*-butoxide (CuO^tBu) is a versatile reagent in coordination chemistry.[117] In 1972, Saegusa *et al.* used the reaction of CuCl and LiO^tBu to produce CuO^tBu.[118,119] From this route, a fine powder of air and light sensitive CuO^tBu decomposes more easily due to the increased surface and limits the use of it as a starting material for further investigations. In our group, the previously investigations of reactions between alkali metal alkoxides and copper(I) halides have shown that the reaction of Potassium-*tert*-butoxide with Copper(I) bromide in THF represents a useful method for the preparation of larger amounts of *crystalline* CuO^tBu.[120]

Since the *crystalline* CuO^tBu can be easily prepared, the reactions of CuO^tBu with carboxylic acid anhydride were investigated. The simple model reaction of CuO^tBu with benzoic acid anhydride which was carried out in THF produced the solvated Cu(I)-benzoate (Scheme 2.1, Figure 2.1).[121]

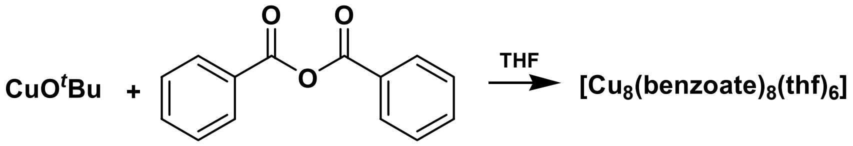

Scheme 2.1 Reaction of CuO^tBu with benzoic acid anhydride

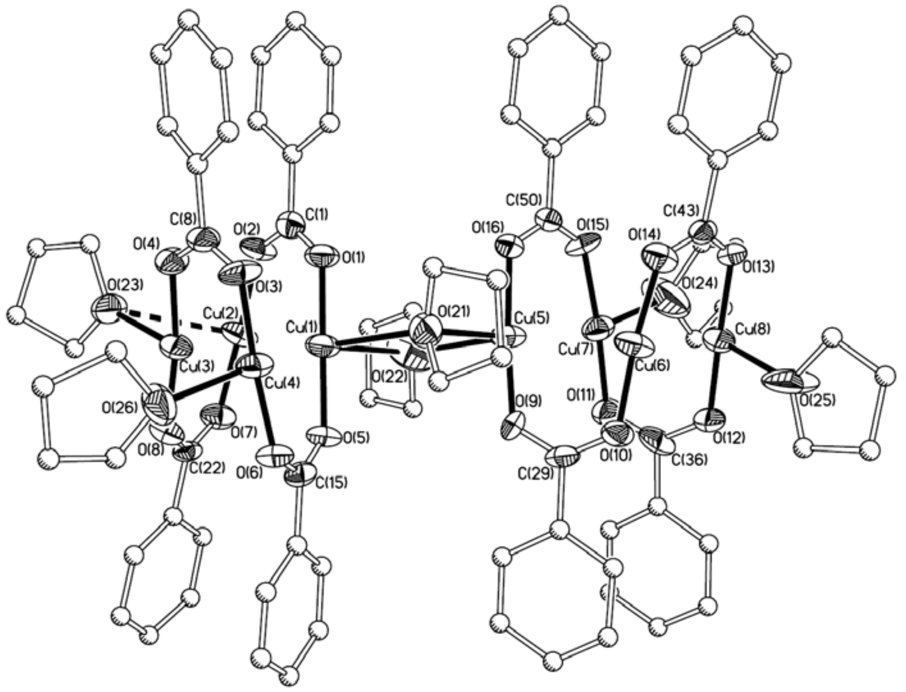

Figure 2.1 Structure of $[Cu_8(benzoate)_8(thf)_6]$

The structure showed that the anhydride bonds CO-O-CO was broken by CuO^{t}Bu, and an acentric structure consisting of two copper(I) benzoate tetramers held together by μ_2-bridging THF molecules was formed. Meanwhile, the insertion reaction of maleic anhydride into the Cu-O bond in CuO^{t}Bu produced the complex [$Cu_2(CO_2C_2H_2CO_2{}^tBu)_4 \cdot (dme)$] (Scheme 2.2, Figure 2.2). [122,123]

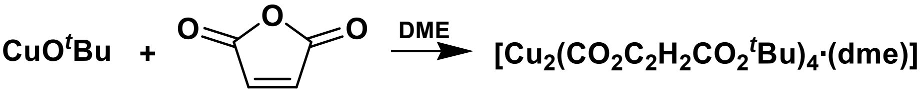

Scheme 2.2 Reaction of CuO^{t}Bu with maleic anhydride

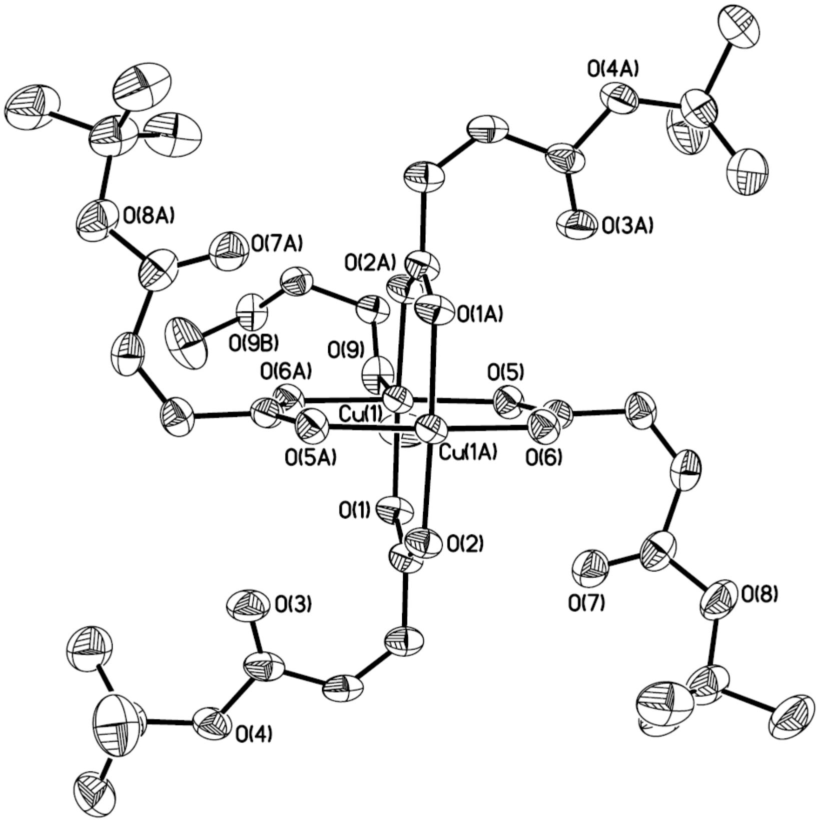

Figure 2.2 Structure of [$Cu_2(CO_2C_2H_2CO_2{}^tBu)_4 \cdot (dme)$]

Here, five-membered ring is opened and the maleic anhydride is transformed into the monoanionic tert-butoxymaleato ligand. It consists of dicopper(II) tetracarboxylate ‘paddlewheel’ units linked by dme into a one-dimensional coordination polymer (Figure 2.2).

So, the original thought was to find out other hybrid anhydrides, Lawesson’s reagent and Woollins’ reagent would react with alkoxides, thiolates and selenolates?

3. Results and Discussions

Initially, 2-Sulfobenzoic acid cyclic anhydride was employed in the reaction, and the structure is showed as follows (Scheme 3.1, Figure 3.1, Table 3.1),

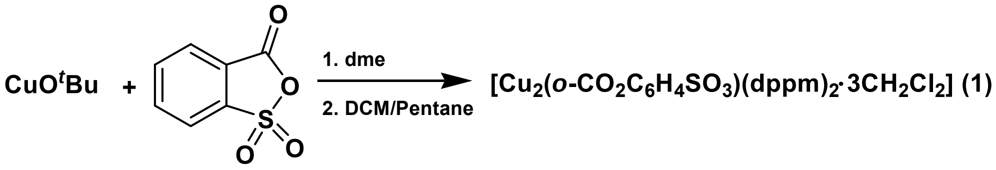

Scheme 3.1 Reaction of CuO^tBu and 2-Sulfobenzoic acid cyclic anhydride

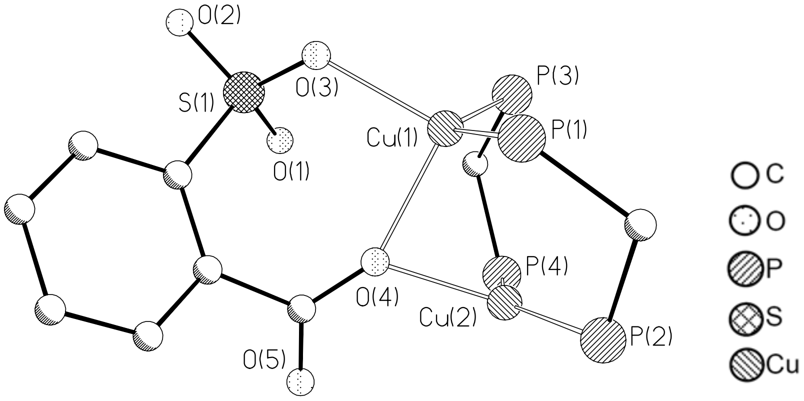

Figure 3.1 Structure of **1** (The phenyl groups of dppm are omitted)

Table 3.1 Selected ranges of bond lengths (Å) and angles (°)

Bond lengths					
S1-O1	1.448(3)	S1-O2	1.451(3)	S1-O3	1.462(3)
Cu1-O3	2.085(3)	Cu1-O4	2.130(3)	Cu1-P1	2.2251(13)
Cu1-P3	2.2460(13)	Cu2-O4	2.025(3)	Cu2-P4	2.2263(13)
Cu2-P2	2.2357(13)				
angles					
O3-Cu1-O4	91.84(11)	O3-Cu1-P1	116.37(9)	O3-Cu1-P3	103.48(9)
P1-Cu1-P3	126.98(5)	O4-Cu2-P4	105.53(10)	O4-Cu2-P2	107.84(10)
P4-Cu2-P2	145.56(5)	S1-O3-Cu1	121.60(15)	C7-O4-Cu2	124.5(2)
C7-O4-Cu1	150.9(3)				

this result is different as the previously studies, that is, O3 and O4 directly coordinated with copper atoms which are held by two dppm, and the O^tBu group is missing. Is 2-Sulfobenzoic acid cyclic anhydride not dried, or is there some special mechanism inside the reaction? That is what we need to find out and because of that, Lawesson's reagent is employed in the reactions with CuO^tBu.

When Lawesson's reagent was heated with 2 equivalents of CuO^{t}Bu in different solvents, and with different phosphorus ligands, different results were obtained (Scheme 3.2).

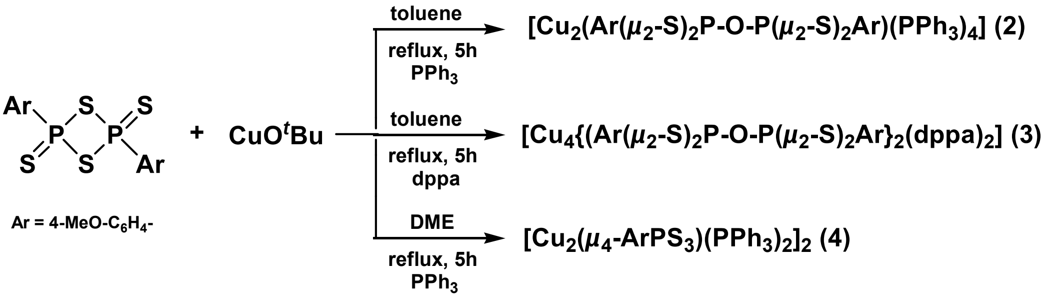

Scheme 3.2 Reactions of CuO^{t}Bu and Lawesson's reagent in different solvents

First, the reaction was carried out in toluene, a yellow precipitate was formed which dissolved upon addition of PPh_3. Crystallization from a mixture of dichloromethane and pentane gave, to our surprise, no phosphane-stabilised copper(I) phosphono-dithioate, which could have been regarded as analogous compound to the sodium phosphono-dithioate salts prepared by Woollins *et al.*. Instead, the Cu(I) pyrophosphonodithioate $[Cu_2(Ar(\mu_2\text{-}S)_2P\text{-}O\text{-}P(\mu_2\text{-}S)_2Ar)(PPh_3)_4]$ (**2**) (Ar = 4-$MeOC_6H_4$-) was obtained in 80% yield. The structure of **2** was initially determined by x-ray analysis (Figure 3.2, Table 3.2).

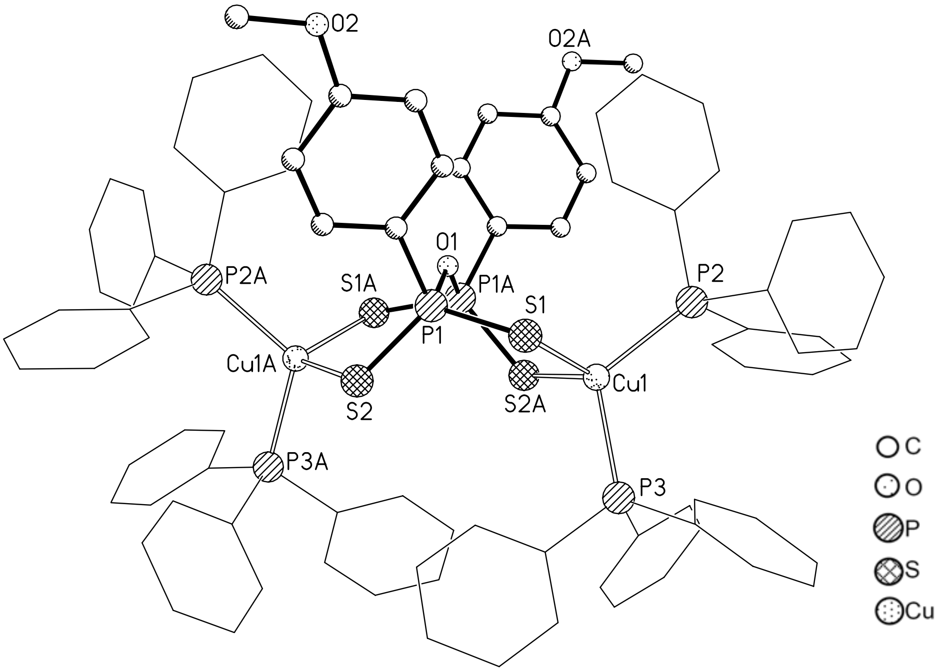

Figure 3.2 Structure of $[Cu_2(Ar(\mu_2\text{-}S)_2P\text{-}O\text{-}P(\mu_2\text{-}S)_2Ar)(PPh_3)_4]$ (**2**)

Table 3.2 Selected ranges of bond lengths (Å) and angles (°)

Bond lengths					
Cu1-P3	2.3181(15)	Cu1-P2	2.3193(14)	Cu1-S1	2.3643(16)
Cu1-S2A	2.3749(15)	P1-O1	1.640(2)	P1-S2	1.9909(17)
P1-S1	1.9927(16)				
angles					
O1-P1-S2	110.33(12)	O1-P1-S1	110.01(7)	S2-P1-S1	117.41(8)
P1A-O1-P1	130.3(3)				

The dianionic ligand $[ArS_2P\text{-}O\text{-}PS_2Ar]^{2-}$ generated in the reaction of CuO^{t}Bu with Lawesson's reagent bridges two $[Cu(PPh_3)_2]^+$ ions. Compound **2** consists of two puckered annulated six-membered $[CuS_2P_2O]$ rings and an organic shell of phenyl rings of the PPh_3 ligands (each one disordered over two positions; 50:50) and anisyl groups from Lawesson's reagent. The Cu(I) centers show a distorted tetrahedral coordination environment. The P-O and P-S distances in **2** are in good agreement with values observed in $[K_2(C_{10}H_6)PS_2(\mu\text{-}O)PS_2]$, which is the closest related compound to **2**.[124] The $^{31}P\{^1H\}$ NMR spectrum was recorded from crystals of **2** dissolved in $CDCl_3$ (verified by redetermination of the unit cell). Resonances at δ = 91.5 ppm for the generated $[ArS_2P\text{-}O\text{-}PS_2Ar]^{2-}$ dianion and at δ = -3.6 ppm for coordinated PPh_3 ligands were observed and the IR spectrum showed a strong band at ν_{as}(P-O-P) = 841 cm^{-1}. In order to know more about the mechanism, the reaction was therefore performed in C_6D_6 and all volatile products were distilled out and the NMR measurement afforded a sample containing $^tBu_2O$ formed in the reaction.

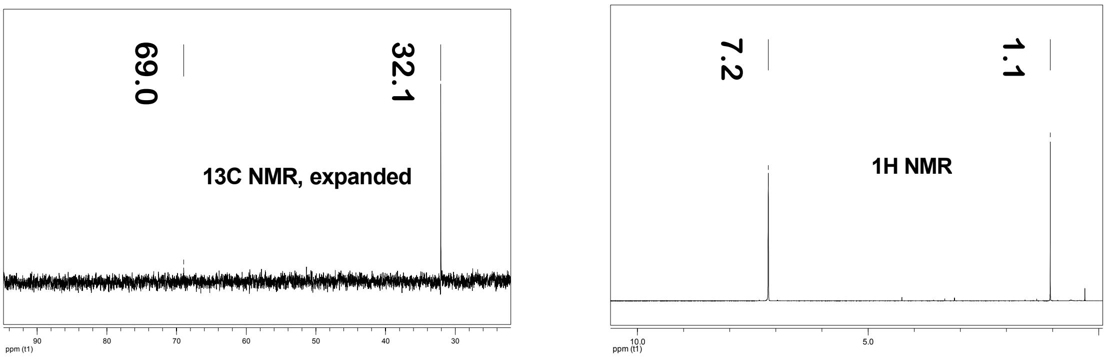

Figure 3.3 NMR spectra of by-product ($^tBu_2O$)

Resonances at δ = 1.1 ppm from the ^1H NMR spectrum and at δ = 32.1 ($C(\underline{C}H_3)_3$), 69.0 ($\underline{C}(CH_3)_3$) ppm from the ^{13}C NMR spectrum for the *tert*-butyl groups which match the values in the literature very well were observed (Figure 3.3). [125,126]

Reactions of CuO^{t}Bu with Lawesson's reagent in the presence of the different phosphane ligand--dppa (dppa = $Ph_2PNHPPh_2$) were also performed and afforded the tetranuclear complex $[Cu_4\{Ar(\mu_2\text{-}S)_2P\text{-}O\text{-}P(\mu_2\text{-}S)_2Ar\}_2(dppa)_2]$ (**3**) (Scheme 3.2, Figure 3.4, Table 3.3). In the solid state **3** consists of two fused adamantane cage frameworks in which two $[ArS_2P\text{- }O\text{-}PS_2Ar]^{2-}$ dianions coordinate the Cu atoms Cu(1, 2, 2A). Cu(3) is located in the periphery of the cluster and the P atoms of the two dppa ligands complete the remaining coordination sites of Cu(2, 2A, 3). Like in **2**, Cu atoms in **3** exhibit distorted tetrahedral coordination environments but the new ligand $[ArS_2P\text{-}O\text{-}PS_2Ar]^{2-}$ now bridges two Cu atoms via the S atoms S(3, 3A, 4, 4A), whilst the remaining S atoms S(1, 1A, 2, 2A) are coordinated to one Cu atom each.

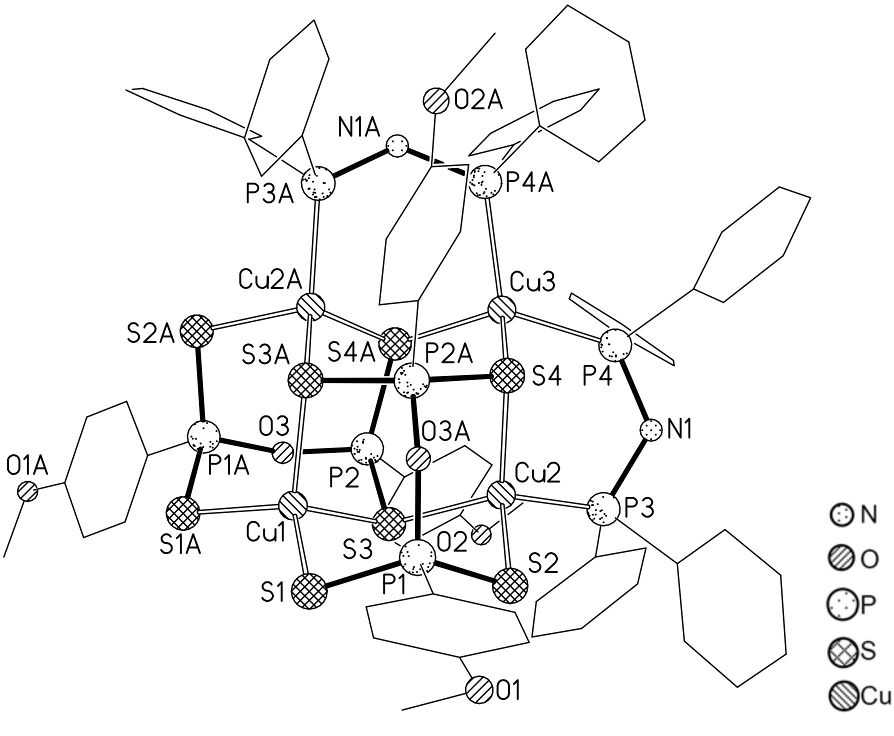

Figure 3.4 Structure of $[Cu_4\{Ar(\mu_2\text{-}S)_2P\text{-}O\text{-}P(\mu_2\text{-}S)_2Ar\}_2(dppa)_2]$ (**3**)

Table 3.3 Selected ranges of bond lengths (Å) and angles (°)

Bond lengths					
Cu1-S1	2.2958(16)	Cu1-S3	2.3394(19)	Cu2-P3	2.2209(19)
Cu2-S3	2.3178(16)	Cu2-S4	2.337(2)	Cu2-S2	2.3570(17)
Cu3-P4	2.3318(18)	Cu3-S4	2.3641(16)	S1-P1	1.994(2)
S2-P1	1.990(3)	S3-P2	2.011(2)	S4-P2A	2.027(2)
P1-O3A	1.662(5)	P2-O3	1.613(4)	P2-S4A	2.027(2)
P3-N1	1.707(6)	P4-N1	1.709(5)		
Angles					
O3A-P1-S2	109.66(19)	O3A-P1-S1	110.14(17)	S2-P1-S1	118.99(12)
O3-P2-S3	108.20(18)	S3-P2-S4A	119.43(10)	P3-N1-P4	127.3(3)
P2-O3-P1A	136.3(3)				

Spectroscopic data and observed bond lengths in **3** verify the uniform composition of crystals of **3** and can be compared with **2** or [$K_2(C_{10}H_6)PS_2(\mu\text{-}O)PS_2$].

The further outcome of the reaction is remarkably different when ethereal solvents are used. In the presence of DME [$Cu_4(\mu_4\text{-}ArPS_3)_2(PPh_3)_4$] (**4**) is formed by asymmetric cleavage of Lawesson's reagent together with tris-1,3,5-Aryl-2,4,6-trioxatriphosphinane-2,4,6-trisulfide [$ArP(S)O]_3$ (Scheme 3.2, Figure 3.5, Table 3.4). The formation of [$ArP(S)O]_3$, which could be regarded as a decomposition product of a hypothetical intermediate [$ArP(S)(O^tBu)_2$], was confirmed by ^{31}P NMR (δ_P 75 ppm, lit. 72 ppm [127]). In the solid state **4** exists as a crystallographically centrosymmetric dimer of two [$Cu_2(ArPS_3)(PPh_3)_2$] units. The Cu atoms exhibit tetrahedral coordination environments and are coordinated by S atoms of [$ArPS_3]^{2-}$ and P atoms of PPh_3 ligands.

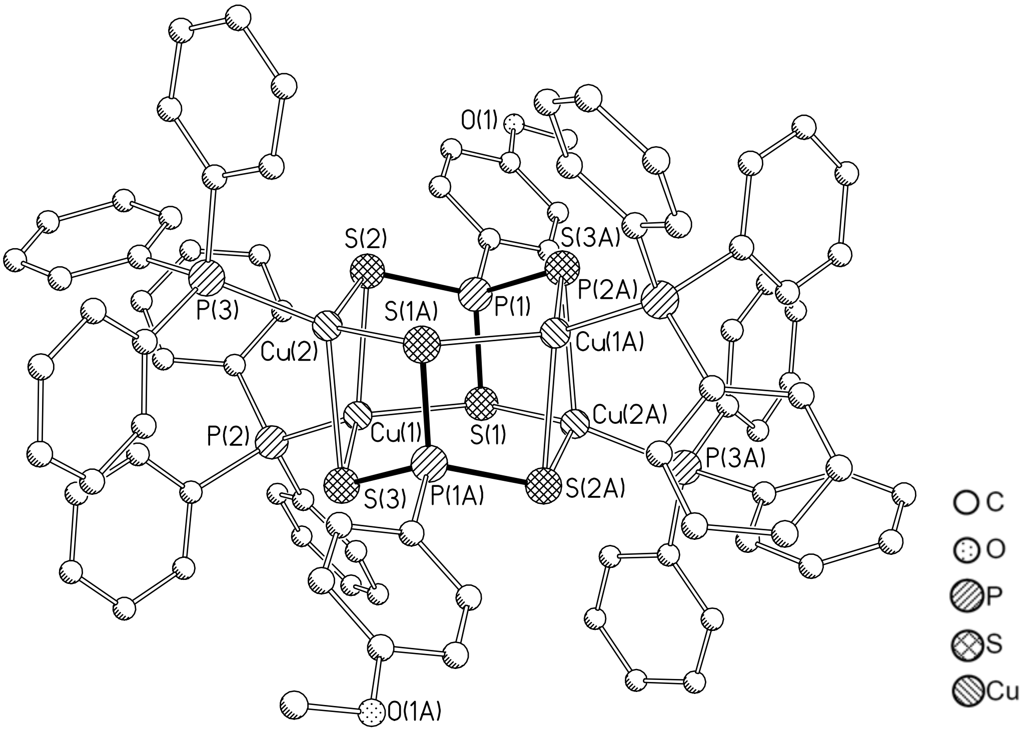

Figure 3.5 Structure of [$Cu_4(\mu_4\text{-}ArPS_3)_2(PPh_3)_4$] (**4**)

Table 3.4 Selected ranges of bond lengths (Å) and angles (°)

Bond lengths					
Cu1-P2	2.2369(8)	Cu2-P3	2.2257(9)	Cu1-S1	2.3958(9)
Cu1-S2	2.5585(13)	Cu1-S3	2.2990(9)	Cu2-S2	2.2672(8)
Cu2-S1A	2.3465(9)	Cu2-S3	2.7115(14)	S1-P1	2.0450(13)
S2-P1	2.0345(10)	P1-S3A	2.0328(10)		
Angles					
P-Cu-S	110.74(3)-116.96(4)	S-Cu-S	82.56(3)-119.17(3)	S3A-P1-S2	116.92(5)
S3A-P1-S1	110.38(4)	S2-P1-S1	109.04(5)	P-S-Cu	78.39(3)-115.38(4)
Cu2A-S1-Cu1	109.84(3)	Cu2-S2-Cu1	69.47(2)	Cu1-S3-Cu2	66.26(2)

According to the results, the possible mechanism is given as follows (Scheme 3.3). The P-S four-membered ring of L.R. is opened by one equivalent CuO^{t}Bu, and the intermediate [ArSP(SCu)-S-(O^{t}Bu)PSAr] is formed. When the second CuO^{t}Bu reacts with the intermediate, there are two possibilities. Symmetric way (a) will produce only one kind of species-[ArSP(O^{t}Bu)SCu], then after one *tert*-butyl ether is eliminated from two [ArSP(O^{t}Bu)SCu] and phosphorous ligands (PPh_3 and dppa) are added, **2** and **3** will be obtained. On the other hand, from asymmetric way (b), [ArSP(O^{t}Bu)$_2$] and [ArSP(SCu)$_2$] will produce [ArP(S)O]$_3$ and **4** separately.

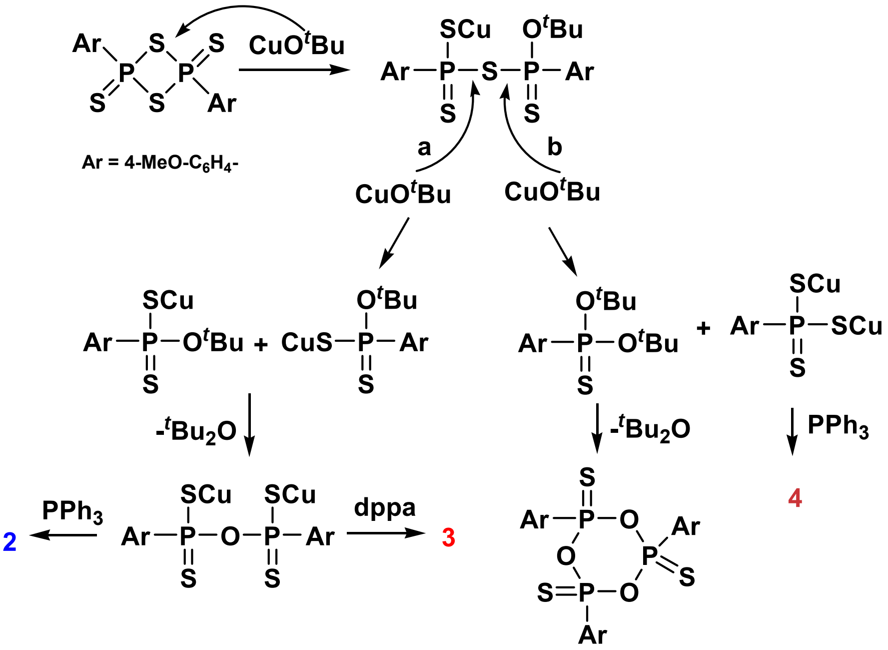

Scheme 3.3 Possible mechanism for the reactions of CuO^{t}Bu and Lawesson's reagent

Since O^{t}Bu is unstable as a substituent on phosphorus atoms, the reactions of Cu(I) thiolates and L.R. were investigated and it turned out that they just worked as well as the reactions between alkoxides and L.R.. Moderate yield of **4** is obtained when refluxing THF or toluene is used, that is to say, [P-S^{t}Bu] is also not stable under elevated temperature. When the reaction was carried out at room temperature in THF, [Cu(ArP(S^{t}Bu)S$_2$)(PPh$_3$)$_2$] (**5**), the first structurally characterised example of a metal complex containing ligands of the type [RP(SR')S$_2$]$^-$ (R, R' = organic group), was obtained in moderate yield (Scheme 3.4, Figure 3.6, Table 3.5).

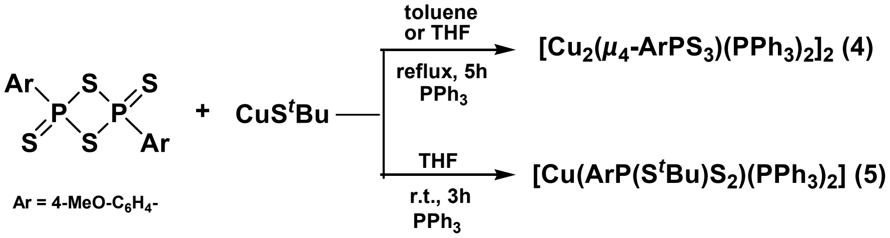

Scheme 3.4 Reactions of CuS^{t}Bu and Lawesson's reagent (with different solvents and temperature)

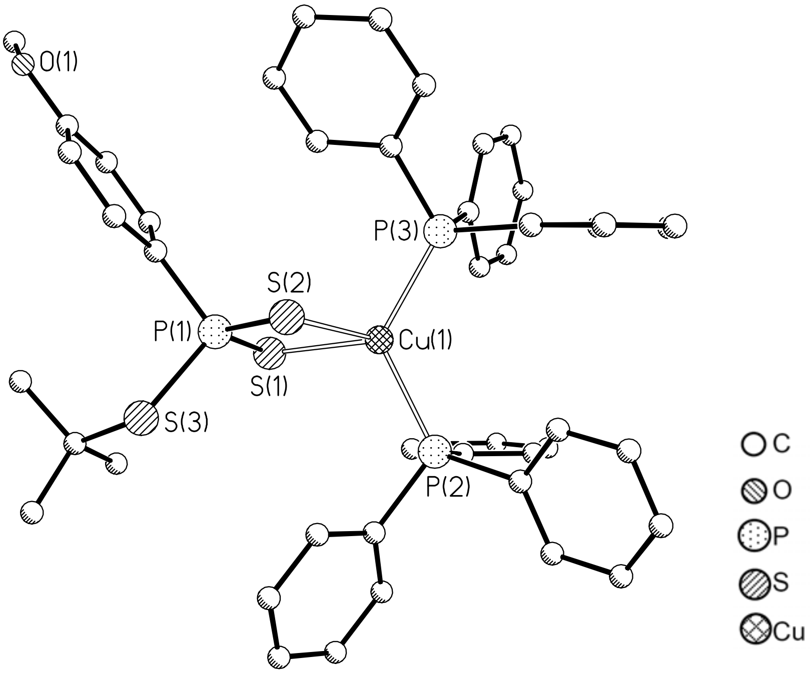

Figure 3.6 Structure of [Cu(ArP(S^{t}Bu)S$_2$)(PPh$_3$)$_2$] (**5**)

Table 3.5 Selected ranges of bond lengths (Å) and angles (°)

Bond lengths					
Cu1-P3	2.2659(5)	Cu1-P2	2.2698(5)	Cu1-S1	2.4538(5)
Cu1-S2	2.4675(6)	P1-S1	1.9903(7)	P1-S2	1.9978(7)
P1-S3	2.1033(7)				
Angles					
P3-Cu1-P2	122.69(2)	P-Cu-S	102.08(2)-120.83(2)	S1-Cu1-S2	84.288(18)
S1-P1-S2	111.79(3)	S1-P1-S3	117.09(3)	S2-P1-S3	100.89(3)

In the solid state **5** exhibits a simple arrangement of one $[ArP(S^tBu)S_2]^-$ ligand chelating Cu(1) *via* S atoms (Figure 3.6). Tetrahedrally surrounded Cu(1) is in addition coordinated by two P atoms of PPh_3 groups. In this case the formation of larger aggregates is hindered by the steric requirements of PPh_3. This product can also be regarded as a proof for the mechanism showed before.

A different approach overcoming the solubility problems of coinage metal complexes was the use of alkali metal alkoxides or thiolates in reactions with L.R.. For alkoxides, alkali metal phosphonodithioate salts are generated, which are commonly prepared *in situ* and used in subsequent metathesis reactions. Up until now, however, no structural evidence for alkali metal phosphonodithioate salts exists. In that sense the synthesis and characterization of **6-10** form the basis of a potentially emerging supramolecular chemistry of alkali metal phosphonodithioate salts (Scheme 3.5, 3.6).

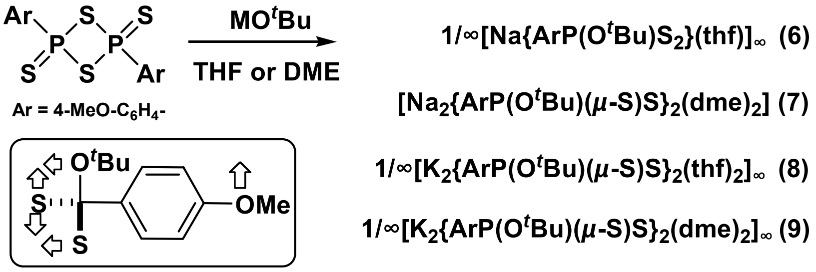

Scheme 3.5 Reactions of MO^tBu and Lawesson's reagent (M = Na, K)

The generated dithiophosphonato anion in these reactions contains four donor centers which could all be involved in metal bonding. In previously examples of metal complexes with similar PS anions, S atoms are commonly chelating metal ions, whereas coordination of O^tBu or methoxy groups to metal atoms has not been detected. A reason for these previous observations might be the rotation of the alkoxy-substituents in solution, their involvement in hydrogen bonding to solvent molecules or a preference of the metal ion for softer donor atoms.[128]

In the solid state **6** exists as a polymer of $[ArP(O^tBu)S_2]^-$ ions held together by Na cations (Figure 3.7, top). The anion and $[Na(thf)]^+$ cation are topologically different (*e.g.*, $[ArP(donor\text{-}center)_3]^-$ and $[(thf)Na(empty\ coordinationsite)_4]^+$). In the extended solid-state structure they are arranged in alternating *cis*/*trans* orientation of neighbouring aromatic and thf rings along the polymer. **7** was obtained from a hexane -DME solution and the structural consequence of the increase of Na coordination

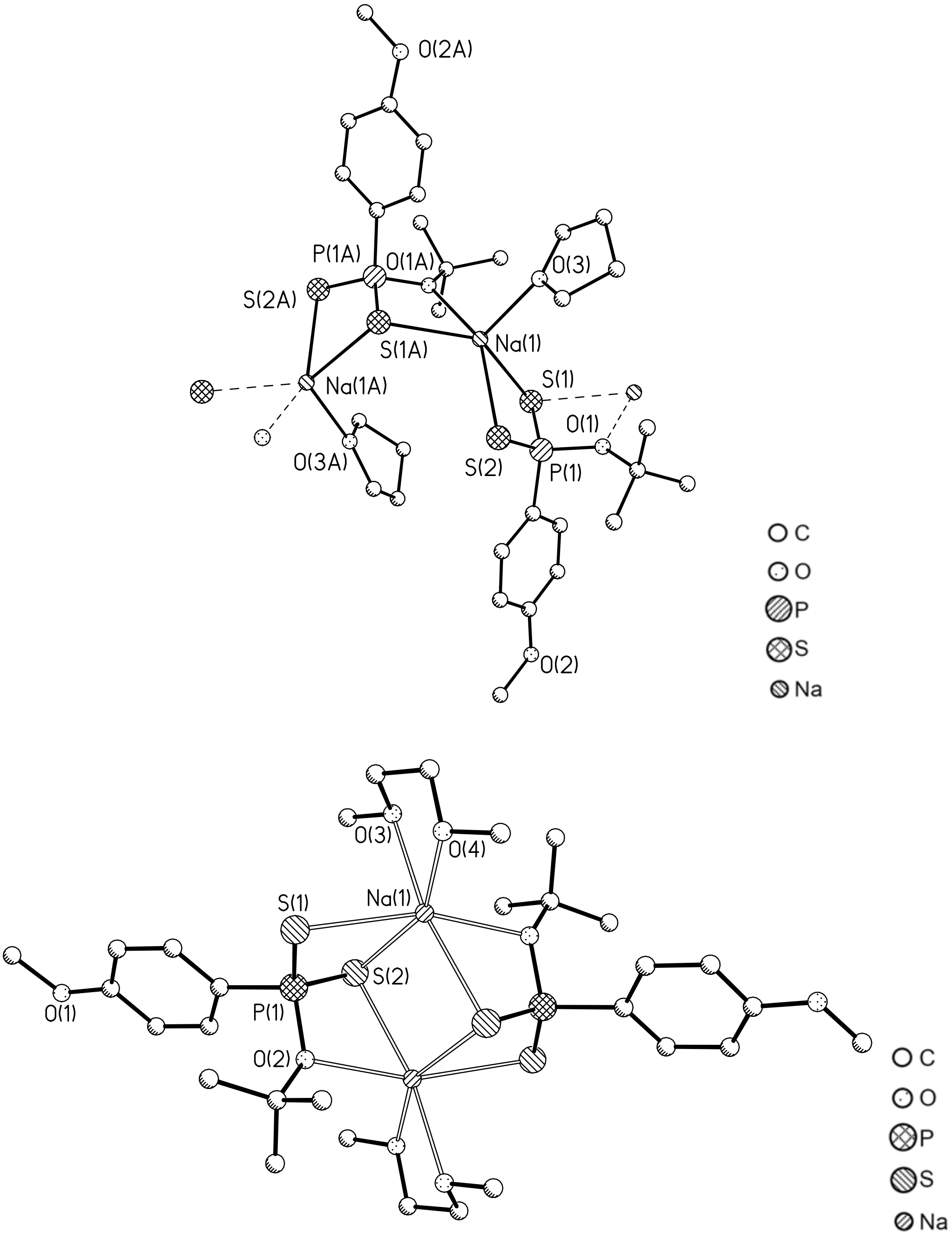

Figure 3.7 Top: Structure of **6**. Bottom: Structure of **7**

Table 3.6 Selected ranges of bond lengths (Å) and angles (°) of 6

Bond lengths					
Na1-O3	2.345(5)	Na1-O1A	2.445(3)	Na-S	2.772(2)-2.874(2)
P1-O1	1.609(3)	P1-C1	1.799(4)	P1-S2	1.9688(16)
P1-S1	1.9973(14)				
Angles					
O3-Na1-O1A	102.59(13)	O-Na-S	65.12(9)-151.04(12)	S1A-Na1-S1	139.26(9)
S1A-Na1-S2	97.31(7)	S1-Na1-S2	72.85(5)	O1-P1-S2	113.98(13)
O1-P1-S1	102.39(11)	S2-P1-S1	116.01(7)		

numbers from five in **6** to six in **7** is displayed in Figure 3.7. In the solid state **7** consists of a centrosymmetric arrangement of two [{ArP(O^{t}Bu)S$_2$}Na(dme)] units with bond lengths similar to those listed for **6** (Table 3.6). The observation of deaggregation by change of solvents seems trivial at first sight. It is assumed, however, that the use of topologically different ions represents a potentially useful concept for the design of alkali metal containing polymers. As a consequence alkali metal ions of different size should result in a variety of alkali metal dithiophosphonate arrangements in the solid state. In the case of the Li$^+$ ion only oily residues were obtained despite various attempts in a range of solvents. Larger K$^+$ ions, however, turned out to have a significant influence on the design of polymeric alkali metal phosphonodithioates. Akin to **7** (Fig 3.7, bottom) the coordination number of the alkali metal ion in **8** (Figure 3.8a) is six hence a similar centrosymmetric arrangement now of two [{ArP(O^{t}Bu)S$_2$}K(thf)] units is formed. The main difference between **7** and **8**, however are increased bond distances of potassium ions to neighboring atoms in comparison to sodium ions in **6** and **7**. As a consequence a higher ordered structure held together by more and weaker electrostatic interactions

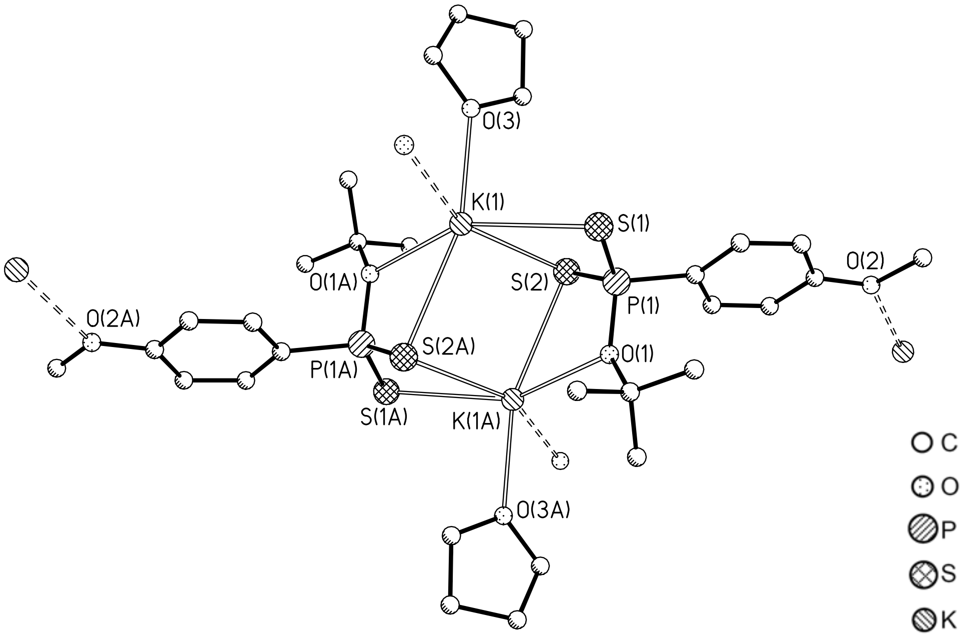

Figure 3.8a Structure of **8**

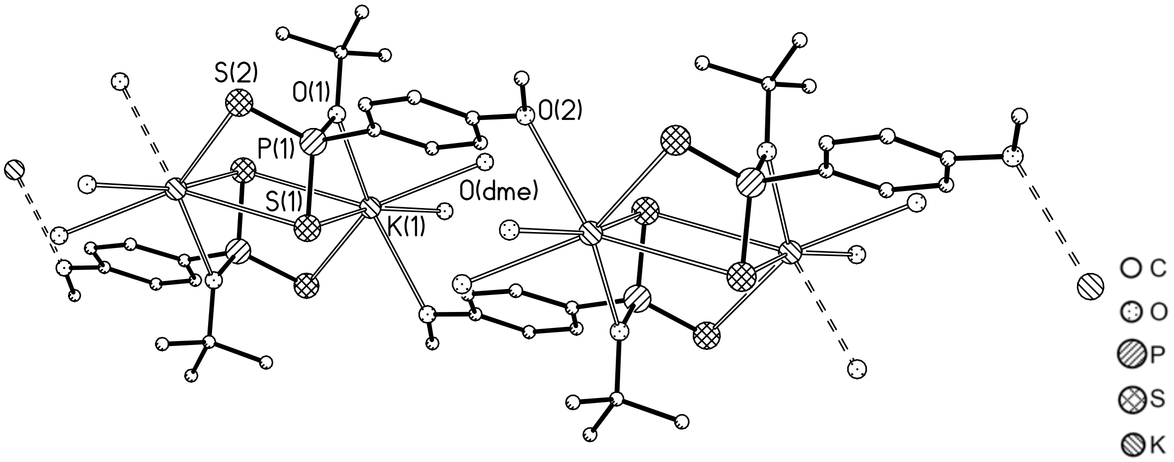

Figure 3.8b Structure of **9**

Table 3.7 Selected ranges of bond lengths (Å) and angles (°) of 8

Bond lengths					
K1-O3	2.635(2)	K1-O1A	2.8715(15)	O2-K	2.7934(16)
K1-S1	3.2164(8)	K1-S2A	3.1632(13)	K1-S2	3.2015(8)
P1-O1	1.6226(17)	P1-C1	1.816(2)	P1-S1	1.9742(8)
P1-S2	1.9830(10)				
Angles					
O1-P1-S1	113.00(7)	O1-P1-S2	103.07(7)	S1-P1-S2	117.64(3)
S-K-S	63.67(2)-106.24(3)	O-K-O	69.03-108.86(4)	O3-K1-S2A	160.81(5)
O-K-S	55.72(4)-155.23(4)				

is found in **8** and the DME solvate **9** (Figure 3.8). A striking feature of **8** and **9** is the fact that coordination of $[ArP(O^tBu)S_2]^-$ ions to the alkali metal involves all donor centers (Scheme 3.5) resulting in $[K_2\{ArP(O^tBu)\ (\mu\text{-}S)S\}_2(thf)_2]$ constitutional units linked into a polymetallacyclophane by coordination of O atoms of 4-anisyl substituents to potassium ions. The use of DME during the synthesis of **9** imposed no major structural changes and bond lengths are similar to those reported for **8** (Table 3.7). At the same time, trithiophosphonates containing $[ArP(S^tBu)S_2]^-$ or related anions is another aspect of current interest. The application of synthetic concepts developed from the first structurally characterized alkali metal phosphonodithioates **6-9** prompted the investigations of solid-state structures of alkali metal trithiophosphonates. It was hoped to achieve the preparation of this new class of compounds with all the ingredients necessary for unusual supramolecular architectures, *e.g.*, a heavier alkali metal and weak electrostatic interactions to S-donor centers in $[ArP(S^tBu)S_2]^-$ anions (Scheme 3.6, Figure 3.9, Table 3.8).

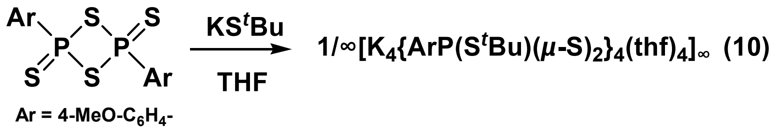

Scheme 3.6 Reaction of KS^{t}Bu and Lawesson's reagent

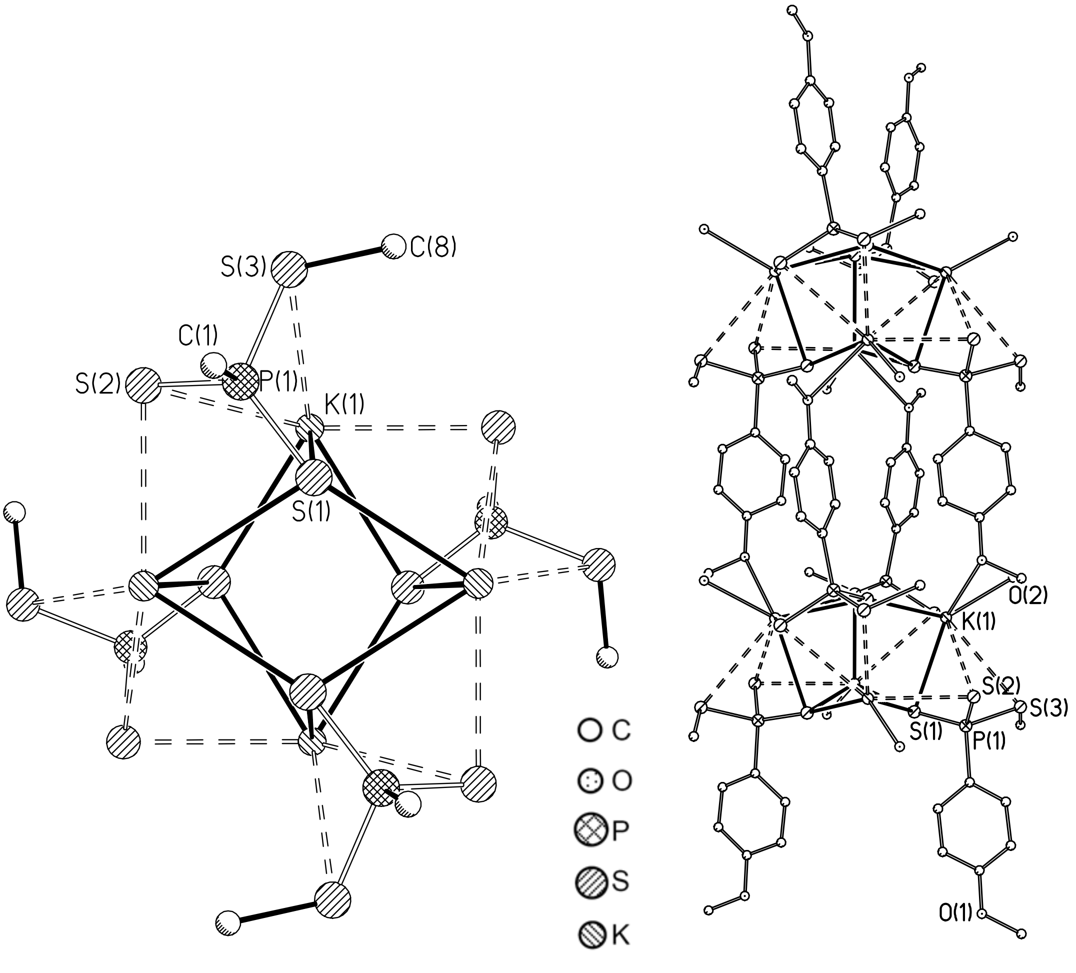

Figure 3.9 Left: Structure of a tetrameric building block of **10**
Right: Arrangement of units in the polymer (only a-C atoms of S^{t}Bu groups and O atoms of THF are displayed).

Table 3.8 Selected ranges of bond lengths (Å) and angles (°)

Bond lengths					
P1-C1	1.814(5)	P1-S1	1.982(2)	P1-S2	1.985(2)
P1-S3	2.123(2)	K1-O	2.758(6), 2.896(4)	K1-S1	3.238(2)
K1-S	3.333(2), 3.370(2),3.437(2)			K1-S2	3.679(2)
K1-S3	3.785(2)	S3-C8	1.877(8)		
Angles					
C1-P1-S1	109.13(19)	C1-P1-S2	111.4(2)	S1-P1-S2	115.07(9)
C1-P1-S3	105.7(2)	S1-P1-S3	115.60(10)	S2-P1-S3	99.26(9)

In the solid state **10** consists of a tetrameric arrangement of [ArP(S^{t}Bu)S$_2$K] units in which K(1), S(1) and symmetry equivalent atoms form a distorted cubic arrangement (Figure 3.9, left) with imposed $\bar{4}$ symmetry held together by coordination of O atoms of methoxy groups to K atoms. Potassium atoms in **10** are seven-coordinated by S and O atoms with rather large distances to O and S atoms. The [ArP(S^{t}Bu)S$_2$K]$_4$ building block in **10** represents a repeating unit with electron donor/acceptor properties.

Till now, the study of the nucleophilic ring-opening of Lawesson's reagent with alkoxides under different conditions showed that metal complexes containing the anionic ligands [ArS$_2$P-O-PS$_2$Ar]$^{2-}$, [ArPS$_3$]$^{2-}$, [ArP(O^{t}Bu)S$_2$]$^-$ or [ArP(S^{t}Bu)S$_2$]$^-$ can be produced selectively by careful selection of the reaction conditions. This study pointed towards a more general approach, in which metal salts with oxygen-containing anions could be used for the similar ring-opening reactions. Hereby CuOAc, AgOAc, Fe(OAc)$_2$ and [Ni(OAc)$_2$·4H$_2$O] are submitted into the reactions with Lawesson's reagent.

When CuOAc is reacted with Lawesson's reagent (and PPh$_3$) in DME or toluene at elevated temperatures (reflux 4h), [Cu$_2$(Ar(μ_2-S)$_2$P-O-P(μ_2-S)$_2$Ar)(PPh$_3$)$_4$] (**2**) (Scheme 3.2) is formed in yields of 68% together with acetic anhydride (δ_C 167, 22 ppm, lit.,[129] 166, 21 ppm). At room temperature, however, [Cu$_{14}$(μ_6-ArP(O)S$_2$)$_6$(μ_3-ArP(O)(OAc)S)$_2$(PPh$_3$)$_6$] (**11**) was isolated in good yield (Scheme 3.7).

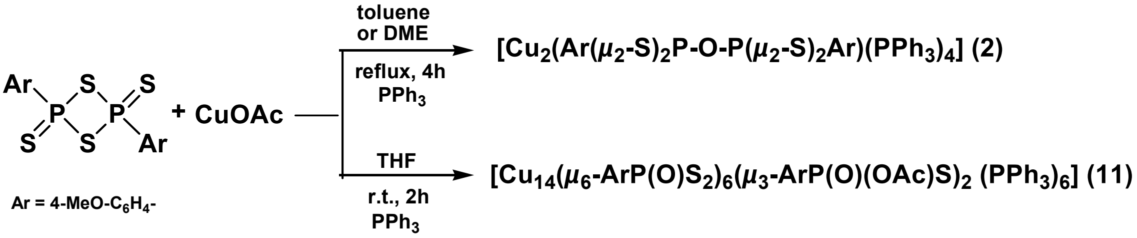

Scheme 3.7 Reactions of CuOAc and Lawesson's reagent

Although NMR investigations of **11** were precluded by its poor solubility, the compound could be unequivocally characterized by IR spectroscopy in combination with x-ray analysis and elemental analysis. The formation of **11** could be rationalized by the nucleophilic addition of four equivalents of CuOAc to Lawesson's reagent, followed by the elimination of acetic anhydride (verified by ^{13}C NMR of the mother liquor) and copper(I) thioacetate [Cu(I)SOCCH$_3$] (Scheme 3.8). The latter elimination product, however, is formed in low yield and it was impossible to obtain direct

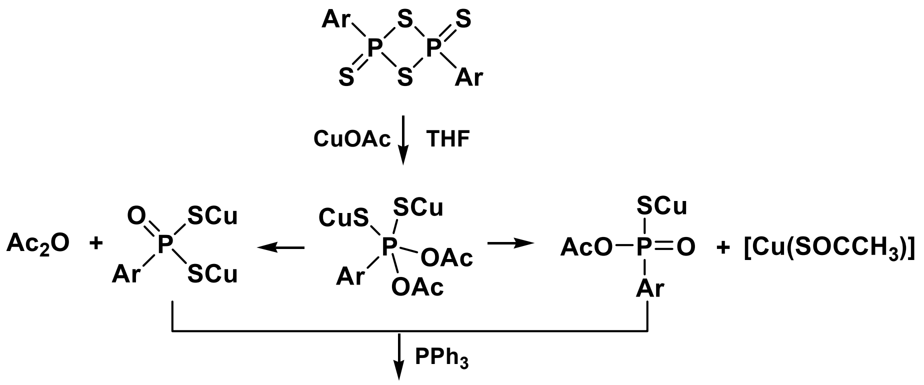

[Cu_{14}(μ_6-ArP(O)S_2)$_6$(μ_3-ArP(O)(OAc)S)$_2$ (PPh_3)$_6$] (11)

Scheme 3.8 Possible mechanism for the reactions of CuOAc and Lawesson's reagent

evidence for its formation by IR or NMR studies. In the solid state **11** consists of a crystallographically-centrosymmetric arrangement of fourteen Cu^+ ions, six $[ArP(O)S_2]^{2-}$, two $[ArP(O)(OAc)S]^-$ anions and six PPh_3 ligands (Figure 3.10, Table 3.9).

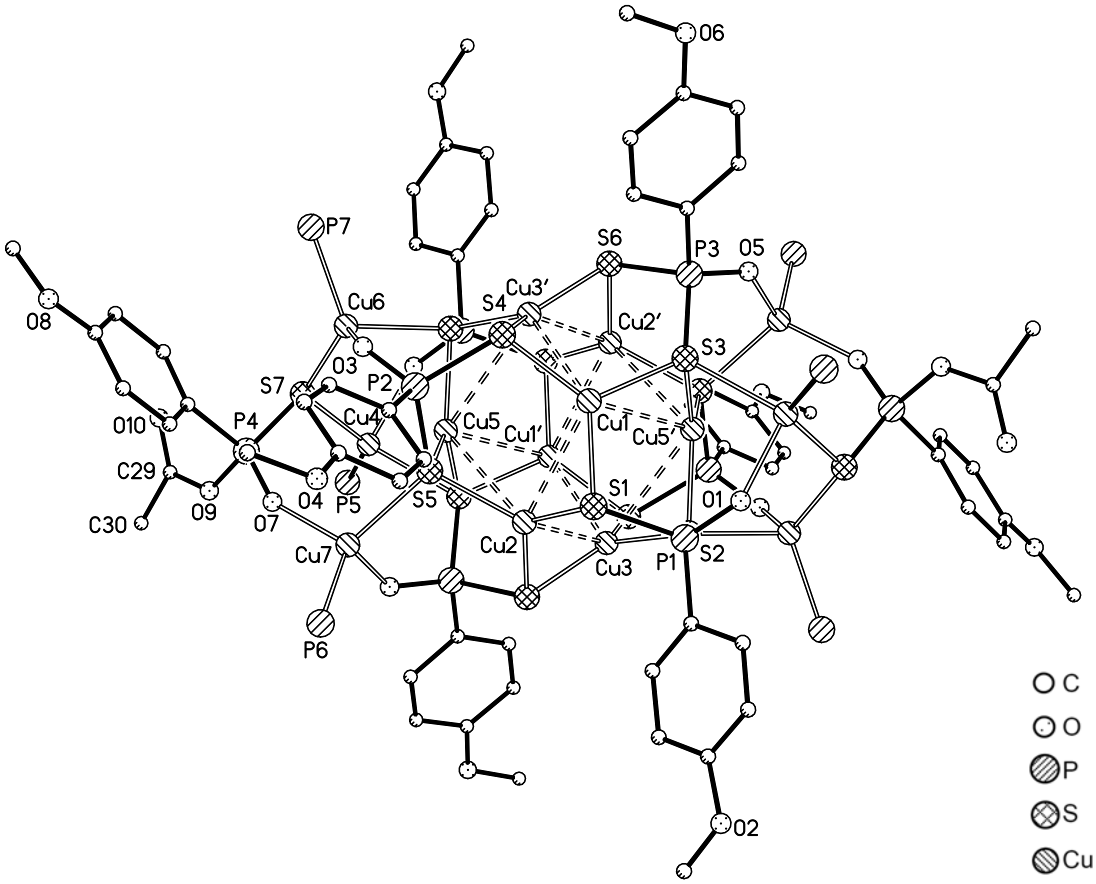

Figure 3.10 Structure of [Cu_{14}(μ_6-ArP(O)S_2)$_6$(μ_3-ArP(O)(OAc)S)$_2$(PPh_3)$_6$] (**11**)

Table 3.9 Selected ranges of bond lengths (Å) and angles (°)

Bond lengths					
Cu-O	2.020(6)-2.153(5)	Cu-P	2.218(2)-2.229(2)	Cu-S	2.2287(18)-2.4144(18)
P-O	1.497(5)-1.505(5)	P4-O9	1.642(8)	P-S	2.076(2)-2.090(2)
P4-S7	1.982(3)				
Angles					
S-Cu-S[a]	110.55(7)-128.56(7)	S-Cu-S[b]	100.04(8)-132.05(7)	O-Cu-P	97.88(15)-113.3(2)
O-Cu-S	95.29(16)-123.26(16)	P-Cu-S	104.28(8)-126.00(9)	O7-P4-O9	102.3(5)
O7-P4-S7	120.1(3)	O9-P4-S7	107.7(3)		

[a] Cu coordination number three; [b] Cu coordination number four.

Above the six faces of the central distorted cubic arrangement (indicated by open dashed connections between Cu atoms in Figure 3.10) six $[ArP(O)S_2]^{2-}$ anions are located. The S atoms of each $[ArP(O)S_2]^{2-}$ ligand coordinate four Cu atoms of one of the cubic faces in μ_2-mode. One of the S atoms is coordinated to an additional Cu atom (located to the right and left of the central cubic $[Cu_8]$ arrangement). In figure 3.10 the coordination of the $[ArP(O)S_2]^{2-}$ anions can best be rationalised by looking at P(2) or P(3). In the periphery of **11**, two $[ArP(O)(OAc)S]^-$ anions are coordinated to three Cu atoms. In contrast to the inner eight three-coordinate Cu atoms the outer Cu atoms Cu(4,6,7) and symmetry equivalents are tetrahedrally surrounded by O and S atoms and additional PPh_3 ligands. Bond lengths and angles found in **11** are not unusual and can be compared with those reported for other metal complexes containing P/S ligands.[8-12] A remarkable feature of **11**, however, is the formation of the $[ArP(O)(OAc)S]^-$ anion. It is the first time that such a substitution pattern is observed for P atoms in an anionic fragment. The long P(4)-O(9) distance of 1.642(8) Å is typical for P-O(carboxylate) bonds [lit.,[130,131] 1.643(5) and 1.662(7) Å] and indicates the lability of this bond. Other P-O distances in **11** are considerably shorter (*ca.* 1.5 Å).

These investigations prompted the synthesis of larger cluster complexes with P/S ligands, so for this purpose the reaction of AgOAc and L.R. was investigated. Initially, a grey precipitate is formed when the reaction is performed in THF. The infra-red spectrum of this insoluble precipitate showed the presence of a carboxylate band at 1777 cm^{-1} and P-S vibrations at *ca.* 530 cm^{-1}. Mass spectrometric investigations (FAB) of the precipitate failed but elemental analysis points towards the composition $[ArP(SAg)_2(OAc)_2]$. The solid residue dissolved upon addition of the tertiary phosphine dppm. Slow diffusion of chilled (0°C) diethyl ether into the filtered reaction mixture within a double Schlenck tube produced crystals of $[Ag_4\{\mu_4\text{-}ArP(O)S_2\}_2(dppm)_4]$ (**12**)

(Ar = 4-anisyl) (Scheme 3.9).

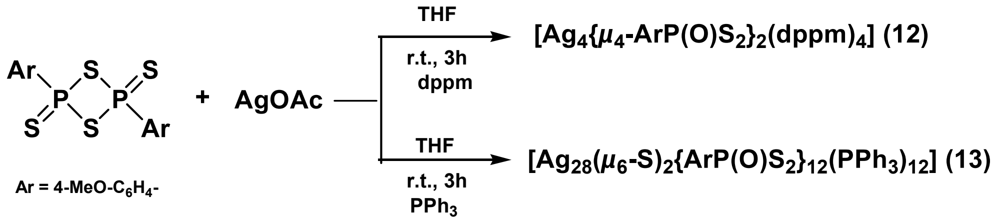

Scheme 3.9 Reactions of AgOAc and Lawesson's reagent

In the solid state **12** exists as a dimer of $[Ag_2\{ArP(O)S_2\}(dppm)_2]$ units (Figure 3.11, Table 3.10). Both $[ArP(O)S_2]^{2-}$ anions in **12** are coordinated to the four Ag atoms forming an adamantane-like core of P, S and Ag atoms in which the remaining coordination sites at Ag atoms are occupied by dppm ligands. Bond lengths and angles in **12** are similar to those observed in $[Ag_{12}(PhS_2P\text{-}PS_2Ph)_6(dppeS)_6]$ [dppeS = $Ph_2PCH_2CH_2P(S)Ph_2$].[132]

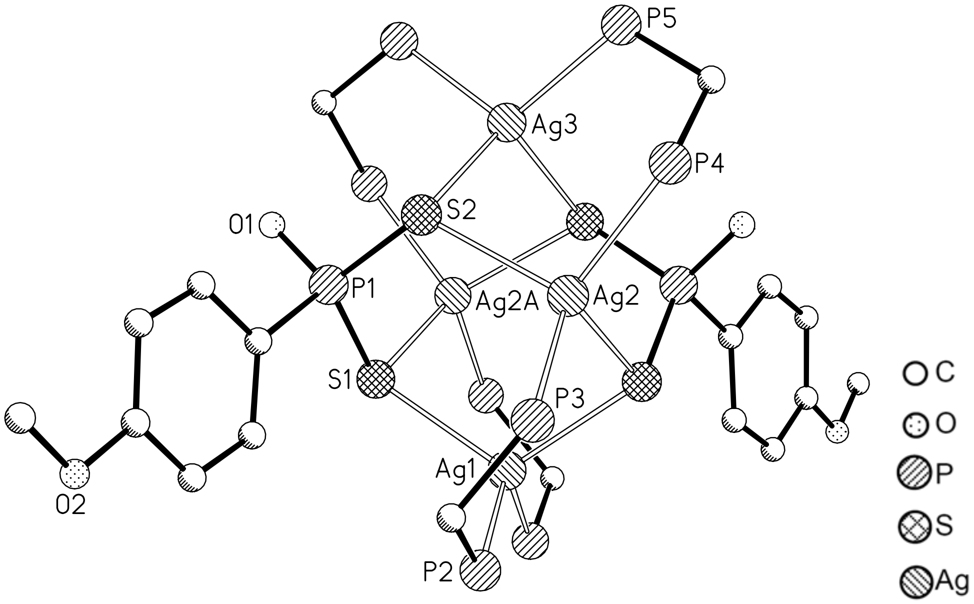

Figure 3.11 Structure of $[Ag_4\{\mu_4\text{-}ArP(O)S_2\}_2(dppm)_4]$ (**12**)
(Ph groups of dppm are omitted)

Table 3.10 Selected ranges of bond lengths (Å) and angles (°)

Bond lengths					
Ag-S	2.5603(7)-2.5889(6)	Ag-P	2.5102(7)-2.5499(7)	P1-S1	2.0533(9)
P1-S2	2.0521(9)	P1-O1	1.5038(18)		
angles					
S2-P1-S1	116.00(4)	S-Ag-S	109.65(3)-114.58(2)	S-Ag-P	102.20(2)-111.55(2)
P-Ag-P	113.01(4)-118.23(3)				

In a separate attempt PPh_3 was used to dissolve the precipitate obtained from the reaction of L.R. and AgOAc. X-ray analysis of the orange product of this reaction gave to our surprise $[Ag_{28}(\mu_6\text{-}S)_2\{ArP(O)S_2\}_{12}(PPh_3)_{12}]$ (**13**), the largest cluster so far containing $[ArP(O)S_2]^{2-}$ ligands (Scheme 2.2.9). The key structural features of **13** are the two central μ_6-S atoms (Ag-S(1) distances 2.4729(17)-2.764(3) Å) coordinating the 10 inner Ag atoms. This arrangement is surrounded by an outer layer of 12 $[ArP(O)S_2]^{2-}$ ligands and the remaining 18 Ag atoms. A closer look at the structure of **13** (Figure 3.12, Table 3.11) reveals a variety of coordination modes of $[ArP(O)S_2]^{2-}$

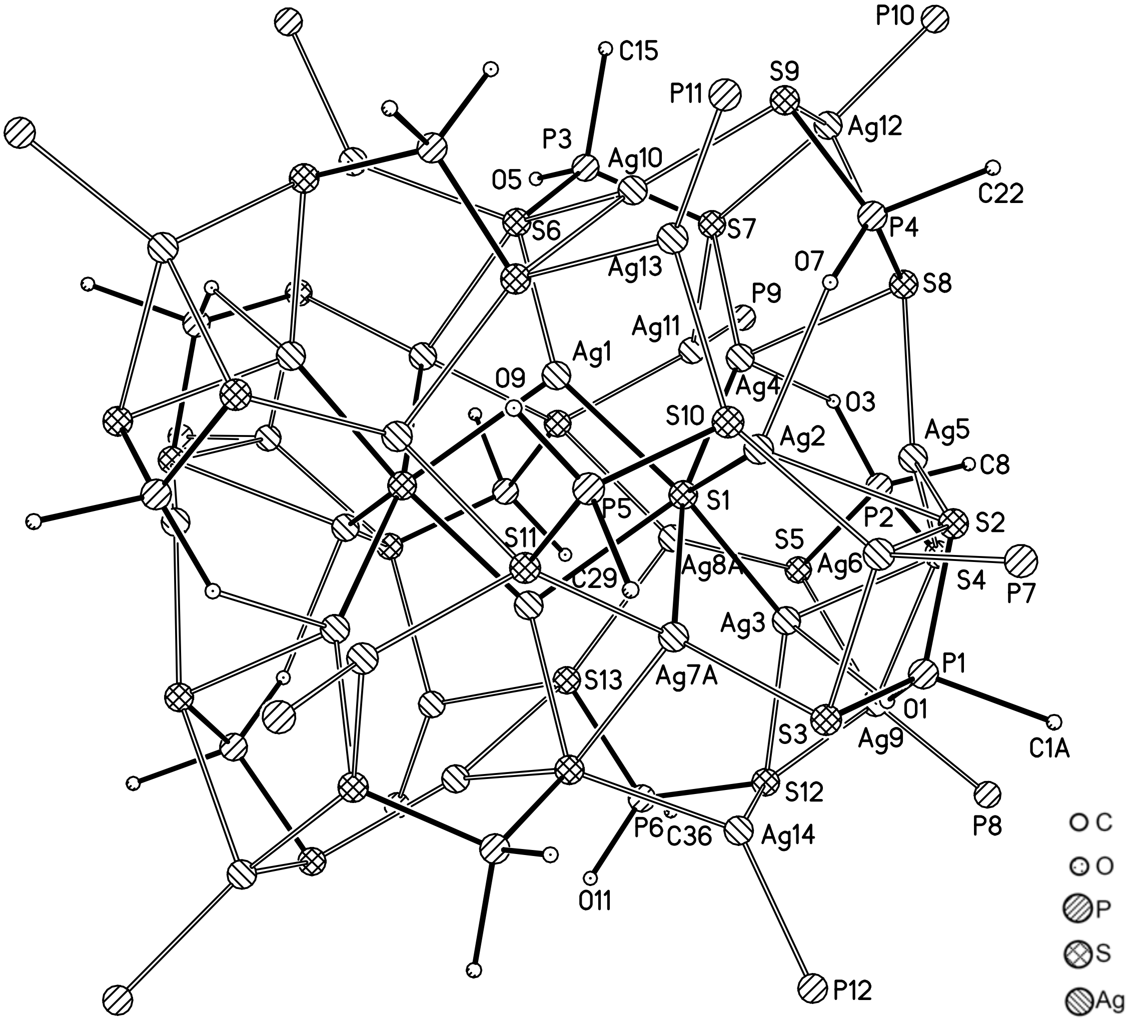

Figure 3.12 Structure of $[Ag_{28}(\mu_6\text{-}S)_2\{ArP(O)S_2\}_{12}(PPh_3)_{12}]$ (**13**) (disordered components and phenyl groups are omitted)

Table 3.11 Selected ranges of bond lengths (Å)

Ag-S	2.212(3)-2.925(2)	Ag-P	2.4077(19)-2.4153(16)	Ag-O	2.426(5)-2.503(4)
P-S	2.037(3)-2.087(2)	P-O	1.489(4)-1.506(4)	Ag··Ag	2.7632(3)-3.3670(18)

ligands, which coordinate Ag^+ ions *via* S- and O-donor centers or just *via* S atoms. Whilst tripodal $[ArP(O)S_2]^{2-}$ ligands tend to form cage complexes with metal ions such as **12**, sulfido ligands tend to form large three-dimensional arrangements with Ag^+ ions (*e.g.*, $[Ag_{344}S_{124}(S^tBu)_{96}]$ [133]). The longest nonbonding distances between symmetry-related Ag atoms in the core of **13** are 1.3 nm. The composition and molecular architecture of **13** reflect the features of both ligand types and also the phenomenon of disordered Ag positions characteristic for larger Ag-S clusters [Ag(1) is disordered over three positions with the occupancy Ag(1) : Ag(1A) : Ag(1B) of 60 : 20 : 20; the inversion center in **13** generates the other three Ag atoms] (Figure 3.13). This illustrates the difficulties involved in the structure determination of larger Ag-S clusters, where Ag-S cores are sometimes treated as ionic liquids and average compositions have to be estimated on the basis of atomic volumes and charge-balance.[133] The generation of both S^{2-} and $[ArP(O)S_2]^{2-}$ ligands in the course of the reaction between AgOAc and L. R. is observed for the first time. The occurrence of two different anions could be explained by competing decomposition reactions of $[ArP(SAg)_2(OAc)_2]$ in the presence of tertiary phosphines (Scheme 3.10).

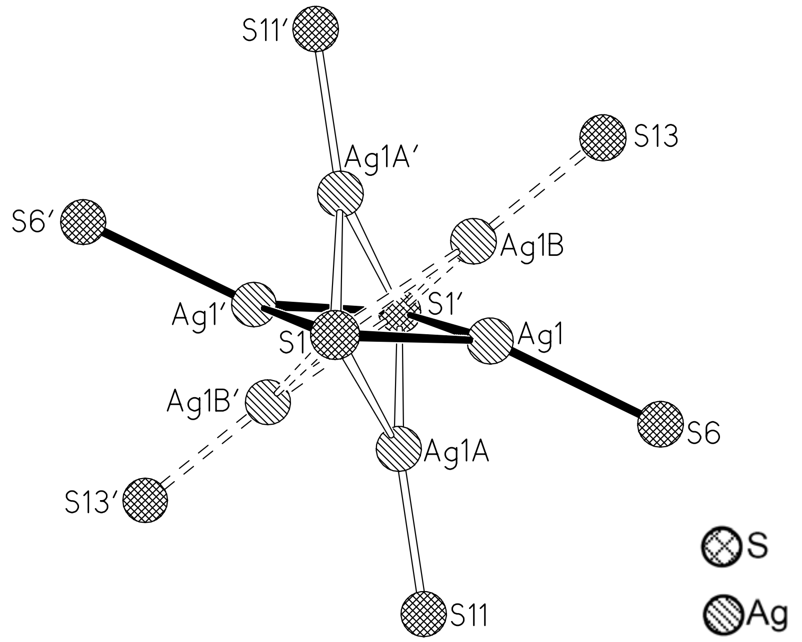

Figure 3.13 The threefold disorder of Ag1 and Ag1’ within the central eight S atoms

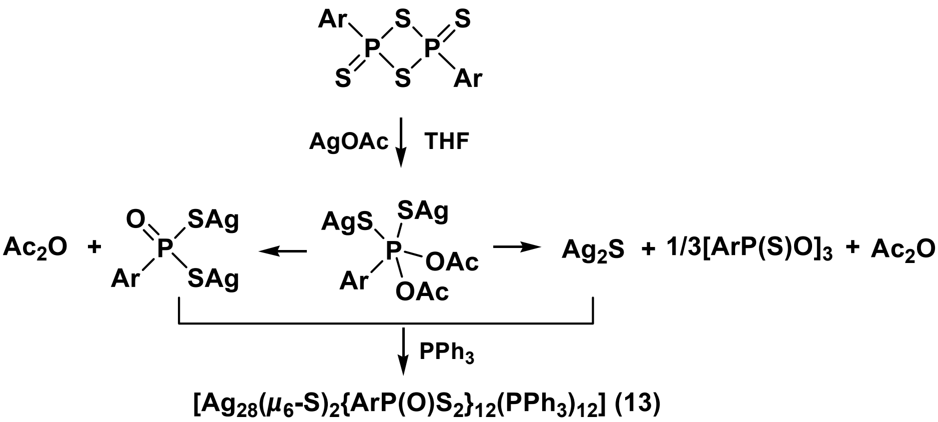

Scheme 3.10 Possible mechanism for the reactions of AgOAc and Lawesson's reagent

Further reactions with other transition-metal carboxylates and Lawesson's reagent were carried out in order to demonstrate the general applicability of this synthetic route for the synthesis of tripodal P/S ligands. In the case of $Fe(OAc)_2$ these efforts resulted in the formation of $[Fe_2(\mu\text{-}ArPS_3)(thf)_4]$ (**14**) (Scheme 3.11, Figure 3.14, Table 3.12).

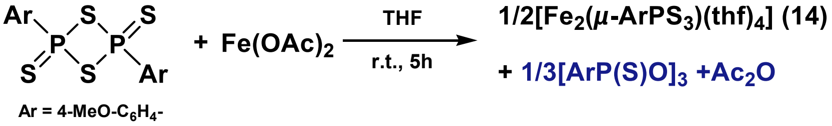

Scheme 3.11 Reaction of $Fe(OAc)_2$ and Lawesson's reagent

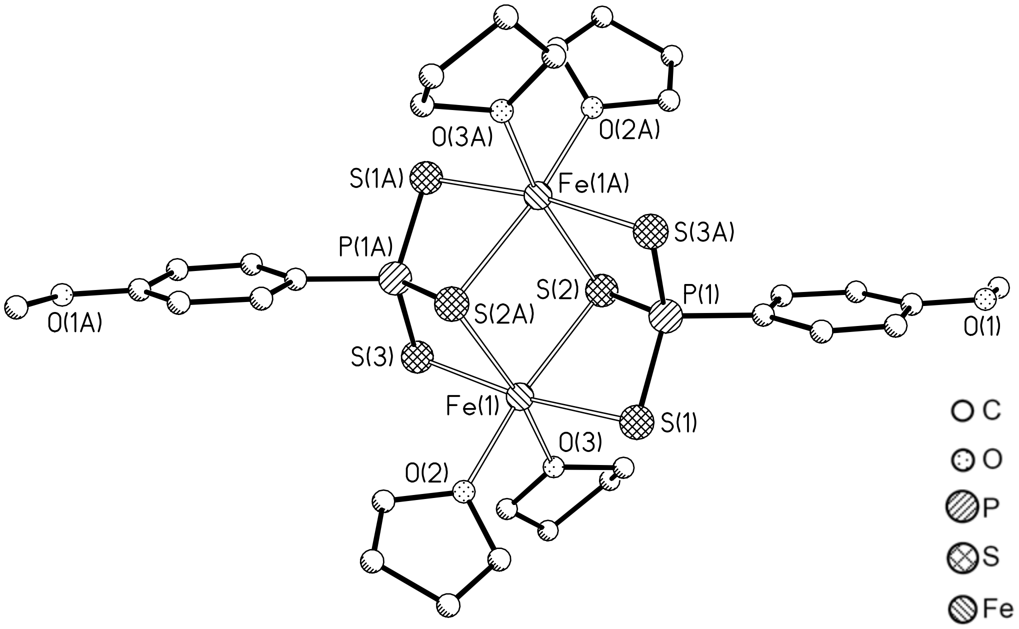

Figure 3.14 Structure of $[Fe_2(\mu\text{-}ArPS_3)(thf)_4]$ (**14**)

Table 3.12 Selected ranges of bond lengths (Å) and angles (°)

Bond lengths					
P1-S1	2.015(3)	P1-S3A	2.024(3)	P1-S2	2.047(3)
Fe1-O2	2.138(6)	Fe1-O3	2.145(7)	Fe1-S3	2.512(3)
Fe1-S1	2.524(3)	Fe1-S2	2.548(2)	Fe1-S2A	2.599(2)
angles					
O2-Fe1-O3	87.3(3)	O2-Fe1-S3	95.91(19)	O2-Fe1-S2A	91.1(2)
O2-Fe1-S2	170.23(19)	S3-Fe1-S1	172.75(10)	S3-Fe1-S2A	79.83(8)
S1-P1-S3A	115.65(13)	S1-P1-S2	107.03(14)	S3A-P1-S2	107.34(14)

In the solid state **14** exists as a centrosymmetric dimer. All the sulfur atoms are involved in metal bonding. The P-S bond to S(2) is slightly longer [P(1)-S(2) 2.047(3) Å] than P-S bonds to non-bridging S atoms [P(1)-S(1) 2.015(3), P(1)-S(3A) 2.024(3)]. The geometry at iron is distorted octahedral, with Fe-S bond lengths of 2.512(3)–2.599(2) Å and Fe-O bond distances to the *cis* THFs of 2.138(6) and 2.145(7) Å. The generation of the $[ArPS_3]^{2-}$ anion follows the reaction mechanism outlined for **4** with the only difference being the formation of the leaving group Ac_2O instead of $^tBu_2O$.

It was important to probe the sensitivity of the reactions to water by employing hydrated metal carboxylates as starting materials in ring-opening reactions of Lawesson's reagent. As a first result of these efforts $[Ni_2\{ArP(O)S_2\}_2(thf)_2(H_2O)_2]_2$ (**15**) was obtained using $[Ni(OAc)_2{\cdot}4H_2O]$ as starting material. Although crystals of **15** were generally twinned and of poor quality, it was possible to establish the basic connectivity by x-ray crystallographic analysis (Scheme 3.12, Figure 3.15, Table 3.13).

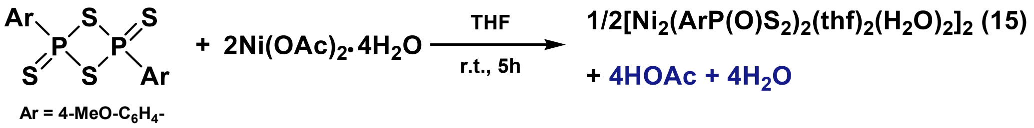

Scheme 3.12 Reaction of $Ni(OAc)_2{\cdot}4H_2O$ and Lawesson's reagent

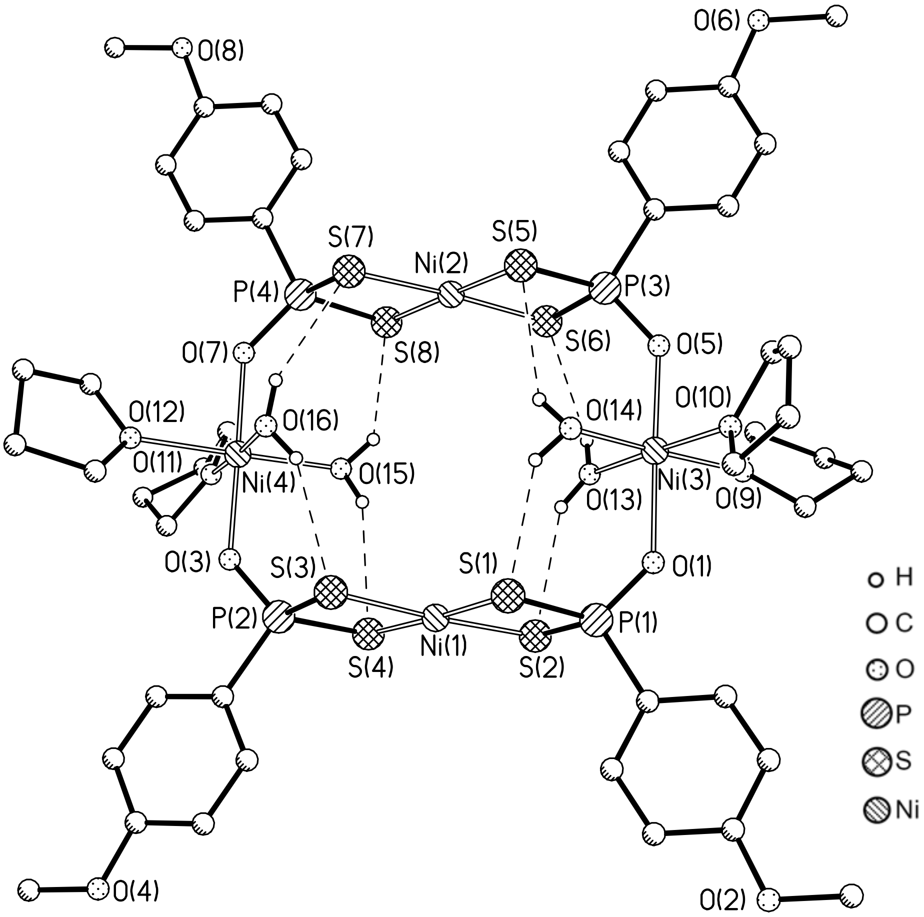

Figure 3.15 Structure of $[Ni_2\{ArP(O)S_2\}_2(thf)_2(H_2O)_2]_2$ (**15**)

Table 3.13 Selected ranges of bond lengths (Å) and angles (°)

Bond lengths					
Ni-S	2.213(5)-2.269(4)	Ni-O(ligand)	1.993(13)-2.086(14)	Ni-O(H_2O)	2.036(15)-2.103(12)
Ni-O(thf)	2.093(14)-2.115(12)	P-S	2.037(6)-2.096(6)	P-O	1.482(12)-1.556(12)
S· · ·H (H_2O ligands O13-O16)			ca.2.5		
angles					
S3-Ni1-S2	176.6(2)	S3-Ni1-S1	93.39(17)	S1-Ni1-S4	177.5(2)
S8-Ni2-S6	92.07(18)	S8-Ni2-S5	179.4(2)	S6-Ni2-S7	177.3(2)
O5-Ni3-O1	177.7(5)	O13-Ni3-O10	177.0(6)	O14-Ni3-O9	177.0(6)
O7-Ni4-O3	179.0(5)	O15-Ni4-O12	179.3(6)	O16-Ni4-O11	176.8(5)
O-P-S	114.0(5)-117.5(6)	S-P-S	96.7(3)-97.7(2)		

In the solid state **15** exists as a dimer of a square-planar and an octahedrally coordinated Ni^{2+} ion held together by two $[ArP(O)S_2]^-$ ions. Inside the cyclic arrangement four molecules of water are located, coordinating the octahedral Ni^{2+}-centers. Similar Ni-O(P) bond distances of *ca.* 2.0 Å to the ones found in **15** have been observed in related methyldiphosphonato and organophosphato Ni-complexes.

[134,135] Weak hydrogen bonds to all S atoms are observed with H···S distances of *ca.* 2.5 Å.[136] Remarkably, **15** is not sensitive to HOAc formed in the course of the reaction (δ_C 172, 20 ppm, lit.,[137] 175, 20 ppm) and water. This complex represents the first example of a mixed high-spin/low-spin d^8-Ni^{2+} complex stabilised by a tripodal P/S ligand. The formation of such a high-spin/ low-spin complex has been favored by the hybrid nature of the ligand, with both hard and soft functionalities. Similar arrangements of tetranuclear square-planar/octahedral Ni^{2+} complexes have so far only proved accessible by ligand design involving multiple reaction steps. [138-140]

As that is mentioned before, initially sodium phosphonodithioate alkali metal salts are formed *in situ* and subsequently reacted with transition metal salts. The generated $[RP(OR')S_2]^-$ ligands are bidentate and chelate metal atoms *via* S atoms to yield complexes of the type ML_2 (L = $[(4\text{-MeO})C_6H_4\{OR\}PS_2]$). [15,89] And little is known about thermal properties of metal phosphonodithioates. In a pilot study following up the previously described ether or acid anhydride elimination during the preparation of $[Cu_2(Ar(\mu_2\text{-}S)_2P\text{-}O\text{-}P(\mu_2\text{-}S)_2Ar)(PPh_3)_4]$ (**2**) (Scheme 3.2 and 3.7) a metathesis reaction with $CdCl_2$ was used to study the thermolysis of $[Cd_2\{ArP(O^tBu)(\mu\text{-}S)S\}_4]$ (**16**) (Scheme 3.13, Figure 3.16, Table 3.14).

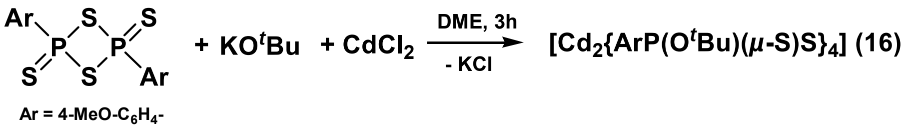

Scheme 3.13 Metathesis reaction with $CdCl_2$

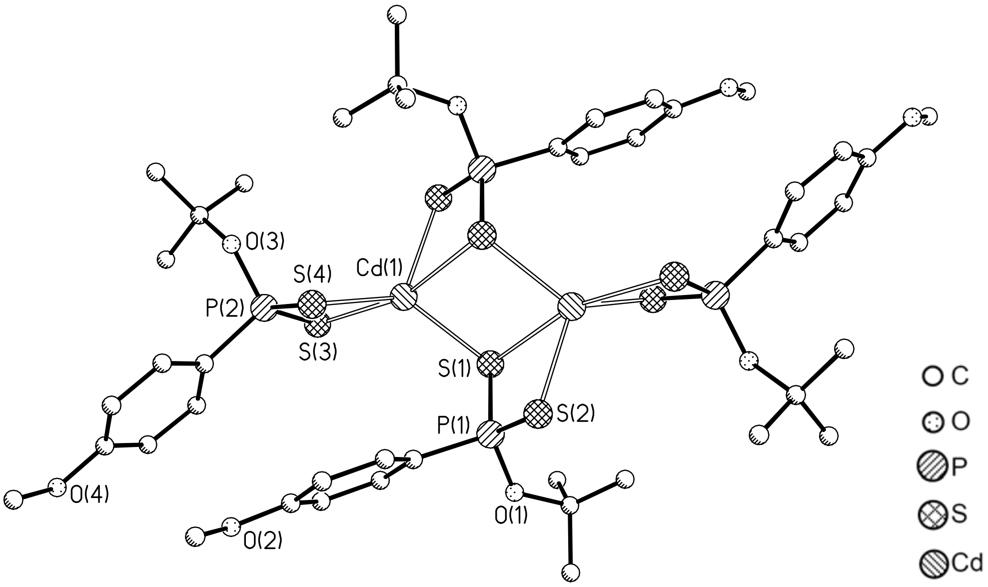

Figure 3.16 Structure of $[Cd_2\{ArP(O^tBu)(\mu\text{-}S)S\}_4]$ (**16**)

Table 3.14 Selected ranges of bond lengths (Å) and angles (°)

Bond lengths					
Cd-S	2.5160(7)-2.9877(7)	P1-O1	1.5804(19)	P2-O3	1.5860(19)
P-S	1.9973(9)-2.0424(8)				
angles					
S4-Cd1-S1	134.00(2)	S4-Cd1-S3	79.16(2)	S-Cd1-S3	106.97(2)
S2-P1-S1	111.75(4)	S3-P2-S4	111.38(4)		

In the solid state **16** exists as a centrosymmetric dimer, a structural motif commonly found in similar Cd complexes.[89,141] A differential thermal analysis of **16** showed that from 126°C on a weight loss of 18.2% occurs which is in fairly good agreement for the expected weight loss of 19.6% for **16**-2^{t}Bu$_2$O (Figure 3.17). Similar observations were made for **6-9** but investigations of their thermal behavior and the characterization of thermolysis products are ongoing.

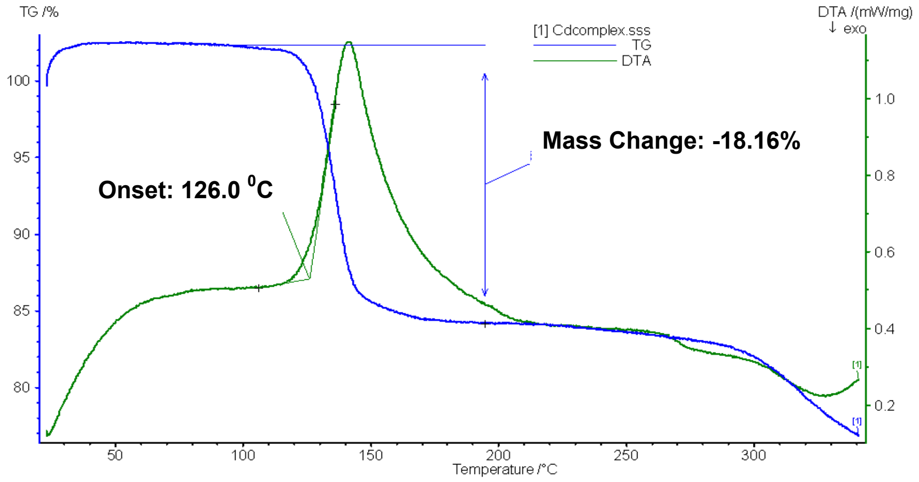

Figure 3.17 DTA of [Cd$_2${ArP(O^{t}Bu)(μ-S)S}$_4$] (**16**)

Since [ArP(O^{t}Bu)S$_2$]$^-$ can be obtained in the metathesis reaction by using alkoxide, would [ArP(S^{t}Bu)S$_2$]$^-$ be synthesized if thiolates are used? In the metathesis reaction of L.R., NaS^{t}Bu and FeCl$_2$, [Fe$_2$(μ-ArPS$_3$)(thf)$_4$] (**17**), the same molecule but in a different crystal space group to compound **14**, was prepared (Scheme 3.14).

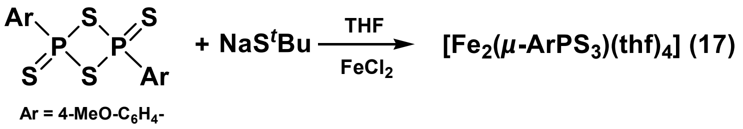

Scheme 3.14 Metathesis reaction with FeCl$_2$

To probe the sensitivity of the reactions to water, metathesis reactions with hydrated Ni(II) salts were subsequently used for controlled hydrolysis of P-chalcogenido anions. The results of these efforts are summarized in scheme 3.15.

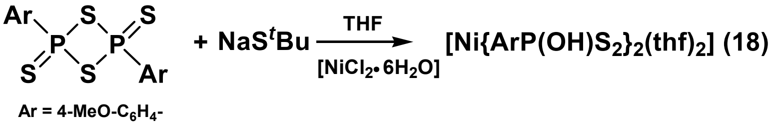

Scheme 3.15 Metathesis reaction with $NiCl_2·6H_2O$

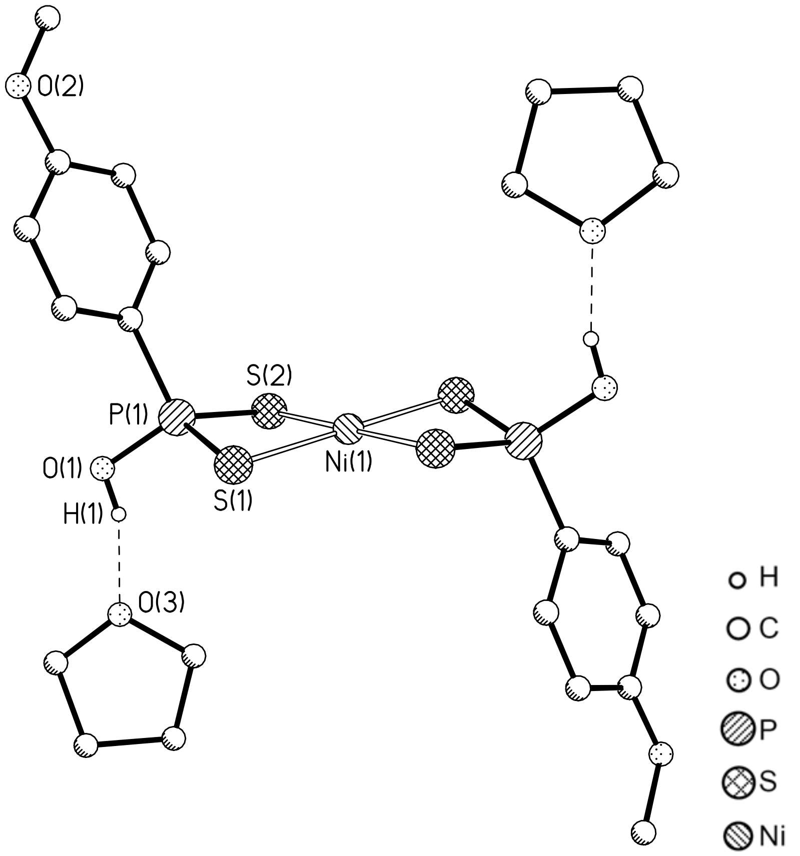

Figure 3.18 Structure of [Ni{ArP(OH)S_2}$_2$(thf)$_2$] (**18**)

Table 3.15 Selected ranges of bond lengths (Å) and angles (°)

Bond lengths					
Ni1-S1	2.2301(8)	Ni1-S2	2.2273(7)	P1-O1	1.569(2)
P1-C1	1.789(3)	P1-S1	2.0099(10)	P1-S2	2.0039(10)
O1· ·O3	2.514(3)				
angles					
S-Ni1-S	87.94(3), 92.06(3)			O1-P1-S2	116.39(10)
C1-P1-S2	112.32(10)	O1-P1-S1	113.07(9)	C1-P1-S1	113.15(10)
S2-P1-S1	100.89(4)				

In the solid state **18** consists of a [Ni{ArP(OH)S$_2$}$_2$] structural motif which has been observed earlier.[11] In **18** THF is strongly hydrogen-bonded to hydroxy groups of the central [Ni{ArP(OH)S$_2$}$_2$] moiety forming an overall monometallic entity (Figure 2.2.18, Table 2.2.15). In d$_6$-DMSO solutions, evidence for the P-OH fragment was found in the ^{1}H NMR spectrum at δ 3.81 indicating that H-bonds are cleaved. In the solid state the P-O bond distance found in the [ArP(OH)S$_2$]$^-$ anion in **18** [P-O 1.569(2) Å] is slightly longer than P-O distances found in the related anion [ArP(O)S$_2$]$^{2-}$ [P-O 1.497(5)-1.505(5) Å] before. **18** could be used in future as a building block for supramolecular assembly reactions but at this stage it serves as an example to illustrate how easy P/S precursors like L.R. can be converted when reacted with an alkali metal salt and, in a second reaction step, with a hydrated transition metal salt (here [NiCl$_2$·6H$_2$O]).

The results presented here show that, in the reactions of L.R. with metal alkoxides or carboxylates and also in the metathesis reactions, metal complexes containing the anionic ligands [ArS$_2$P-O-PS$_2$Ar]$^{2-}$, [ArPS$_3$]$^{2-}$, [ArP(O^{t}Bu)S$_2$]$^-$, [ArP(S^{t}Bu)S$_2$]$^-$ or [ArP(OH)S$_2$]$^-$ can be produced selectively. Besides studying the coordination chemistry of P/S-containing anions, the chemistry of complexes containing P-Se functional groups is also studied intensively.[15,109,110,142-151] In order to further develop this area, the availability of P-Se-containing starting materials is a key issue. For the synthesis of Woollins' reagent (W.R.) [PhP(Se)(μ-Se)]$_2$ (which is commercially available), (PhP)$_5$ was prepared and subsequently reacted with elemental selenium.[101,103] Similarly to the fragmentation of L.R. in reactions with metal alkoxides or carboxylates, a new approach to the coordination chemistry of P-Se based ligands is described here.

First, alkali metal alkoxides and thiolates are employed in the reaction with W.R.. By reacting KO^{t}Bu with W.R. in THF, single crystals of potassium phosphonodiselenolate 1/∞[K$_2${PhP(O^{t}Bu)Se$_2$}$_2$(thf)]$_\infty$ (**19**) were obtained by diffusion of hexane into the reaction mixture (Scheme 3.16).

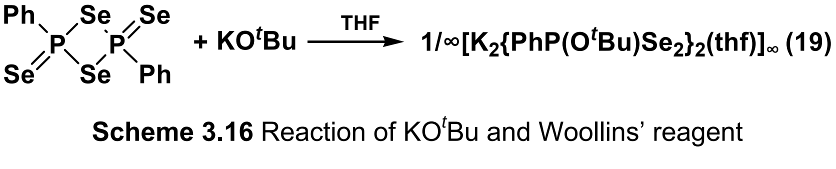

Scheme 3.16 Reaction of KO^{t}Bu and Woollins' reagent

In the solid state, **19** consists of a polymeric arrangement, for which the asymmetric unit contains two independent [PhP(O^{t}Bu)Se_2]$^{2-}$ anions held together by two K^+ ions. A closer look at the structure reveals that [PhP(O^{t}Bu)Se_2]$^{2-}$ anions bridge the K^+ cations in different modes (Figure 3.19, Table 3.16). A [PhP(O^{t}Bu)(μ_2-Se)$_2$]$^{2-}$ anion (containing P(1)) bridges K(1) and K(2) through Se-donor centers. The O^{t}Bu group of this anion is not involved in metal coordination. In contrast, in the [PhP(μ_4-O^{t}Bu)(μ_4-Se)(μ_2-Se)]$^{2-}$ anion (containing P(2)), both O- and Se-donor centers are involved in metal coordination. K-Se distances in **19** span a broad range of 3.2847(19)–3.8982(18) Å and indicate that the highly ordered arrangement in **19** is held together by electrostatic interactions of various strengths. Similar coordination has not yet been observed for [PhP(OR)Se_2]$^-$ ligands (R = Et, ^{i}Pr), which commonly

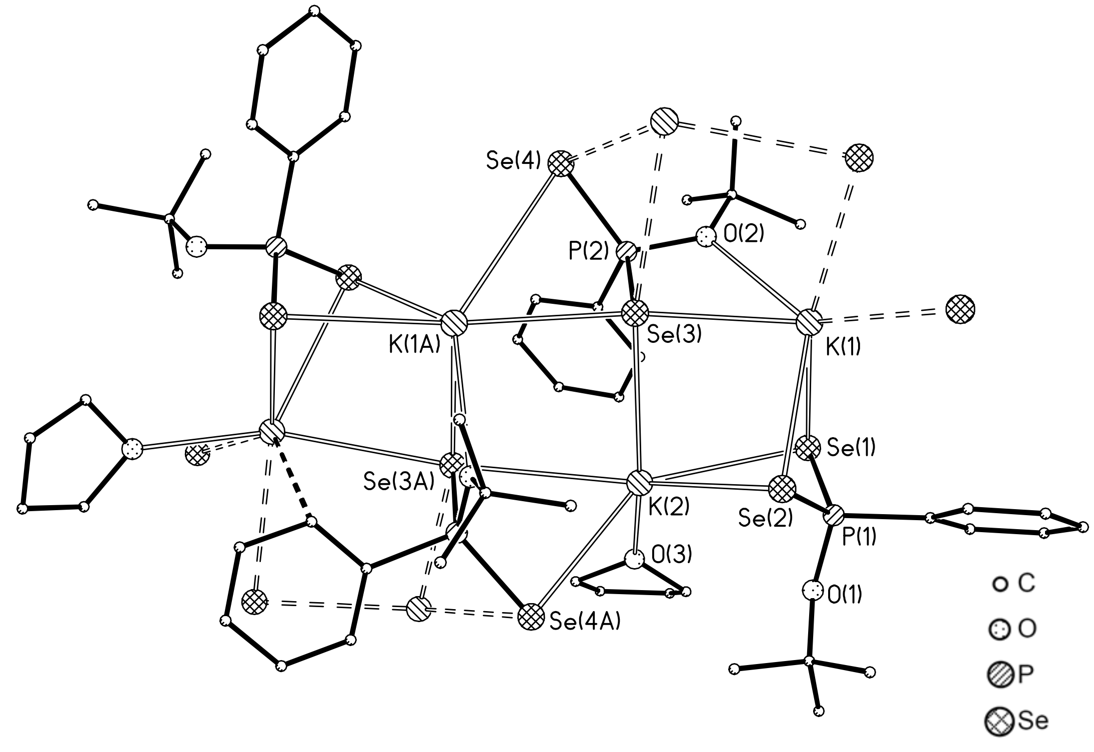

Figure 3.19 Structure of 1/∞[K_2{PhP(O^{t}Bu)Se_2}$_2$(thf)]$_\infty$ (**19**)

Table 3.16 Selected ranges of bond lengths (Å) and angles (°)

Bond lengths					
Se-P	2.1240(18)-2.1565(16)	K-Se	3.2847(19)-3.8982(18)	P1-O1	1.601(4)
P2-O2	1.616(4)	K1-O2	3.074(5)	K2-O3	2.764(7)
K2···C16	3.235(7)				
angles					
K1-Se3-K1A	167.48(4)	Se2-K2-Se3A	147.47(5)		

are bidentate and chelate metal atoms through chalcogen atoms, while the introduced alkoxide group is not involved in metal coordination.[15] In **19**, K(1) and K(2) are six-coordinated by five Se atoms and an oxygen atom belonging to a $[PhP(O^tBu)Se_2]^{2-}$ anion [K(1)] or the auxiliary ligand THF [K(2)]. Another difference in the coordination environments of the potassium ions is the close contact between K(2) and C(16). Similar contacts are not observed for K(1).

When NaS^tBu is reacted with W.R., $1/\infty[PhPSe_3Na_2(thf)_3]_\infty$ (**20**) is obtained in moderate yield as colourless crystals together with $PhPSe(S^tBu)_2$ (Scheme 3.17). The asymmetric cleavage of W.R. by NaS^tBu and the formation of $PhPSe(S^tBu)_2$ was observed by GC-MS and NMR of the mother liquor ($PhP(S^tBu)_2$ *m/z* 286, loss of Se because of high injection temperatures, $\delta_{Se} = -51$ ppm, $^1J_{P\text{-}Se} = 801$ Hz). Unusually, however, is the structure of **20** in the solid state (Figure 3.20).

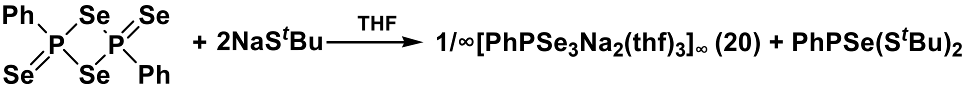

Scheme 3.17 Reaction of NaS^tBu and Woollins' reagent

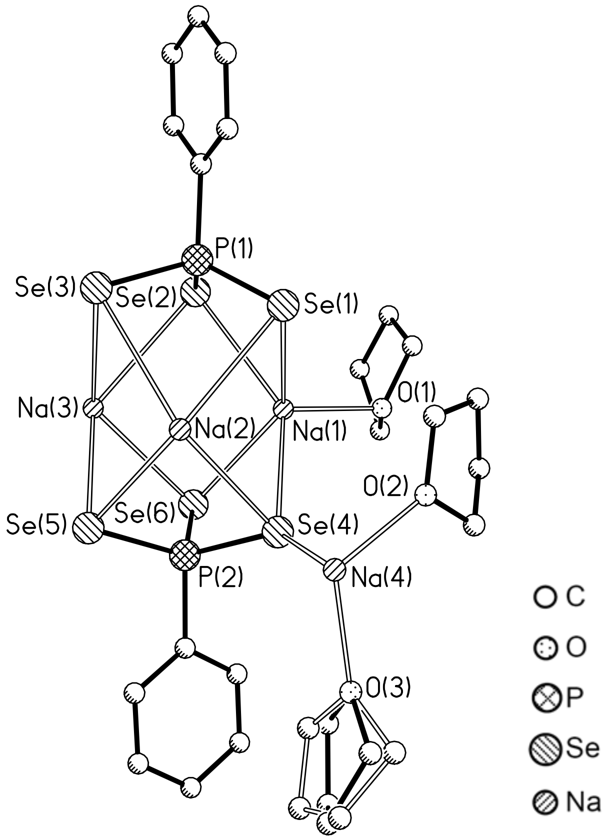

Figure 3.20a The asymmetric unit in **20**, thf at O3 is disordered over two sites.

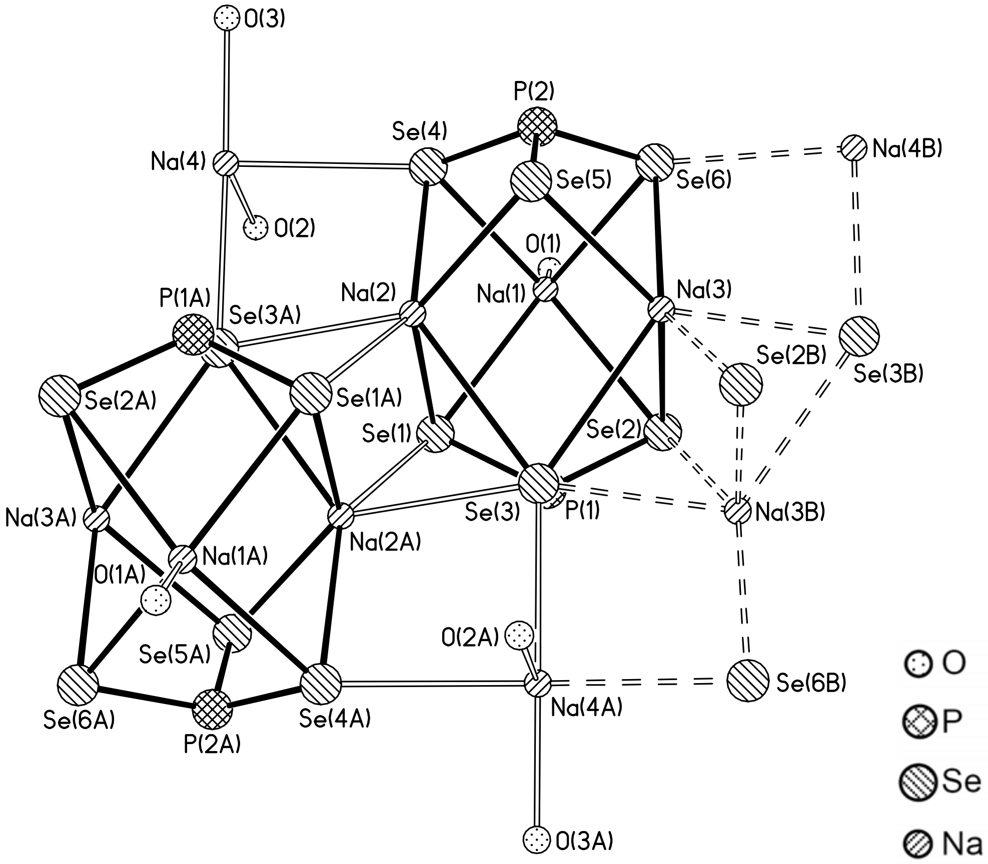

Figure 3.20b 1-D polymeric structure of **20**, C and H are omitted.

In figure 3.20a, the building block for polymeric **20** is displayed. It consists of two $[PhPSe_3]^{2-}$ anions, forming a cage arrangement with the sodium ions bridging the tripodal ligands. Na(4) is not accommodated within the cage and is coordinated by Se(4) and two thf molecules. The consequence of this arrangement is that 'outer-cage' Na^+-ions act as templates for the arrangement of cages in the extended solid-state structure of **20** (Figure 3.20b). Na(4) is surrounded by three Se atoms of two different cages and two thf ligands in a distorted square-pyramidal coordination geometry. In addition to Na(4), cage units are held together by coordination of Na(2), Se(1) and Se(3) to symmetry related atoms of a neighboring cage, resulting in a 1-D polymeric arrangement of the asymmetric unit $[Na_2(thf)_3Se_3PPh]$ found in **20**. This result is to the best of our knowledge the first example, in which tripodal cage complex units are connected by alkali-metal ions to a one dimensional polymer. In the solid state **20** is composed of an inner sodium-triseleno- phosphonate polymer stabilized by an organic layer consisting of phenyl groups and coordinated thf solvent. In a d_8-thf solution of crystals of **20**, two resonances in the ^{31}P NMR and ^{77}Se satellites indicate that the cage structure of **20** with two different environments for P atoms in $[PhPSe_3]^{2-}$ anions is retained. It is noteworthy in this context that a general feature of $[PhPSe_3]^{2-}$

ligands is the fact that due to the low abundance of the ^{77}Se isotope (I = 1/2, 7.63%), the isotopomeric anion observed in prolonged NMR experiments is of the type $[PhPSe_2(^{77}Se)]^{2-}$.

Now, the aim was to synthesize a series of alkali-metal complexes analogous to **20** using Li, K and Rb cations and thereby study the influence of the cation size on the dimensionality of the resulting alkali metal triselenophosphonate polymers. Whilst reactions of W.R. with LiS^tBu so far did not yield any product that could be fully characterized, a reaction with KS^tBu, followed by solvent diffusion of hexane into the reaction mixture, afforded yellow crystals of $1/\infty[(PhPSe_2Se\text{-}SeSe_2PPh)K_2(thf)_4]_\infty$ (**21**) (Scheme 3.18). In the solid state **21** consists of the new dianion $[PhPSe_2Se\text{-}SeSe_2PPh]^{2-}$, which is coordinated to two K^+ ions (Figure 3.21 top). The thf completes the coordination sphere of the potassium ions. The extended solid-state structure of **21** can be described as a ladder of two dimerized KSe-strands (indicated by bonds shown as solid lines; Figure 3.21 bottom, Table 3.17). Inner-strand K-Se distances are slightly shorter than K-Se distances between strands and anions are located on both sides of the ladder arrangement in an alternating fashion. This ligand orientation results in a corrugated K-Se ladder in the one dimensional polymer **21**. In addition to x-ray crystallographic characterization of **21** investigations of the reaction mechanism likely to be involved in the formation of **21** included a ^{31}P NMR study and GC-MS of the mother liquor. Both $PhP(Se)(S^tBu)_2$ and $PhP(S^tBu)_2$ were identified as soluble by-products and their identity checked by separate targeted synthesis (Scheme 3.18). The solid residue of the reaction consists of **21** and a colourless precipitate of possibly amorphous potassium selenides, K_2Se and/or K_2Se_2, which immediately turns red upon exposure to air. Based on these results it is assumed that reactions of W.R. with heavier alkali-metal thiolates initially led to the formation of $[PhPSe_3]^{2-}$ anions,

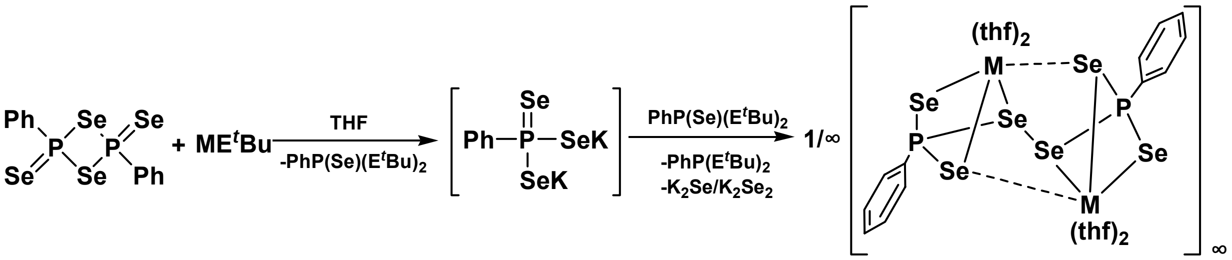

M = K, E = S, $1/\infty[(PhPSe_2Se\text{-}SeSe_2PPh)K_2(thf)_4]_\infty$ (21)
M = Rb, E = O, $1/\infty[(PhPSe_2Se\text{-}SeSe_2PPh)Rb_2(thf)_4]_\infty$ (22)

Scheme 3.18 Reactions of KS^tBu or RbO^tBu and Woollins' reagent

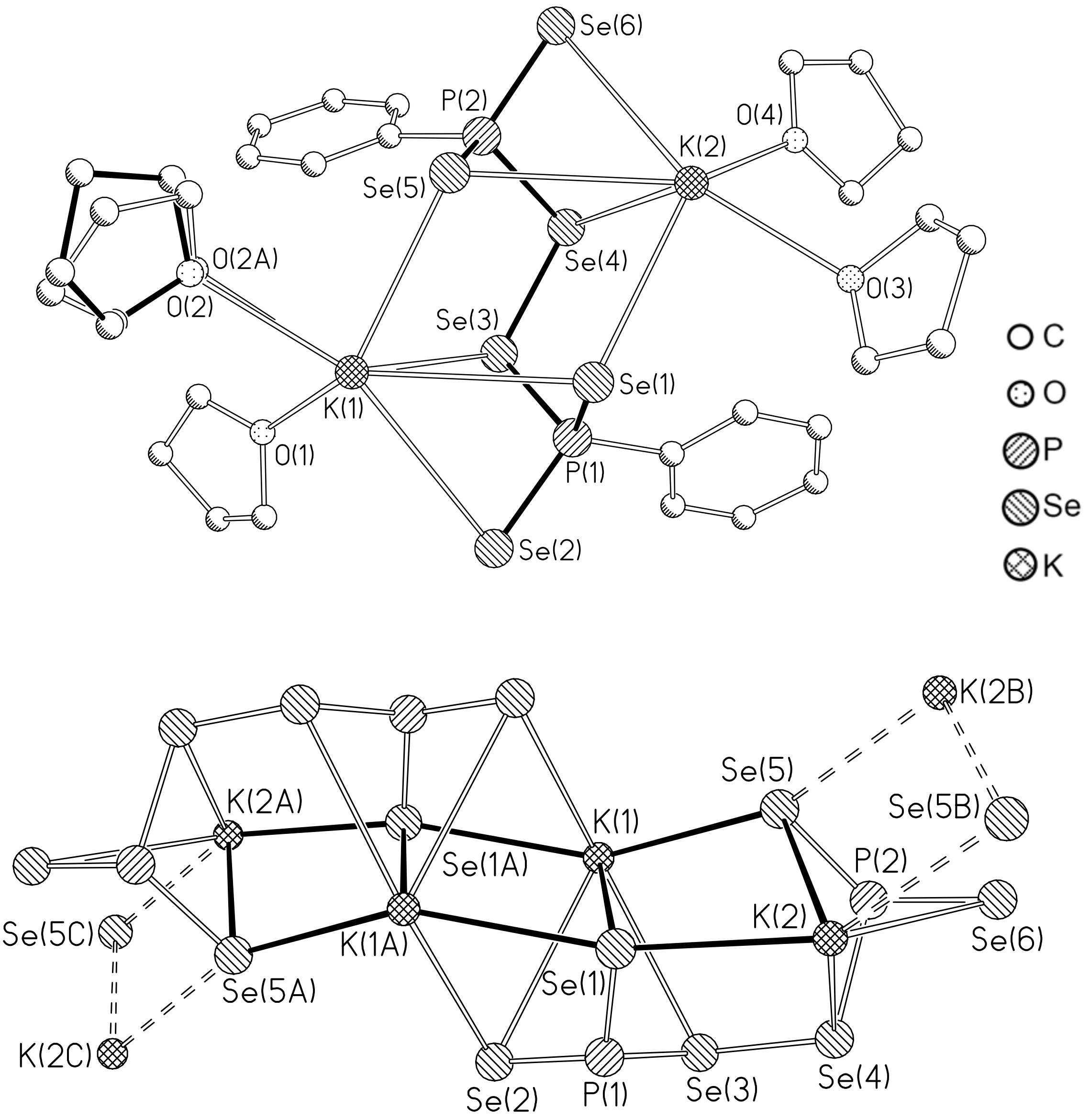

Figure 3.21 Top: the asymmetric unit in **21**, thf at O(2) is disordered over two sites.
Bottom: the polymeric arrangement of **21** (C and H atoms were omitted).

Table 3.17 Selected ranges of bond lengths (Å) and angles (°)

Bond lengths					
K1-Se1A	3.3051(16)	K1-Se5	3.3443(16)	K2-Se1	3.3403(16)
K2-Se5B	3.3074(16)	other K-Se distances are longer			3.4365(18)-3.8402(18)
P1-Se1,2	2.1233(19) and 2.1283(18)			P1-Se3	2.285(2)
P2-Se5,6	2.1192(19) and 2.1283(18)			P2-Se4	2.2889(18)
Se3-Se4	2.3364(10)	K-O	2.716(6)-2.834(16)		
Angles					
Se1A-K1-Se5	148.14(6)	K1A-Se1-K2	160.47(5)	Se5B-K2-Se1	148.98(6)
K2B-Se5-K1	161.00(4)				

which are then oxidized by $PhPSe(S^tBu)_2$ in the presence of potassium ions. The different outcome of the reactions leading to the formation of **20** and **21** is possibly caused by increased Se-metal distances (Na-Se: 2.929(2)-3.227(2) Å, K-Se 3.3051(16)-3.8402(18) Å) for the larger cations, which apparently do not form cage architectures such as **20** with $[PhPSe_3]^{2-}$ anions. A similar observation was made in the presence of Rb^+ ions which resulted in the formation of $[Rb_2(PhPSe_2Se\text{-}SeSe_2PPh)(thf)_4]$ (**22**) (Scheme 3.18, Figure 3.22). Compound **22** (in space group *C*2/*c*) is isostructural with compound **21** (in space group *P*2$_1$/*c*) and the structure won't be discussed.

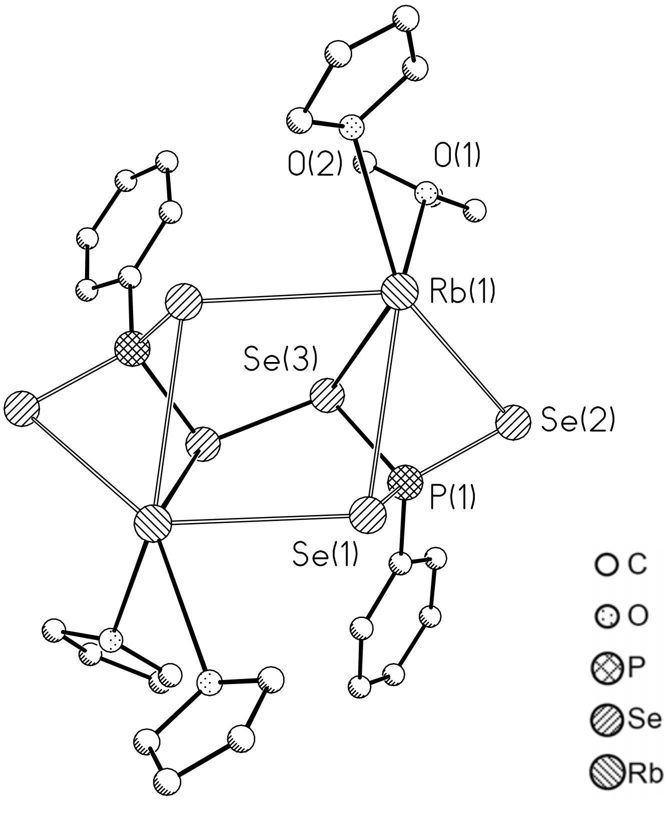

Figure 3.22 Structure of $[Rb_2(PhPSe_2Se\text{-}SeSe_2PPh)(thf)_4]$ (**22**)

Just like using NaS^tBu to react with L.R., $NaSe^tBu$ was also used in the reaction with W.R.. Surprisingly In the case of $NaSe^tBu$, this resulted in the formation of $1/\infty[Na_2\{PhSe_2P\text{-}PSe_2Ph\}(thf)_3]_\infty$ (**23**), which was obtained as single crystals by solvent-diffusion methods (Scheme 3.19). Although the reaction mechanism leading

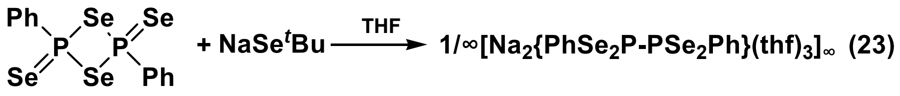

Scheme 3.19 Reaction of $NaSe^tBu$ and Woollins' reagent

to the formation of **23** has not been investigated in detail, it seems likely that mixtures of W.R. and NaSe^{t}Bu initially form Na complexes containing a $[PhP(Se^tBu)Se_2]^-$ anion that decomposes into $(^tBuSe)_2$ and the $[PhSe_2P\text{-}PSe_2Ph]^{2-}$ anion observed in **23**. A decomposition reaction with a similar outcome was observed in the reaction of $PhPS(SSiMe_3)_2$ with $Ag(CF_3CO_2)$, in which $1/\infty[Ag_2(PhS_2P\text{-}PS_2Ph)(dppe)_2]_\infty$ was formed (dppe=1,2-bis(diphenylphosphino)ethane).[132] Compound **23** is soluble in THF or dimethylsulfoxide (DMSO) and the anion remains intact, allowing characterization

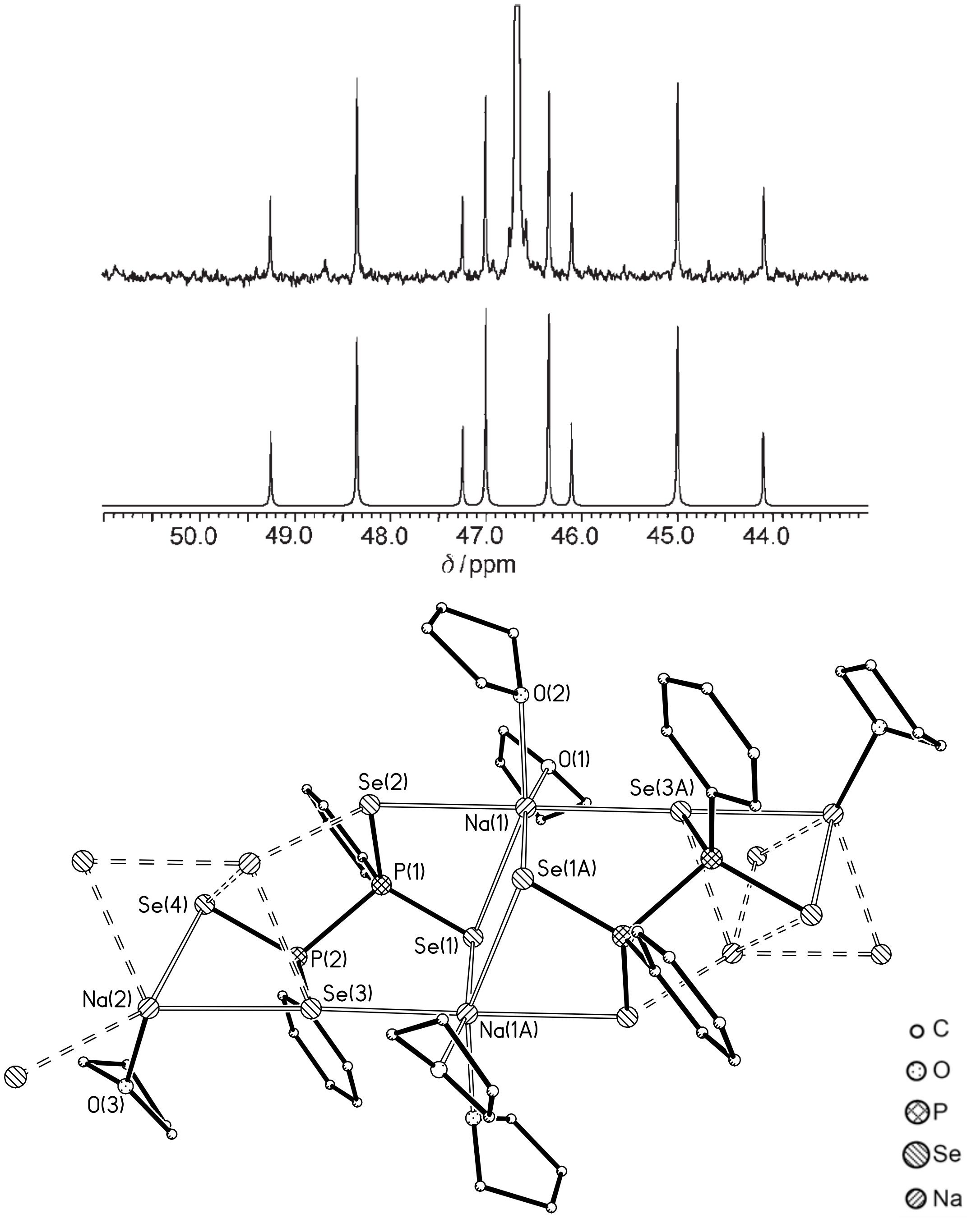

Figure 3.23 ^{77}Se satellites in the $^{31}P\{^1H\}$ NMR spectrum of **23** (top) and simulation (middle). Section of polymeric **23** in the solid state (bottom).

Table 3.18 Selected ranges of bond lengths (Å) and angles (°)

Bond lengths					
Se1-P1	2.1461(13)	Se-Na	3.0221(19)-3.284(2)	Se2-P1	2.1500(12)
Se3-P2	2.1544(12)	Se4-P2	2.1459(13)	P1-P2	2.2625(16)
O1-Na1	2.378(4)	O2-Na1	2.395(4)	O3-Na2	2.291(4)
angles					
Se1-P1-Se2	117.01(6)	Se1-P1-P2	109.21(6)	Se2-P1-P2	106.90(6)
Se4-P2-Se3	113.61(5)	Se4-P2-P1	108.89(6)	Se3-P2-P1	107.43(6)

by NMR. Figure 3.23 (top) shows the $^{31}P\{^{1}H\}$ NMR spectrum of **23** in which a singlet resonance is observed at $\delta = 46.8$ ppm. Upon prolonged recording times centered around this singlet, eight satellite lines become visible, indicating the presence of an ABX three-spin system, which is in good agreement with an optimized simulated $^{31}P\{^{1}H\}$ NMR spectrum (Figure 3.23, middle) (Ph(^{77}Se)SeP-PSe$_2$Ph; $^{1}J_{P\text{-}P} = -146$ Hz, $^{1}J_{P\text{-}Se} = -659$ Hz, $^{2}J_{P\text{-}Se} = 9$ Hz; $^{1}J_{P\text{-}Se}$ and $^{2}J_{P\text{-}Se}$ coupling constants have opposite signs).[152,153] Other isotopomeric compounds present in solution cannot be detected. In the solid state, **23** consists of a one-dimensional polymeric arrangement of $[PhSe_2P\text{-}PSe_2\ Ph]^{2-}$ anions held together by penta-[Na(2)] and hexacoordinated [Na(1)] alkali-metal ions (bottom). The P-P backbone of dianions is located in an alternating fashion above and below a band of two corrugated one-dimensional Na-Se(2) and Na-Se(3) strands, with Se(1) and Se(4) bridging the Na ions. The *gauche* conformation of phenyl groups in $[PhSe_2P\text{-}PSe_2Ph]^{2-}$ anions apparently favours this arrangement and the NMR study indicates that rotation of the P-P bond in solutions of **23** at room temperature is hindered.

Having shown that reactions of W.R. and alkali-metal alkoxides, thiolates and selenolates produce a range of novel complexes containing the anions $[PhP(O^{t}Bu)Se_2]^{2-}$, $[PhPSe_3]^{2-}$, $[PhPSe_2Se\text{-}SeSe_2PPh]^{2-}$ and $[PhSe_2P\text{-}PSe_2Ph]^{2-}$, next efforts were directed towards exploration of reactions between the P-Se precursor W.R. and metal carboxylates. Initial attempts with coinage metal acetates, same as copper alkoxides, often produced amorphous precipitates of metal selenides which terminated the reaction to form other new metal complexes containing P/Se ligands. Optimized reaction conditions finally yielded crystals of $1/\infty[K_2(PhPSe_2Se\text{-}SeSe_2\ PPh)(thf)_2]_\infty$ (**24**) from a reaction mixture of W.R. and KOAc in THF (Scheme 3.20).

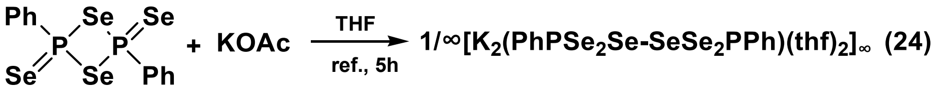

Scheme 3.20 Reaction of KOAc and Woollins' reagent

In the solid state, **24** exists as a one-dimensional polymeric ladder of two dimerised [KSe] strands isostructural to a compound obtained from reactions of W.R. and KS^{t}Bu (Figure 3.24, top). The one-dimensional polymeric strands in **24** exhibit an orientation relative to each other in which close contacts between phenyl carbon atoms and potassium centers result in densely packed polymers (Figure 3.24, bottom). The mechanism likely to be involved in the formation of **24** was investigated for similar reactions of L.R. by conducting GC/MS and ^{31}P NMR spectroscopy. To investigate potentially broader applications of nucleophilic ring-opening reactions of W.R. in organometallic-polymer synthesis, hydrated metal salts were employed for combined nucleophilic ring-opening/hydrolysis of W.R..

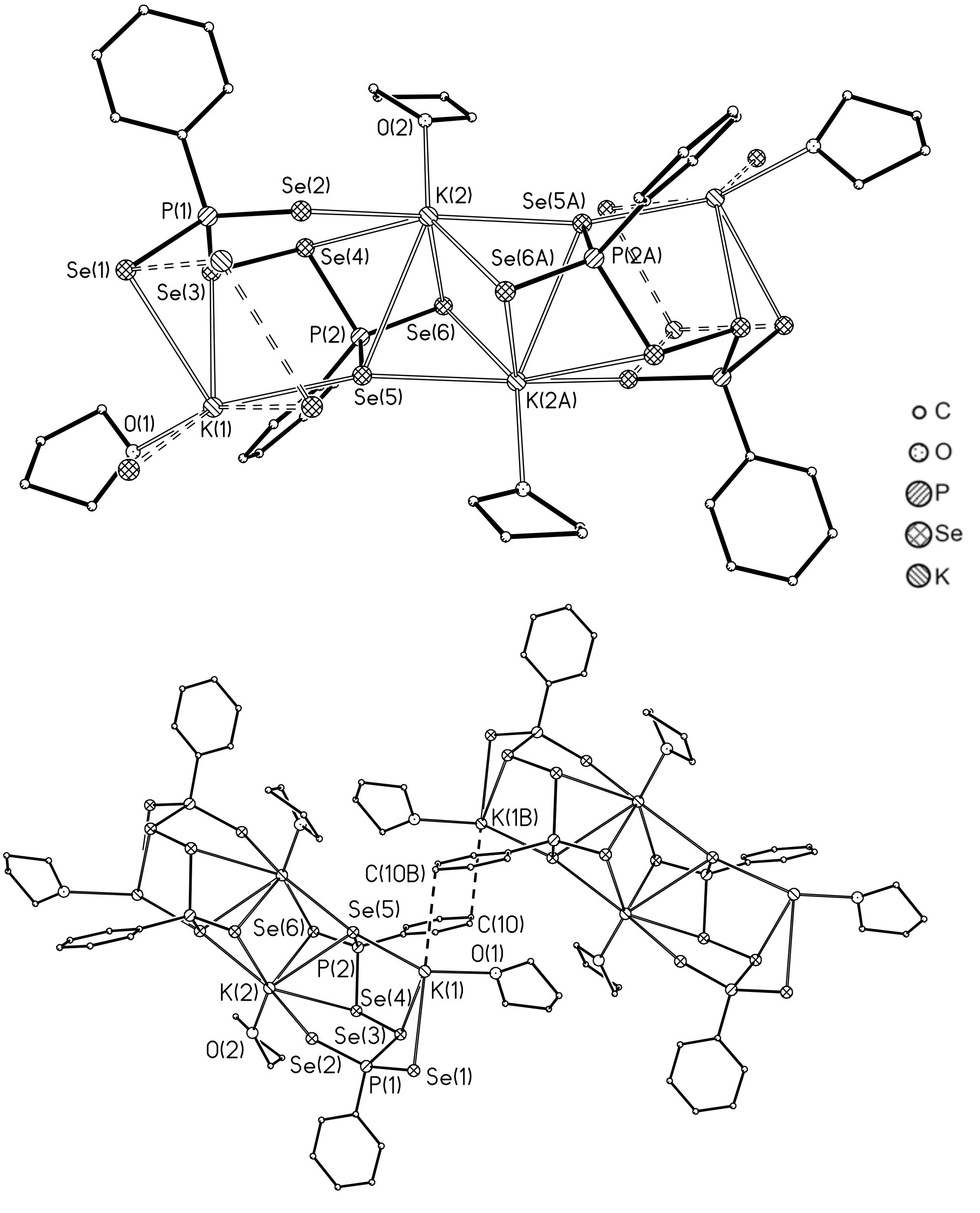

Figure 3.24 Top: Section of polymeric **24** in the solid state. Bottom: Arrangements of one-dimensional coordination polymeric strands of **24** in the solid state.

Table 3.19 Selected ranges of bond lengths (Å) and angles (°)

Bond lengths					
Se-P	2.1296(8)-2.2996(8)	Se4-Se3	2.3369(4)	K-Se	3.2282(8)-3.6150(7)
K1-O1	2.698(3)	K2-O2	2.661(3)	K1···C10B	3.463(3)
angles					
P2-Se4-Se3	102.56(2)	P1-Se3-Se4	107.23(2)	Se5-P2-Se6	117.69(3)
Se5-P2-Se4	111.49(3)	Se6-P2-Se4	99.28(3)	Se2-P1-Se1	118.54(4)
Se2-P1-Se3	114.61(3)	Se1-P1-Se3	97.56(3)		

In the case of NaOAc·3H_2O, crystals of 1/∞[$Na_2(PhPSe_2O)(H_2O)_4$(thf)]$_\infty$ (**25**) were obtained (Scheme 3.21). Once isolated, **25** was then insoluble in d_8-THF and D_2O, preventing characterization by NMR. The solid-state structure of a building block in **25** (Figure 3.25a, Table 3.20) consists of two crystallographically independent Na atoms

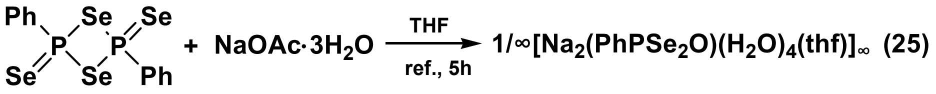

Scheme 3.21 Reaction of NaOAc·3H_2O and Woollins' reagent

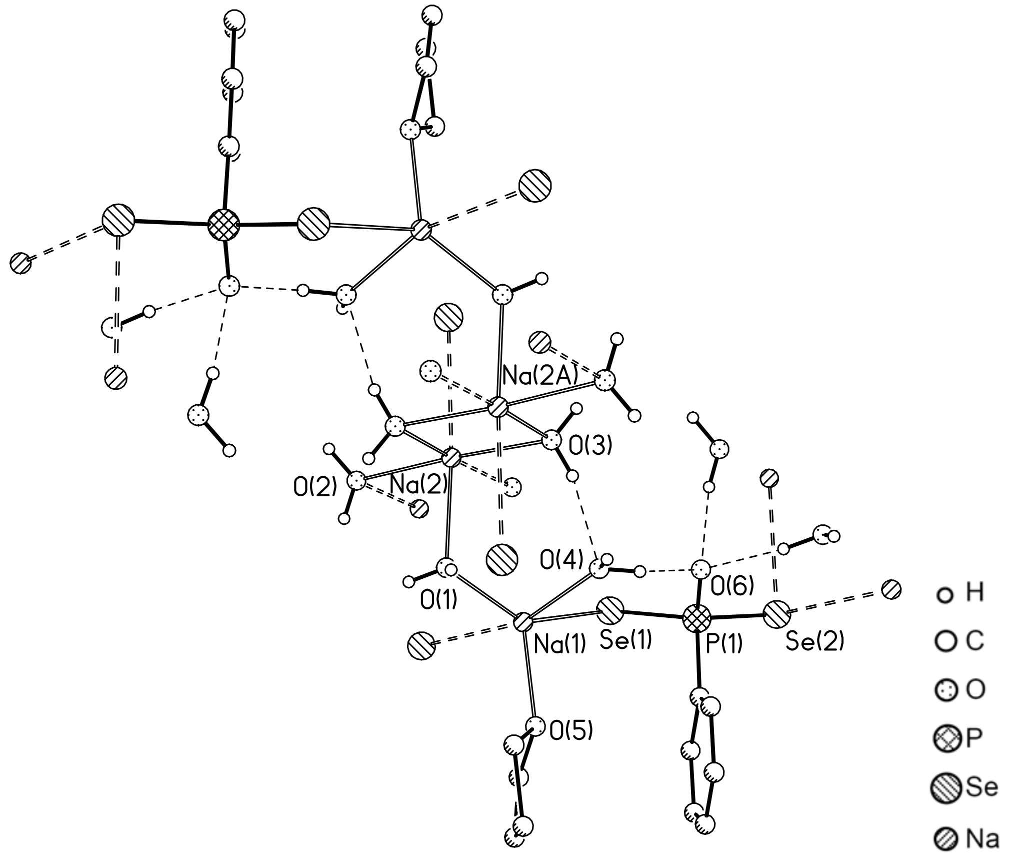

Figure 3.25a Structure of a building block of **25** in the solid state.

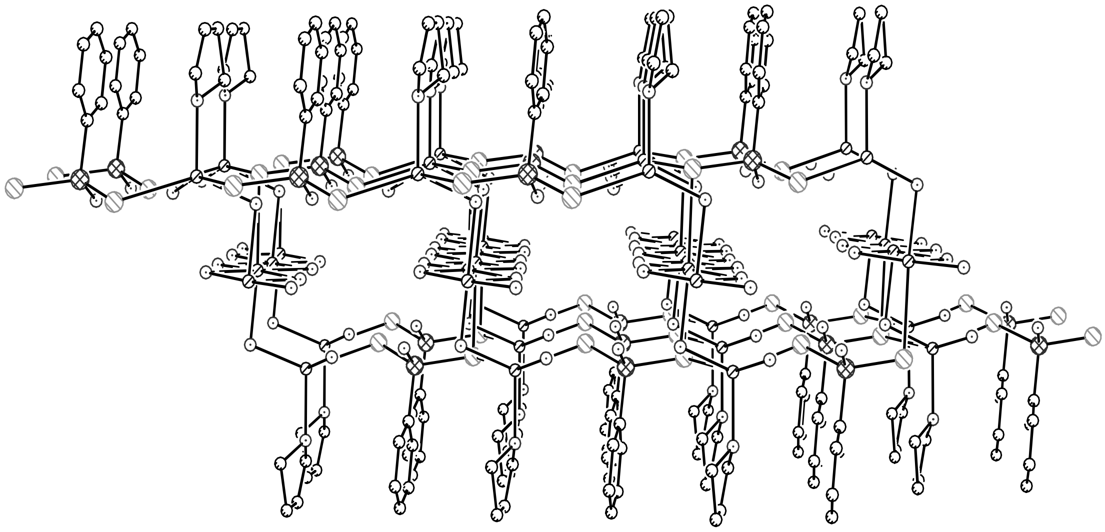

Figure 3.25b Packing diagram of **25**.

Table 3.20 Selected ranges of bond lengths (Å) and angles (°)

Bond lengths					
Na-O(H_2O)	2.27(2)-2.443(6)	Na1-O5	2.29(3)	Na-Se	3.023(3)-3.057(3)
P1-O6	1.525(5)	P1-Se2	2.1592(18)	P1-Se1	2.1651(18)
angles					
Na2A-O3-Na2	92.1(2)	O6-P1-Se2	111.5(2)	C1-P1-Se2	105.0(2)
O6-P1-Se1	111.5(2)	C1-P1-Se1	107.3(3)	Se2-P1-Se1	113.59(8)

and symmetry-equivalent Na atoms held together by an elaborate arrangement of $[PhP(O)Se_2]^{2-}$ anions and hydrogen-bonded water. Na(1) is coordinated by Se-donor centers and O atoms of THF and water. As part of a one-dimensional polymeric strand, Na(1) is in an environment similar to that of the alkali-metal atoms in compounds **19**, **23** and **24**. Perpendicular to this arrangement Na(2), Na(2A) and symmetry-equivalent atoms are arranged by bridging μ-H_2O ligands into another one-dimensional polymeric motif observed in **25**. Altogether, this results in a self assembled layer-sandwich structure of lipophilic surface groups (topologically similar, but electronically inverse $[Na(thf)]^+$ and $[PhP(O)Se_2]^{2-}$ ions) held together by an inner polar arrangement of Na^+ and H_2O (Figure 3.25b).

The investigations in which tetrahedrally and octahedrally surrounded metal atoms are incorporated to give crosslinked organometallic polymers based on P-Se anions are still at an early stage. With the successful experiences of alkali metal salts, somewhat unpredictable results have been observed when other transition metal salts are used in the reaction with W.R. under optimized conditions, as shown in the following example. The reaction of CuOAc with W.R. and successive treatment with PPh_3 afforded the crystalline compound $[Cu_4(PhSeP\text{-}O\text{-}PSePh)_2(PPh_3)_4]$ (**26**) besides the huge amount of copper selenide (Scheme 3.22). In the solid state, **26** exhibits a cage arrangement of four distorted-tetrahedrally coordinated Cu^+ ions and the

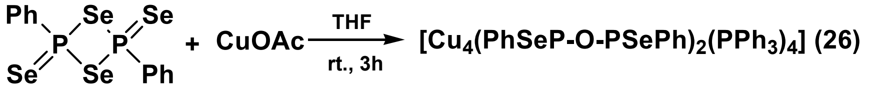

Scheme 3.22 Reaction of CuOAc and Woollins' reagent

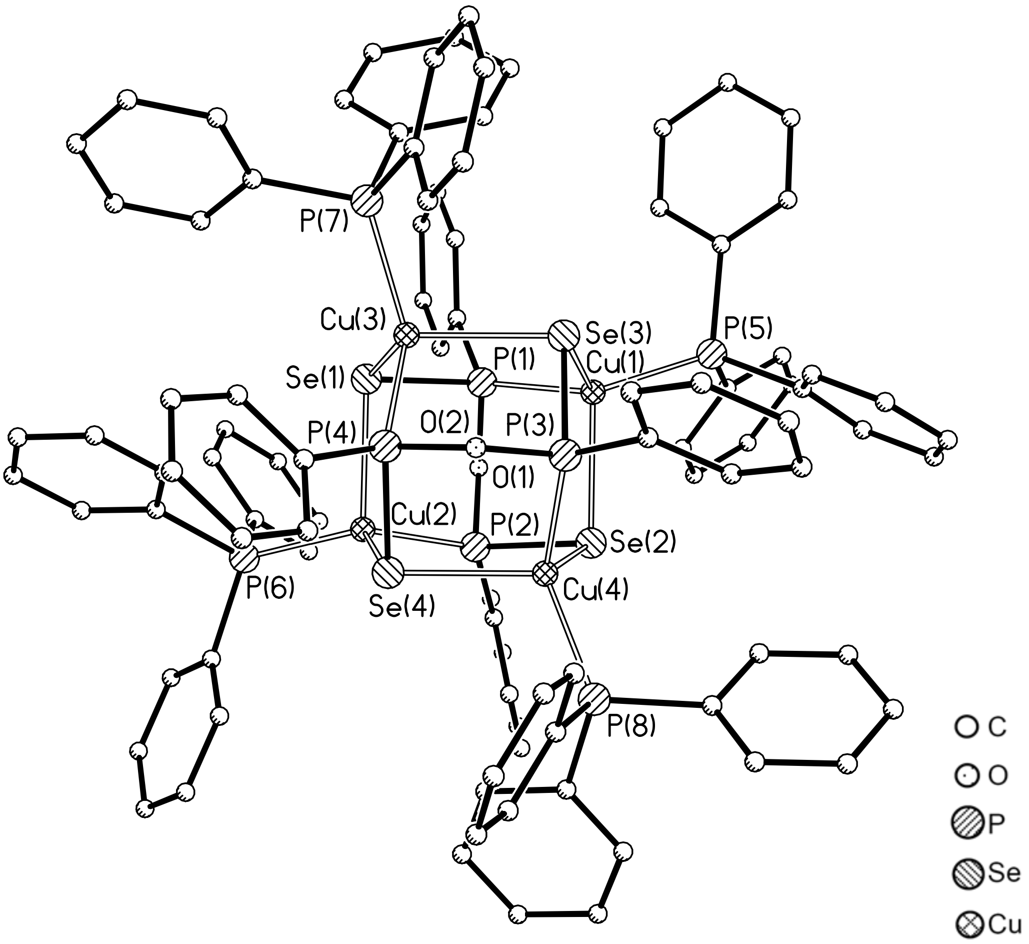

Figure 3.26 Structure of $[Cu_4(PhSeP\text{-}O\text{-}PSePh)_2(PPh_3)_4]$ (**26**)

Table 3.21 Selected ranges of bond lengths (Å) and angles (°)

Bond lengths					
Se-Cu	2.4353(9)-2.5077(9)	Cu1-P1	2.2643(15)	Cu2-P2	2.2573(17)
Cu3-P4	2.2466(17)	Cu4-P3	2.2407(15)	Cu-P(PPh$_3$)	2.2331(16)–2.2462(16)
Se1-P1	2.2363(17)	Se2-P2	2.2380(14)	Se3-P3	2.2394(15)
Se4-P4	2.2414(16)	P1-O1	1.662(5)	P2-O1	1.658(4)
P3-O2	1.657(4)	P4-O2	1.676(4)		
angles					
O1-P1-Se1	103.67(15)	O1-P1-Cu1	103.70(16)	Se1-P1-Cu1	113.68(7)
O1-P2-Se2	103.34(14)	O1-P2-Cu2	103.63(17)	Se2-P2-Cu2	114.71(6)
O2-P3-C13	97.94(19)	O2-P3-Se3	103.70(16)	O2-P3-Cu4	104.00(15)
Se3-P3-Cu4	115.26(6)	O2-P4-Se4	103.41(16)	O2-P4-Cu3	103.09(15)
Se4-P4-Cu3	115.27(7)	P2-O1-P1	114.8(2)	P3-O2-P4	113.6(2)

dianion [PhSeP-O-P SePh]$^{2-}$ (Figure 3.26, Table 3.21). The formation of this anion indicates that reduction of P atoms has occurred during the reaction. It is likely that intermediates of the type [Cu$_2$(PhSe$_2$P-O-PSe$_2$Ph)] are formed initially, together with Ac$_2$O. Subsequently, the PPh$_3$ present in solution acts both as ligand and reducing agent to give **26** and P(Se)Ph$_3$. Reduction of W.R. in the presence of phosphines was also encountered in other investigations.

Similar to reactivity studies of Lawesson's reagent, hydrated metal carboxylates are also employed as starting materials in ring-opening reactions of Woollins' reagent. The synthetic route was applied for the synthesis of the Se compound [Ni{PhP(OH)Se$_2$}$_2$(thf)$_2$] (**27**) (Scheme 3.23, Figure 3.27, Table 3.22) which is isostructural to **18** (Figure 3.18). [PhP(OH)Se$_2$]$^-$ anions were formed during the course of the reaction. The substitution pattern at the phosphorus atom in **27** is rare and only few examples of P-based ligands are known which both contain hydroxyl groups and Se atoms.[154] Crystals of **27** were soluble in d$_8$-THF and a proton resonance of the hydroxyl group in the P-O-H···O(thf) fragment was observed at δ12.19. The P-O bond distances found in the [PhP(OH)Se$_2$]$^-$ anions in **27** [P-O 1.561(5) and 1.565(6) Å] are slightly longer than the P-O distance found in the related anion [PhP(O)Se$_2$]$^{2-}$ in **25** [P-O 1.525(5) Å].

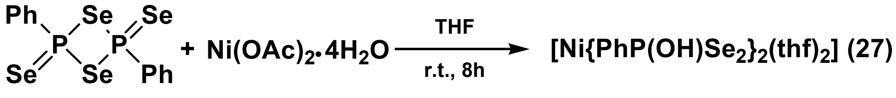

Scheme 3.23 Reaction of Ni(OAc)$_2$·4H$_2$O and Woollins' reagent

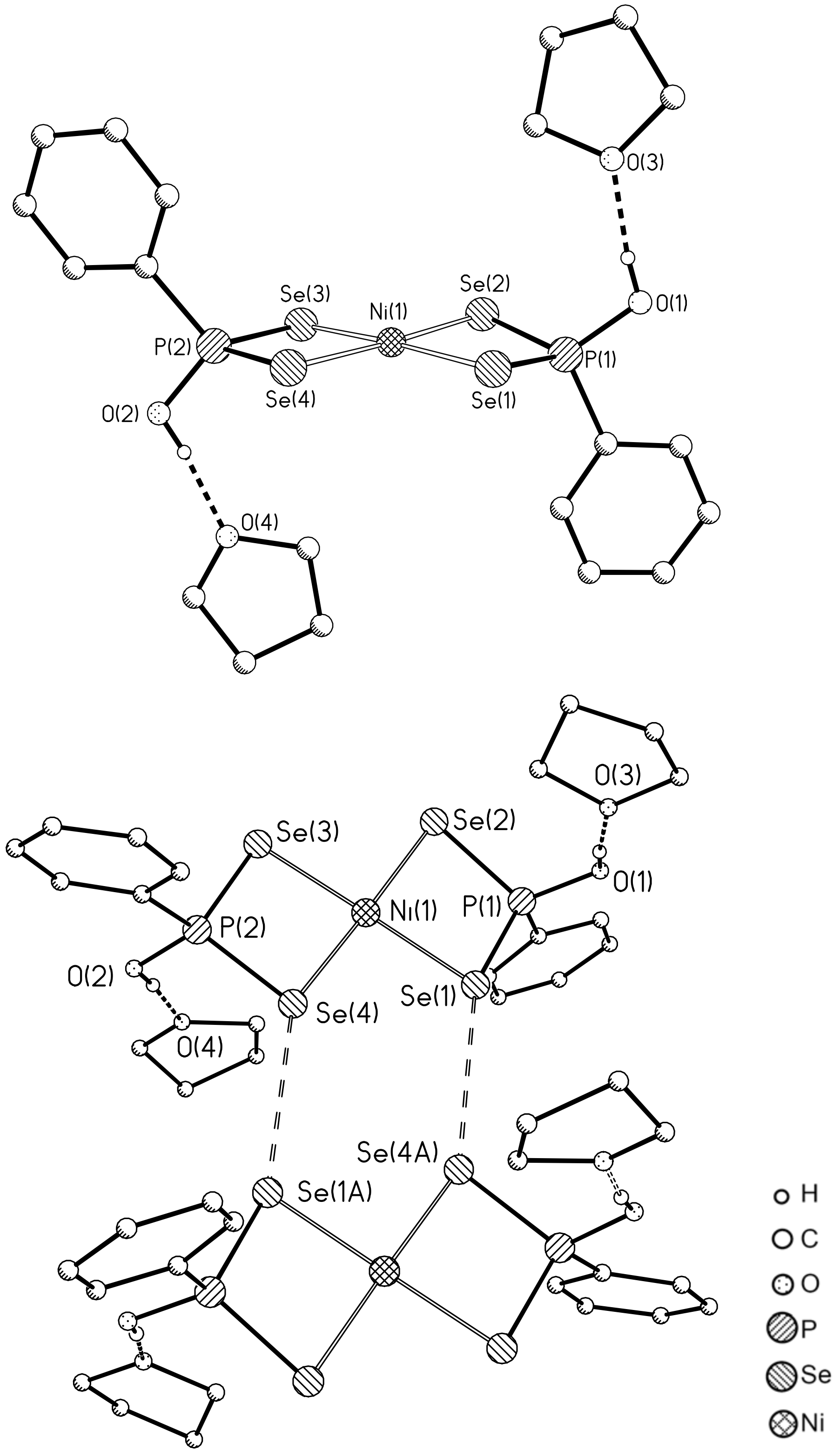

Figure 3.27 Top: Molecular structure of **27** (50% probability ellipsoids)

Bottom: Pseudodimeric arrangement of two molecules of **27**

Table 3.22 Selected ranges of bond lengths (Å) and angles (°)

Bond lengths					
Se1-Ni1	2.3498(11)	Se2-Ni1	2.3509(11)	Se3-Ni1	2.3307(11)
Se4-Ni1	2.3507(11)	Se1-P1	2.1610(18)	Se2-P1	2.1592(18)
Se3-P2	2.1619(17)	Se4-P2	2.1716(19)	P1-O1	1.561(5)
P2-O2	1.565(6)	O1···O3	2.549(9)	O2···O4	2.527(9)
Se1···Se4A	ca. 3.8				
Angles					
Se1-Ni1-Se2	90.32(4)	Se1-Ni1-Se4	91.02(4)	Se3-Ni1-Se1	177.04(6)
Se3-Ni1-Se4	89.60(4)	Se3-Ni1-Se2	89.16(4)	Se4-Ni1-Se2	177.58(5)
Se2-P1-Se1	100.98(7)	Se3-P2-Se4	99.15(7)	P-Se-Ni	83.78(5)-85.27(5)
O-P-Se	114.6(2)-115.7(2)	C-P-Se	111.0(2)-113.7(2)		

In the solid-state molecules of **27** form pseudo dimeric arrangements with nonbonding Se···Se distances of ca. 3.8 Å (Figure 3.27 bottom).

The reactions of [PhPSe(*μ*-Se)]$_2$ (W.R.) with the hydrated metal carboxylate [$NaOAc\cdot 3H_2O$] and [$Ni(OAc)_2\cdot 4H_2O$] were shown that the presence of water played a crucial role in the formation of the resulting coordination polymer $1/\infty[Na_2(PhPSe_2O)(H_2O)_4(thf)]_\infty$ (**25**) and [Ni{PhP(OH)Se$_2$}$_2$(thf)$_2$] (**27**). As an extension of this initial report, more hydrated metal carboxylates were reacted with W.R., compounds **28-30** with a new kind of dianion [PhP(O,Se)Se-Se(Se,O)PPh]$^{2-}$ were produced (Scheme 3.24).

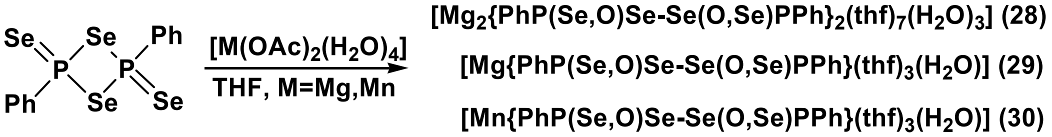

Scheme 3.24 Reaction of $M(OAc)_2\cdot 4H_2O$ and Woollins' reagent (M = Mg, Mn)

28 crystallizes in the orthorhombic space group *P*ca2$_1$ with two differently-coordinated Mg atoms in the asymmetric unit. The constituting magnesium complexes [Mg{PhP(Se,O)Se-Se(O,Se)PPh}(thf)$_3$(H$_2$O)] and [Mg{PhP(Se,O)Se-Se(O,Se) PPh}(thf)$_4$(H$_2$O)$_2$] in **28** exhibit an octahedral metal coordination environment (Figure 3.28, Table 3.23). The new generated ligand [PhP(Se,O)Se-Se(O,Se)PPh]$^{2-}$ chelates the magnesium atoms and coordinates in a similar fashion like the neutral related ligand 1,2-*bis*-diphenylphosphine-oxide.[155,156] The two isolated units are connected by a weak hydrogen bond between Se(5) and O(6) (distance Se5···O6 *ca.* 3.35 Å).[157]

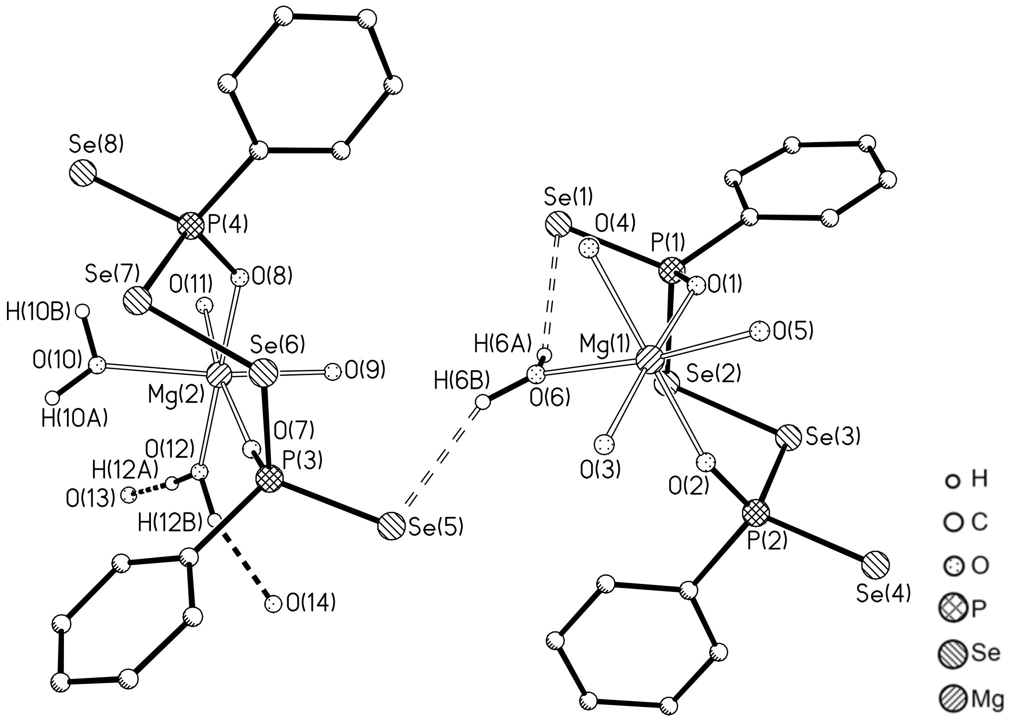

Figure 3.28 Structure of [Mg$_2${PhP(Se,O)Se-Se(O,Se)PPh}$_2$(thf)$_7$(H$_2$O)$_3$] (**28**)

Table 3.23 Selected ranges of bond lengths (Å) and angles (°)

Bond lengths					
Se-P	2.113(2)-2.261(2)	Se2-Se3	2.3302(12)	Se6-Se7	2.3360(12)
P1-O1	1.503(5)	P2-O2	1.499(5)	P3-O7	1.493(6)
P4-O8	1.485(6)	Mg1-O1	2.008(6)	Mg1-O2	1.986(6)
Mg2-O8	2.025(6)	Mg2-O7	2.036(6)	Mg-O(H$_2$O)	2.057(6)-2.091(6)
Mg-O(3,4,5,9,11; thf)		2.089(6)-2.151(6)		Se5···O6	*ca.* 3.35
Se1···O6	*ca.* 3.43	O12···O13	*ca.* 2.68	O12···O14	*ca.* 2.69
Angles					
P1-Se2-Se3	99.35(6)	P2-Se3-Se2	99.62(6)	P3-Se6-Se7	103.44(6)
P4-Se7-Se6	100.38(6)	O1-P1-Se1	118.2(2)	O1-P1-Se2	110.3(2)
Se1-P1-Se2	101.40(8)	O2-P2-Se4	119.3(2)	O2-P2-Se3	110.4(2)
Se4-P2-Se3	102.20(8)	O7-P3-Se5	120.3(2)	O7-P3-Se6	113.0(2)
Se5-P3-Se6	98.27(8)	O8-P4-Se8	118.3(2)	O8-P4-Se7	111.1(2)
Se8-P4-Se7	100.99(9)	O2-Mg1-O1	93.7(2)	O8-Mg2-O7	91.5(2)

Other hydrogen bonds present include the strongly bound THF at O(12) and a weak H-bond between Se(1) and O(6). **29** is almost identical to **28**. Slightly modified experimental conditions, however have led to a slight change in the substitution pattern of the magnesium atom in [Mg{PhP(Se,O)Se-Se(O,Se)PPh}(thf)$_3$(H$_2$O)] (**29**) (Figure 3.29, Table 3.24).

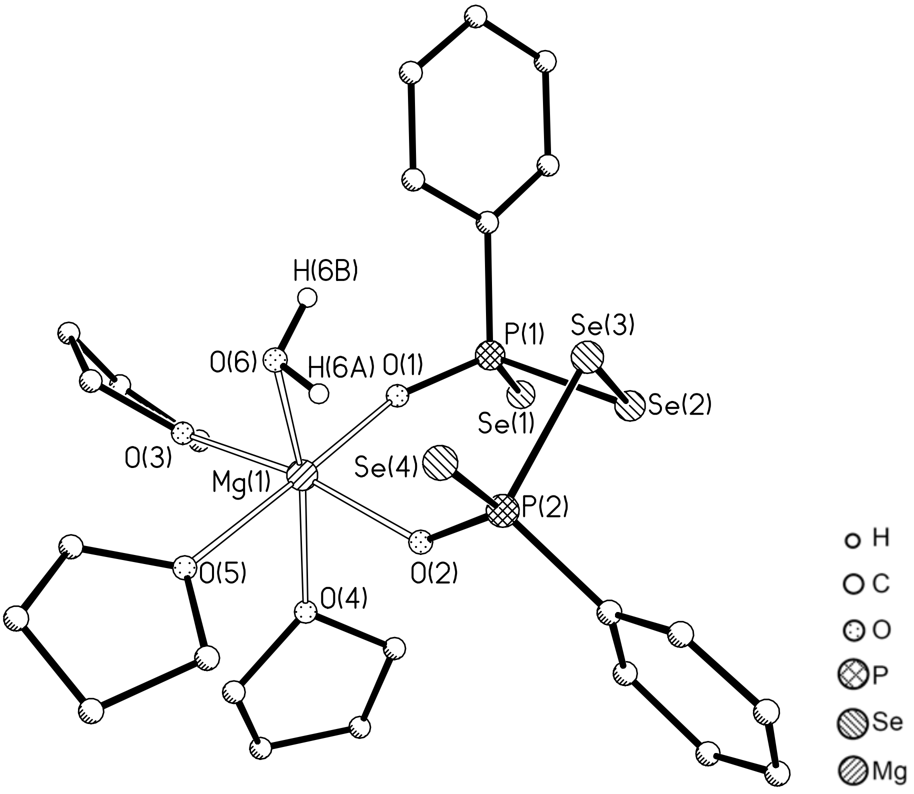

Figure 3.29 Structure of [Mg{PhP(Se,O)Se-Se(O,Se)PPh}(thf)$_3$(H$_2$O)] (**29**)

Table 3.24 Selected ranges of bond lengths (Å) and angles (°)

Bond lengths					
Se-P	2.127(4)-2.329(2)	P1-O1	1.496(10)	P2-O2	1.519(8)
Mg1-O1	1.996(11)	Mg1-O2	2.016(9)	Mg1-O6	2.090(9)
Mg1-O(3,4,5; thf)		2.02(2)-2.190(16)			
Angles					
P1-Se2-Se3	98.54(11)	P2-Se3-Se2	100.11(11)	O1-P1-Se1	118.6(4)
O1-P1-Se2	111.0(4)	Se1-P1-Se2	102.48(16)	O2-P2-Se4	117.8(4)
O2-P2-Se3	111.1(4)	Se4-P2-Se3	99.73(14)	O1-Mg1-O2	93.1(4)

29 crystallizes in the monoclinic space group $P2_1/c$ with two crystallographically independent molecules in the asymmetric unit. Attempts to characterize the new anion spectroscopically were also made and indicated that **29** slowly decomposes in d$_6$-DMSO. It was, however, possible to dissolve **29** by stirring crystals in d$_8$-THF overnight. In the ^{31}P{^{1}H} NMR a singlet resonance for the [PhP(Se,O)Se-Se(O,Se) PPh]$^{2-}$ dianion was observed together with two satellite sets, which can be ascribed to $^1J_{P\text{-}Se}$ coupling to chemically inequivalent terminal and 'inner' Se atoms.[114] In the ^{77}Se NMR of **28** and **29**, however, one weak resonance at *ca.* δ 40 ppm was detected, whilst at δ 131 ppm a further resonance could be ascribed to the different Se environments present. Generally, NMR investigations are complicated by low solubility of **28** and **29**.

The incorporation of paramagnetic metal ions into the new ligand framework was finally exemplified by treating W.R. with [Mn(OAc)$_2$·4H$_2$O] and x-ray analysis of crystals of **30** (Figure 3.30, Table 3.25)**.**

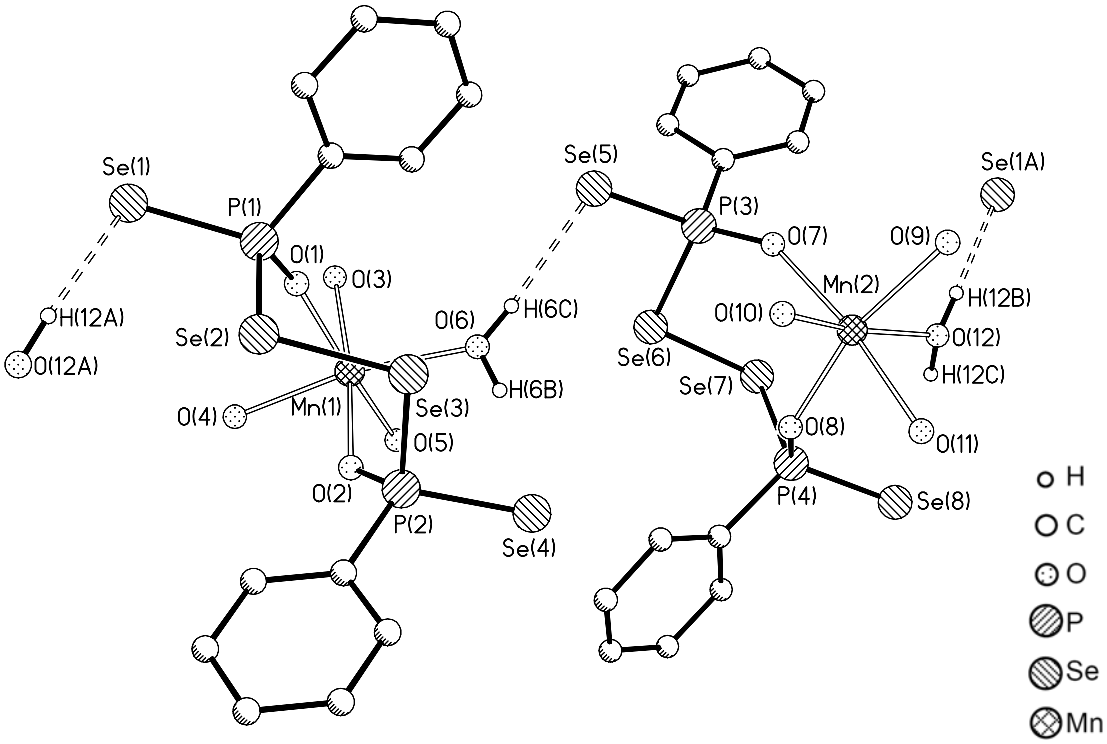

Figure 3.30 Structure of [Mn{PhP(Se,O)Se-Se(O,Se)PPh}(thf)$_3$(H$_2$O)] (**30**)

Table 3.25 Selected ranges of bond lengths (Å) and angles (°)

Bond lengths					
Se-P	2.118(2)-2.264(2)	Mn1-O1	2.078(6)	Mn1-O2	2.124(6),
Mn2-O7	2.138(6)	Mn2-O8	2.096(6)	Mn1-O6	2.206(6)
Mn2-O12	2.186(7)	Se2-Se3	2.3353(12)	Se6-Se7	2.3306(14)
Mn-O(3,4,5,9,10,11; thf)		2.188(6)-2.284(6)		P1-O1	1.497(6)
P2-O2	1.517(6)	P3-O7	1.505(6)	P4-O8	1.502(6)
Se1···O12A	ca. 3.36				
Angles					
O1-Mn1-O2	95.9(2)	O8-Mn2-O7	94.6(2)	P-Se-Se	98.46(7)-102.02(6)
O-P-Se	110.2(3)-120.8(3)	Se-P-Se	98.13(9)-102.23(9)		

30 crystallizes in the monoclinic space group $P2_1/c$ with two crystallographically independent but chemically equivalent [Mn{PhP(Se,O)Se-Se(O,Se)PPh}$(thf)_3(H_2O)$] (**30**) complexes in the asymmetric unit. In the extended solid-state structure **30** forms a 1D polymeric arrangement held together by weak hydrogen bonds (Se1···O12A *ca.* 3.36 Å).

The formation of the $[PhP(Se,O)Se\text{-}Se(O,Se)PPh]^{2-}$ dianion represents a new development in P-Se chemistry. The new ligand can be regarded as the product of an oxidation of the recently reported $[PhP(O)Se_2]^{2-}$ anion. During the ring-opening reactions of Woollins' reagent, metathesis reaction is also one kind of very important reaction. Here, the reactions with Ni salts were investigated (Scheme 3.25).

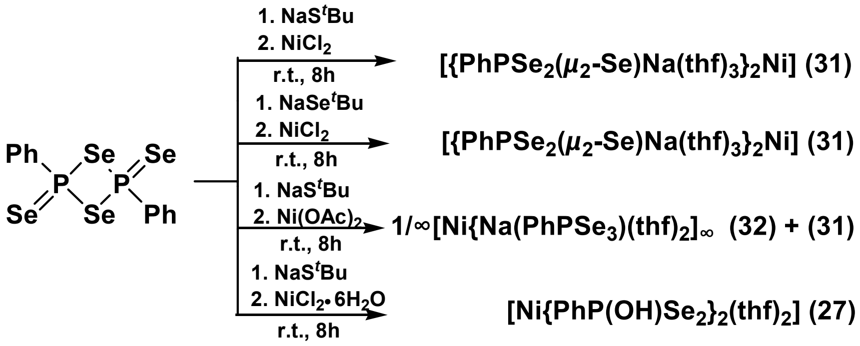

Scheme 3.25 Metathesis reactions of Ni(II) salts.

In the metathesis reaction with $NiCl_2$, thiolate (NaS^{t}Bu) and senelonate (NaSe^{t}Bu) produced the same crystal [{$PhPSe_2(\mu_2\text{-}Se)Na(thf)_3$}$_2$Ni] (**31**). In the solid state **31** consists of a centrosymmetric arrangement of two $[PhPSe_3]^{2-}$ ligands chelating square- planar coordinated Ni(1), which is located on the inversion center (Figure 3.31, Table 3.26).

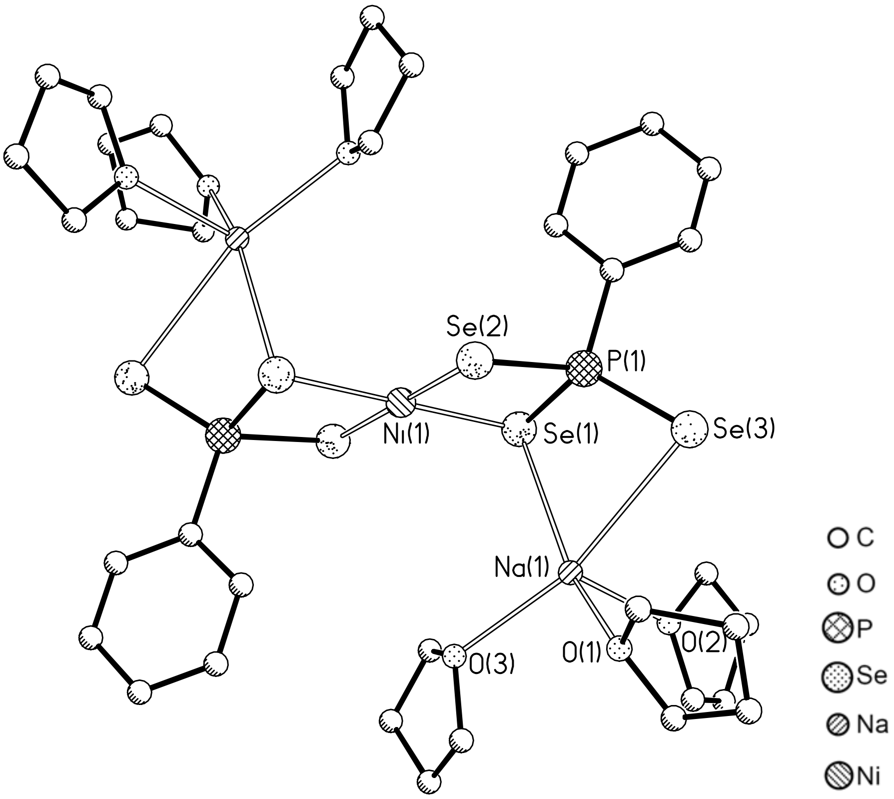

Figure 3.31 Structure of $[\{PhPSe_2(\mu_2\text{-}Se)Na(thf)_3\}_2Ni]$ (**31**)

Table 3.26 Selected ranges of bond lengths (Å) and angles (°)

Bond lengths					
Ni1-Se1	2.3430(11)	Ni1-Se2	2.3254(10)	P1-Se1	2.212(2)
P1-Se2	2.225(3)	P1-Se3	2.113(3)	Na1-Se1	3.074(4)
, Na1-Se3	3.128(4)	Na-O	2.274(8)-2.431(14)		
Angles					
Se3-P1-Se1	116.17(11)	Se3-P1-Se2	116.91(12)	Se1-P1-Se2	94.13(9)
Se1-Ni1-Se2	88.18(4)				

Two thf-solvated Na^+ ions are located above and under the plane defined by the $NiSe_4$ unit and are coordinated by chelating triselenophosphonato anions. The different chemical environments of the Se donor centers are reflected in the ^{31}P NMR by ^{77}Se satellites showing $^1J_{P\text{-}Se}$ coupling constants of 390 and 350 Hz. Both P-Se bond distances and $^1J_{P\text{-}Se}$ coupling constants are in good agreement with previously reported values for $RPSe_3$-dianions (R = cyclohexyl, phenyl).[113,158] When $Ni(OAc)_2$ was used in stead of $NiCl_2$, the polymeric $1/\infty[Ni\{Na(PhPSe_3)(thf)\}_2]_\infty$ (**32**) was isolated together with previously **31** (Scheme 3.25). Although crystals of **32** were generally of poor quality, the solid-state structure could be established (Figure 3.32).

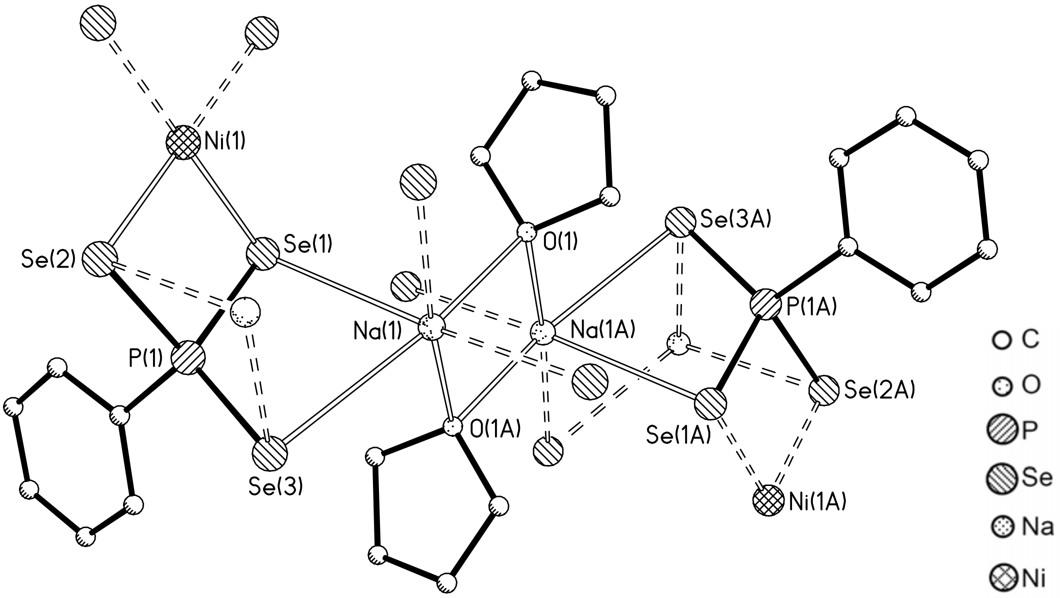

Figure 3.32 Section of polymeric **32** in the solid state

As showed in **19**, **23** and **24**, the alkali-metal ions in **32** form a one-dimensional polymer with $[PhPSe_3]^{2-}$ anions, however, these are now linked by the square-planar coordinated Ni(1) into a two-dimensional sheet. The Se atoms in the $[PhPSe_3]^{2-}$ anions bridge between Na atoms, whereas Ni(1) is chelated by two Se atoms belonging to anions of different one-dimensional polymeric strands.

Metathesis reactions with hydrated Ni(II) salts were subsequently used for controlled hydrolysis of P-Se anions as same as P-S anions. In the case of $NiCl_2 \cdot 6H_2O$, $[Ni\{ArP(OH)Se_2\}_2(thf)_2]$ (**27**) (Figure 3.27, Table 3.22) was obtained, as the same result in the reaction of $Ni(OAc)_2 \cdot 4H_2O$ and W.R..

Based on the results from the reactions of metal alkoxides, carboxylates and thiolates with P/S ligand precursors (L.R.) and P/Se ligand precursors (W.R.), another type of P/S ligand precursors--Phosphorus trisulfide (P_4S_6) and Phosphorus pentasulfide (P_4S_{10}) was investigated. It is well-known that the alcoholysis of P_4S_n (n = 6 or 10) is an important chemical process but reactions with coinage metal alkoxides or carboxylates have to the best of our knowledge not been described.[64] P_4S_n (n = 6 or 10) is, like L.R., a strong sulfur transfer reagent and reactions with metal salts often give amorphous precipitates of metal sulfides. In the reaction of CuO*t*Bu with $P_4S_{(n = 6, 10)}$, however, some new complexes containing P/S ligands were produced (Scheme 3.26).

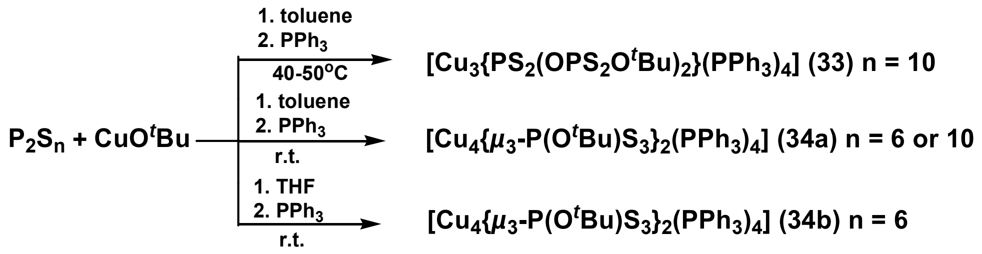

Scheme 3.26 Reactions of CuO^{t}Bu and P_4S_n (n = 6 or 10)

The formation of $[Cu_3\{PS_2(OPS_2O^tBu)_2\}(PPh_3)_4]$ (**33**) proceeds via alkoxide-induced cage fragmentation of P_4S_{10}. In the solid state the $[PS_2(OPS_2O^tBu)_2]^{3-}$ anion chelates three Cu^+ ions. The conformation of the anion is fixed by Cu(1), which is coordinated to S(3-5). Cu(2,3) are coordinated by S atoms of the central dithiophosphato group

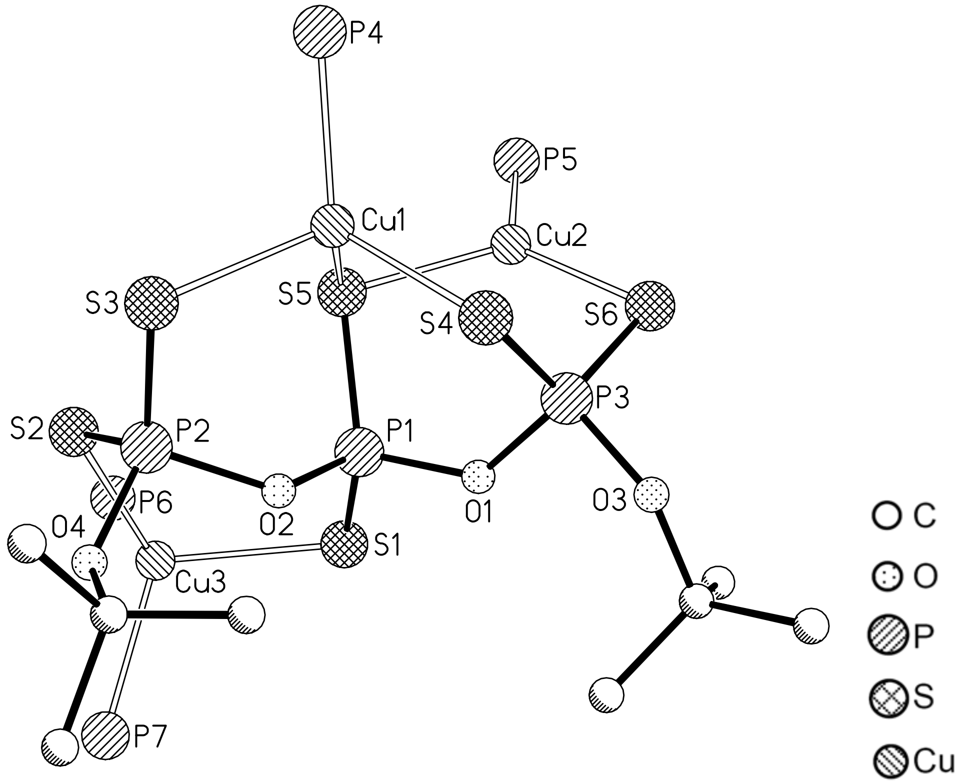

Figure 3.33 Structure of $[Cu_3\{PS_2(OPS_2O^tBu)_2\}(PPh_3)_4]$ (**33**)
(The phenyl groups of PPh_3 are omitted)

Table 3.27 Selected ranges of bond lengths (Å) and angles (°)

Bond lengths					
Cu-P	2.2139(9)-2.2981(8)	Cu-S	2.2334(9)-2.4223(8)	P1-O1	1.605(2)
P1-O2	1.601(2)	P2-O2	1.653(2)	P2-O4	1.622(2)
P3-O1	1.645(2)	P3-O3	1.585(3)	P-S	1.9611(11)-2.0155(11)
Angles					
S-P-S	116.30(5)-118.75(6)	O2-P1-O1	99.37(11)	O4-P2-O2	101.05(12)
O3-P3-O1	101.34(12)				

and the peripheral S atoms S(2,6). The tetrahedral [Cu(1) and Cu(3)] and trigonal [Cu(2)] coordination spheres are completed by triphenylphosphine ligands (Figure 3.33, Table 3.27). The thermal instability of **33** and the insolubility of amorphous by-products (*e.g.*, [Cu_3PS_4]) once formed, prevented a more detailed reaction study. The formation of P-O-P bonds in **33** is likely to occur via ether elimination connecting P-O^{t}Bu groups to P-O-P structural motifs.

When a mixture of CuO^{t}Bu and P_4S_6 (or P_4S_{10} sometimes) are dissolved in THF or toluene, crystals of [$Cu_4\{\mu_3$-P(O^{t}Bu)$S_3\}_2(PPh_3)_4$] (**34a**, **34b**) were obtained after addition of the auxiliary ligand PPh_3 (Figure 3.34, Table 3.28). In the unit cell of **34a** there are two independent molecules lying about inversion centers, and in the polymorph **34b** there is one molecule in the unit cell, also lying about an inversion center (bond lengths in both compounds are similar). **34a** consists of a centrosymmetric distorted hexagonal prismatic arrangement of two [P(O^{t}Bu)$S_3]^{2-}$ anions and four [Cu(PPh_3)]$^+$ units. Each of the S-donor atoms bridges two Cu atoms resulting in tetrahedral coordination environments for Cu atoms with Cu-S and Cu-P bond distances in commonly observed ranges. The most striking feature of **34a** is the formation of [^{t}BuOP$S_3]^{2-}$ ligands which is mechanistically difficult to rationalize. The moderate yield in which **34a** is formed indicates the complexity of the reaction.

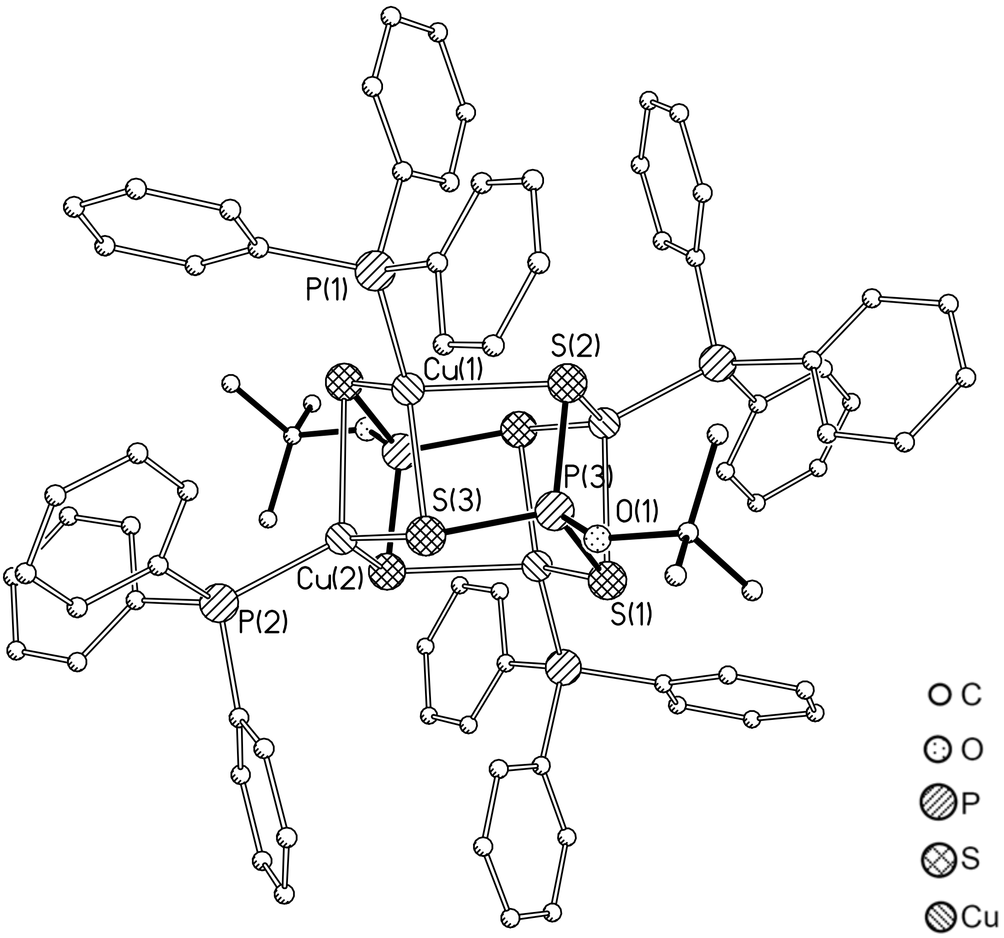

Figure 3.34 Structure of [$Cu_4\{\mu_3\text{-}P(O^tBu)S_3\}_2(PPh_3)_4$] (**34**)

Table 3.28 Selected ranges of bond lengths (Å) and angles (°)

Bond lengths					
Cu-P	2.2264(9)-2.2467(10)	Cu-S	2.2739(9)-2.7390(12)	P3-O1	1.601(2)
P3-S1	2.0302(12)	P3-S2	2.0304(13)	P3-S3	2.0416(11)
Angles					
P-Cu-S	99.75(4)-121.99(3)	S-Cu-S	81.62(3)-125.52(3)	O1-P3-S2	113.32(10)
S1-P3-S2	109.47(5)	O1-P3-S3	97.72(10)	S1-P3-S3	117.19(5)
S2-P3-S3	108.73(5)				

Attempts to gain a mechanistic insight by NMR experiments in a variety of solvents failed. So far reactions of CuO^tBu with P_4S_6 and P_4S_{10} are of limited practical value despite the fact that the novel compounds **33** and **34** were obtained.

In the following, another attempt to generate further example of P/S anions is described, which potentially opens up new synthetic routes to sulfur analogs of known metal phosphates and phosphonates.[3,159-161] The reaction of P_4S_{10} with NaS^tBu was performed. Layering of the reaction mixture with hexane resulted in the formation of the 2D-polymer 1/∞$[Na_2(S_3PS^tBu)(dme)]_\infty$ **35** (Scheme 3.27, Figures 3.35, Table 3.29).

$$\mathbf{P_2S_5 + NaS^{\mathit{t}}Bu \xrightarrow[r.t.]{DME} 1/\infty[Na_2(S_3PS^{\mathit{t}}Bu)(dme)]_\infty\ (35)}$$

Scheme 3.27 Reaction of NaS^tBu and P_4S_{10}

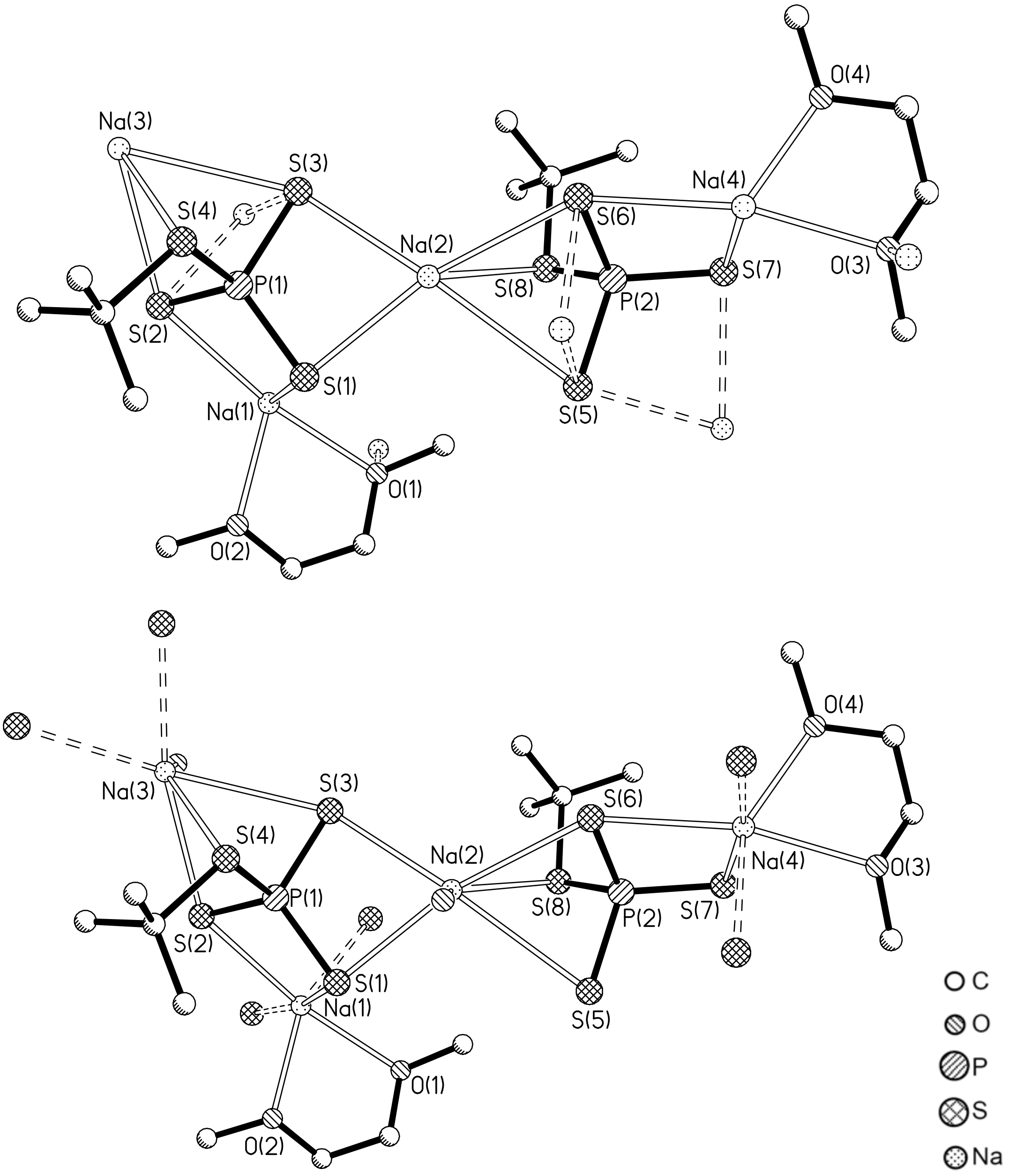

Figure 3.35a Top: Environments of S and O donor centers to Na. (dashed bonds)
Bottom: Coordination environment of Na^+ to donor centers of adjacent units. (dashed bonds)

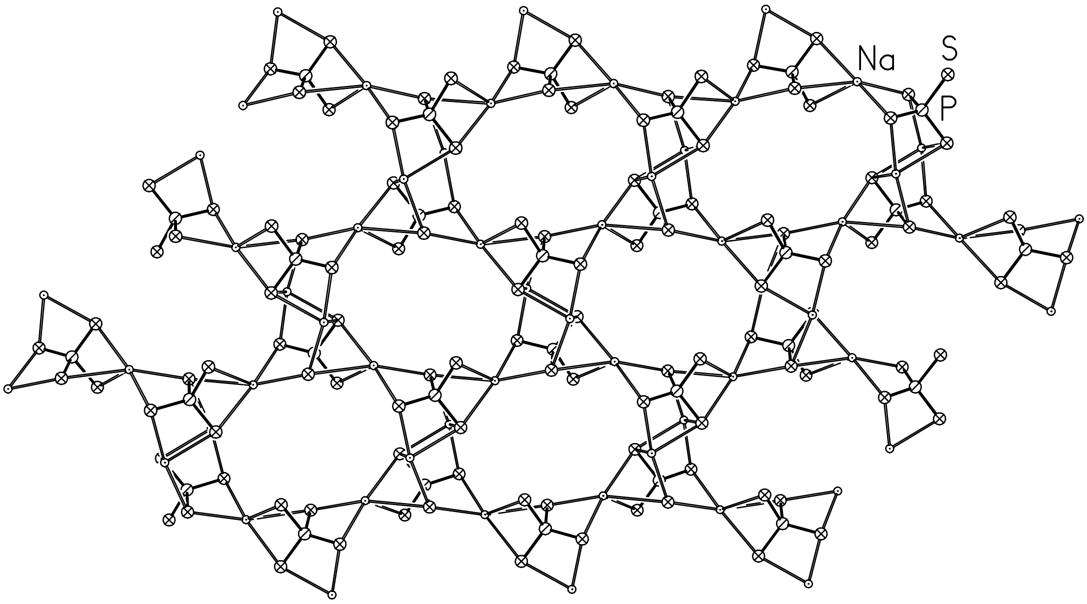

Figure 3.35b Packing diagram of **35** (C, H and O atoms have been omitted).

Table 3.29 Selected ranges of bond lengths (Å) and angles (°)

Bond lengths					
Na-S	2.8150(7)-3.2191(8)	Na-O	2.3453(12)-2.5157(14)	S4-P1	2.1347(6)
S8-P2	2.1291(6)	S-P	2.0187(6)- 2.0228(6)	S4-C	1.8636(16)
S8-C	1.8626(16)				
angles					
O-Na-O	72.35(4)-72.31(4)	O-Na-S	77.08(3)-161.84(4)	S-Na-S	59.031(16)-171.53(2)
S3-P1-S4	96.33(2)	S5-P2-S8	96.48(2)	S-P-S	109.00(2)-113.56(2)

In the solid state, the generated $[^{t}BuSPS_3]^{2-}$ anions in **35** coordinate metal atoms via three edges and one face of a PS_4-tetrahedral building block. The auxiliary ligand DME coordinates in the common chelating mode but O(1) and O(3) are additionally bridging Na atoms (Figure 3.35a top).[162] The Na atoms are six-coordinated (Figure 3.35a bottom) and act as flexible multiacceptor centers in the extended solid-state structure of **35**. A section of the aesthetic arrangement of polymeric **35** is displayed in figure 3.35b. A close look reveals a honeycomb-like architecture consisting of six $[^{t}BuSPS_3]^{2-}$ anions held together by Na^+ ions. In the $^{31}P\{^1H\}$ NMR of a d_8-THF solution, a single resonance at δ 93.3 for the P atom in the $[^{t}BuSPS_3]^{2-}$ anion was observed.

And similar to the former investigation, an metathesis reaction of P_4S_{10} with $NiCl_2{\cdot}6H_2O$ was performed and $[Ni\{P(OH)_2S_2\}_2(thf)_4]$ (**36**) was obtained in moderate yield (Scheme 3.28, Figure 3.36, Table 3.30). In the solid state **36** consists of two $[P(OH)_2S_2]^-$ anions coordinating Ni(1) via the soft S donor centers whilst hydroxyl groups are involved in hydrogen-bonding. So far the closest related compound to 3 represents sodium dithiophosphate $Na_3PO_2S_2$ by Jansen *et al.*, which was synthesized to investigate its ionic conducting properties.[163-165] Currently, the mechanistic investigations of the fragmentation of P/S-cage molecules were in the present case hindered by the poor solubility of byproducts.

$$\mathbf{P_2S_5 + NaS^{\mathit{t}}Bu \xrightarrow[NiCl_2\cdot 6H_2O]{THF} [Ni\{P(OH)_2S_2\}_2(thf)_4]\ (36)}$$

Scheme 3.28 Metathesis reaction of P_4S_{10} with $NiCl_2{\cdot}6H_2O$

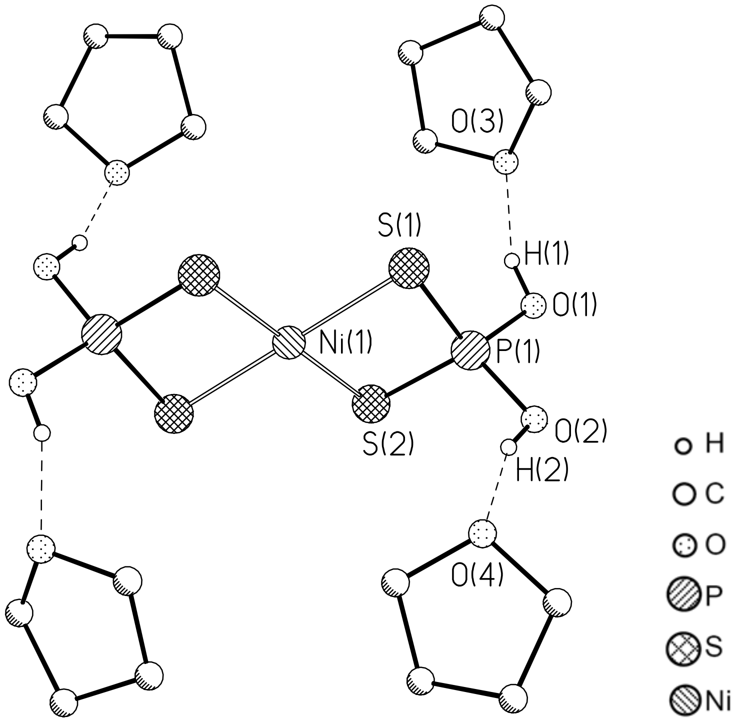

Figure 3.36 Structure of $[Ni\{P(OH)_2S_2\}_2(thf)_4]$ (**36**)

(Hydrogen bonds are shown as dashed lines)

Table 2.2.30 Selected ranges of bond lengths (Å) and angles (°)

Bond lengths					
Ni1-S1	2.2187(11)	Ni1-S2	2.2368(16)	P1-S1	2.0140(16)
P1-S2	2.0002(14)	P1-O1	1.549(3)	P1-O2	1.555(2)
Angles					
S-Ni-S	87.98(6), 92.02(6), 179.999(2)			O1···O3	2.507(4)
O2···O4	2.527(4)	O1-P1-O2	99.41(14)	O1-P1-S1	114.69(11)
O1-P1-S2	115.34(11)	O2-P1-S1	114.25(11)	O2-P1-S2	112.99(12)
S2-P1-S1	100.87(6)				

Till now, an amount of metal complexes containing P/S or P/Se ligands were abtained. According to the literatures, one of the two bridging S atoms can be easily replaced by O or N atom.[166-169] That thiazadiphosphetanes could be given in the reaction of L.R. and phenyl isocyanate helps to solve the key issue-the synthesis of starting materials (Scheme 3.29, Figure 3.37, Table 3.31).

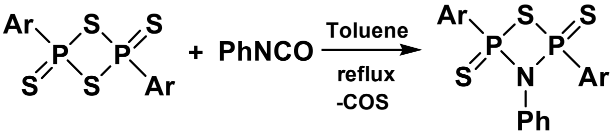

Scheme 3.29 Synthesis of [ArPS(μ-S)(μ-NPh)SPAr] (**37**)

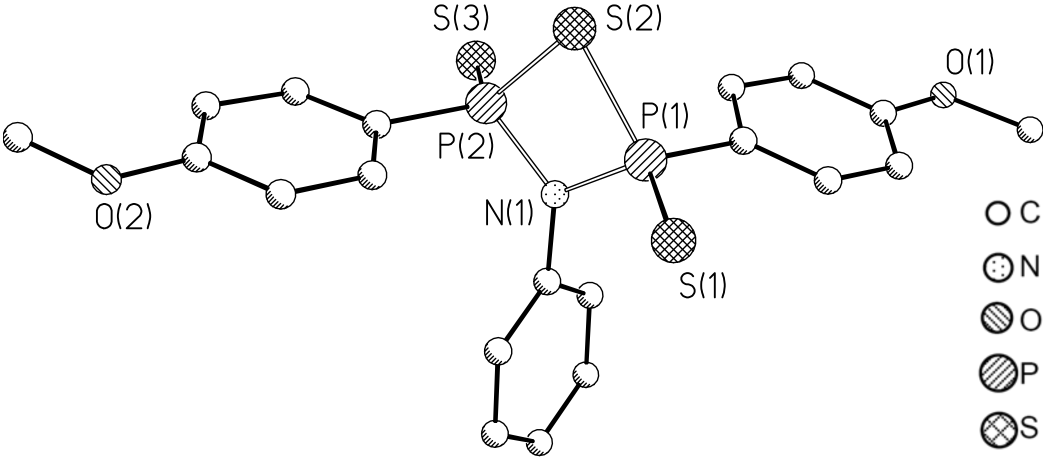

Figure 3.37 Structure of [ArPS(μ-S)(μ-NPh)SPAr] (**37**)

Table 3.31 Selected ranges of bond lengths (Å) and angles (°)

Bond lengths					
N1-P1	1.690(4)	N1-P2	1.685(4)	P1-C1	1.796(5)
P1-S1	1.926(2)	P1-S2	2.1159(17)	P2-C8	1.791(5)
P2-S3	1.9320(19)	P2-S2	2.1264(17)		
Angles					
P2-N1-P1	106.5(2)	N1-P1-S1	115.13(15)	N1-P1-S2	87.14(14)
N1-P2-S3	117.17(15)	N1-P2-S2	86.93(15)	P1-S2-P2	79.17(6)

In the solid state, the angle of P(1)-S(2)-P(2) is 79.17(6)°, a little smaller than that in Lawesson's reagent (87.15°). The bond length of P(1) and the bridging S atom changes from 2.1238(12) to 2.1159(17) Å.[88] So the ring-opening reactions would be a little more difficult than L.R., but a new kind of complexes containing P/S/N ligands would be obtained if the four-membered ring is opened successfully in future!

4. Experimental Section

All operations were carried out under purified dinitrogen. All solvents were dried over the appropriate drying agent and freshly distilled prior to use. Toluene was dried with sodium, dichloromethane was dried with CaH_2, pentane, hexane, DME (dimethoxyethane) were dried with sodium, diethyl ether was dried with molecular sieves 4Å and freshly distilled.

Chemicals (Lawesson's reagent, P_2S_5, P_2S_3, PPh_3, dppm, NaO^tBu, KO^tBu, $FeCl_2$, $CdCl_2$, $NiCl_2$, $NiCl_2{\cdot}6H_2O$, KOAc, AgOAc, $Ni(OAc)_2$, $Fe(OAc)_2$, $Ni(OAc)_2{\cdot}4H_2O$, $Mg(OAc)_2{\cdot}4H_2O$, $Mn(OAc)_2{\cdot}4H_2O$ and $NaOAc{\cdot}3H_2O$) were purchased from Aldrich, Fluka or Merck and used without further purification. CuO^tBu, CuOAc, CuSR (R = Et, ^tBu and Cyclohexyl), KS^tBu, NaS^tBu, $NaSe^tBu$, RbO^tBu, dppa (1,2-Bis-diphenylphosphinoamine) and Woollins' reagent were synthesized according to published procedures. [101,103,119,120,170,171]

Elemental analysis was obtained on a Vario elemental analyser. NMR spectra were recorded on a BRUKER AMX300WB-Spectrometer. For ^{31}P NMR, 65% $H_3PO_4(aq)$ is used as an internal standard. Infra-red spectra were measured on a BRUKER XIFS 28-Spectrometer. GC-MS was measured by HP-5890, and GC Conditions: analyzed by a flame ionization detector (FID) and a HP-5 analytical column (30-m fused silica column with an internal diameter of 0.32 mm and a film thickness of 0.25 μm). The initial oven temperature was 70°C, which was ramped by 10 K/min to the final temperature of 270°C.

4.1 Syntheses of starting materials

The synthetic procedures of CuO^tBu, CuSR (R = Et, ^tBu and Cyclohexyl), dppa, Woollins' reagent, $PhP(S^tBu)_2$ and $PhP(Se)(S^tBu)_2$ are as follows:

4.1.1 CuO^tBu [120]

A three-necked 250 mL flask equipped with a 100 mL dropping funnel, a nitrogen inlet and a magnetic stirrer bar is charged with 34.0 g (237 mmol) CuBr. CuBr is suspended in 100 mL THF. In a 100 mL flask 24.0 g (214 mmol) KO^tBu are dissolved in 80 mL THF and the solution is transferred into the dropping funnel. The CuBr suspension is cooled using an ice-bath and the KO^{t}Bu solution is added to the suspension dropwise. After the addition is complete the mixture is allowed to warm to room temperature and the dropping funnel is replaced by a stopper. The mixture is stirred for 14 hours to give a pale yellow suspension. The solvent is carefully removed under reduced pressure and the solid residue is transferred to an extractor equipped with a nitrogen inlet. The charged extractor replaces the a stopper of a three-nacked 250 mL flask with 200 mL hexane, equipped with a nitrogen inlet. In a counter current of inert gas a reflux condenser with a nitrogen inlet is placed on the extractor. The hexane is stirred and heated with a heating mantel distilling *ca.* 60 mL hexane via the sidearm of the extractor onto the solid residue (**caution**: Teflon tap is open). The heating mantel is removed and the Teflon tap *closed*. After filtration the Teflon tap is opened and hexane is distilled onto the solid residue again. This procedure is repeated for about 3h. Stop heating and the flask is cooled down to room temperature overnight allowing the product to crystallize. Yield 18 g (61%) yellow crystals of CuO^{t}Bu.

4.1.2 CuSR (R = ^{t}Bu, Et and Cyclohexyl)

To an ice-cold mixture of 50 mL conc. NH_3(aq.) and 100 mL H_2O was added $CuSO_4·5H_2O$ 12.6 g (50.4 mmol) forming a royal blue solution. Over a period of 90 minutes, solid $NH_2OH·HCl$ 7.9 g (56.0 mmol) was added. Stirring overnight at room temperature under nitrogen purge produced a colourless solution. Then a solution of ^{t}BuSH (4.65 g, 51.7 mmol) in 250 EtOH was added dropwise. A pale yellow solid formed immediately. The solid product was collected via filtration and washed with H_2O, EtOH and ether in succession and vacuum-dried (5.7g, 37.4 mmol, 74.2%). Other Cu(I) thiolates were prepared similarly. Found: C, 31.10; H, 5.82. C_4H_9CuS (152.7) requires C, 31.46; H, 5.94%.

4.1.3 dppa (1,2-Bis-diphenyphosphinoamine)

2.12 mL $((CH_3)_3Si)_2NH$ was dissolved in 30 mL toluene and the solution was heated with a heating mantel to 50°C for 40 minutes. Then the temperature was raised to 70°C and 3.6 mL Ph_2PCl was added dropwise. The resulting yellow solution was stirred at 70°C for 3h. The solvent was removed under reduced pressure and the solid residue was washed with hexane and vacuum-dried.

4.1.4 Woollins' reagent [101,103]

a. $(PPh)_5$

To a suspension of 20 g (2.5 mol) LiH in 500 mL THF, 137 mL $PhPCl_2$ was added dropwise under nitrogen. The mixture was heated to reflux for 1h, and then filtered. The solvent was removed under reduced pressure and 150 mL toluene was added to the residue. The resulting yellow solution was heated to reflux and the filtration was cooled down to room temperature overnight allowing the product to crystallize. Yield 40 g (37%) yellow crystals of $(PPh)_5$. In order to improve the purity one can use benzene to recrystallize the product.

b. Woollins' reagent

Woollins' reagent was prepared according to published procedures. A mixture of $(PPh)_5$ and ten equivalents of Se powder in toluene was refluxed for 5h, during this time the formation of a red precipitate was observed. The mixture was filtered and the residue was washed with cold toluene and vacuum-dried, yield 90%. Found: C, 26.72; H, 1.92. $C_{12}H_{10}P_2Se_4$ requires C, 27.09; H, 1.89%.

4.1.5 $PhP(S^tBu)_2$

1.12 g (10.0 mmol) NaS^tBu was suspended in 15 mL THF, and a solution of 0.90 g (5.0 mmol) $PhPCl_2$ in 5 mL THF was added dropwise. The mixture was stirred for 4h at room temperature, then THF was removed and 20 mL toluene was added. The precipitate was filtered off, and the solution was concentrated to obtain a colourless oil. 1.08 g, yield 76%. (For NMR and GC-MS studies) δ_H (400 MHz, $CDCl_3$, 25ºC) 1.55 (18H, s, 2 × $C(CH_3)_3$), 7.41 (3H, m, ArH), 7.87 (2H, m, ArH); δ_P (162 MHz, $CDCl_3$, 25ºC, 65% H_3PO_4) 40.3; GC-MS retention time (min) 16.43; *m/z* (relative intensity) 286 (11, M^+), 230 (34, $-C_4H_8$), 174 (100, $-C_4H_8$), 141 (29, M_1^+, -SH), 107 (34, M_1^+-SH_2), 77 (8, M_1^+-PSH) (M = $PhP(S^tBu)_2$, M_1 = PhPSH).

4.1.6 $PhP(Se)(S^tBu)_2$

0.16 g (2.0 mmol) Se powder was suspended in 10 mL toluene, and a solution of 0.57 g (2.0 mmol) $PhP(S^tBu)_2$ was added dropwise. The mixture was refluxed for 4h and then filtered. The remaining yellow solution was concentrated to obtain a yellow solid. (For

NMR and GC-MS studies) δ_H (400 MHz, $CDCl_3$, 25 ºC) 1.55 (18H, s, $C(CH_3)_3$), 7.51 (3H, m, ArH), 8.28 (2H, m, ArH); δ_P (162 MHz, $CDCl_3$, 25 ºC, 65% H_3PO_4) 43.6 (s + d satellites, $^1J_{P\text{-}Se}$ = -801 Hz); δ_{Se} (76 MHz, $CDCl_3$, 25ºC) -50.7 (d, $^1J_{P\text{-}Se}$ = -801 Hz); GC-MS retention time (min) 16.42; *m/z* (relative intensity) 286 (6, M^+-80), 230 (21, -C_4H_8), 174 (77, -C_4H_8), 141 (26, M_1^+, -SH), 107 (17, M_1^+-SH_2), 77 (9, M_1^+-PSH), 57 (100) (M = $PhP(S^tBu)_2$, M_1 = PhPSH).

4.2 Syntheses of new complexes

4.2.1 [Cu_2(*o*-$CO_2C_6H_4SO_3$)(dppm)$_2$]•3CH_2Cl_2 (1)

To a solution of 184 mg (1.0 mmol) 2-Sulfo-benzoesäureanhydrid in toluene (or DME) (10 mL) was added dropwise a solution of 136 mg (1.0 mmol) CuO^tBu in 5 mL toluene (or DME). The resulting yellow solution was heated for about 5 minutes, and then a solution of 384 mg (1.0 mmol) dppm in 5 mL toluene (or DME) was added. The solvent was removed under reduced pressure after 1h. Addition of CH_2Cl_2 (3 mL) and pentane (5 mL) and storage of the solution at room temperature for 3 days produced colourless crystals. 0.30 g, yield 44%.

4.2.2 [Cu_2(μ_2-ArS_2P-O-PS_2Ar)(PPh_3)$_4$]•CH_2Cl_2 (Ar = 4-anisyl) (2)

a) To a solution of 202 mg (0.5 mmol) Lawesson's reagent in toluene (12 mL) was added dropwise a solution of 136 mg (1.0 mmol) CuO^tBu in 10 mL toluene. The resulting yellow solution was refluxed for about 5 hours during which time a colour change to brown and the formation of a yellow precipitate was observed. The precipitate was dissolved upon addition of a solution of 524 mg (2.0 mmol) PPh_3 in 10 mL toluene. The solvent was removed under reduced pressure. Addition of CH_2Cl_2 (3 mL) and pentane (5 mL) and storage of the solution at room temperature for one day produced colourless crystals. 0.68 g, yield 81%; m.p. 194ºC; found: C, 64.4; H, 4.6. $C_{86}H_{74}Cu_2O_3P_6S_4$ (M = 1594.2) requires C, 64.6; H, 4.6%; ν_{max}/cm^{-1} (KBr) 3046w, 1593s, 1431 (P-C), 1250s, 1105s, 841s (P-O-P), 657s (P=S). δ_H (400 MHz, $CDCl_3$, 25°C) 7.9-6.7 (19H, m, ArH), 3.8 (3H, s, OCH_3); δ_C (100 MHz, $CDCl_3$, 25°C) 161.5-113.1 (ar. C), 55.3 (s, $O\underline{C}H_3$); δ_P (162 MHz, $CDCl_3$, 25°C, 65% H_3PO_4) 91.2 (s, $ArPS_2O$), -3.6 (s, $CuPPh_3$).

b) A mixture of Lawesson's reagent (202 mg, 0.5 mmol) and CuOAc (123 mg, 1.0 mmol) was dissolved in 15 mL toluene (or DME). The resulting yellow solution was refluxed for about 4h during which time a yellow precipitate was observed. The precipitate was dissolved upon addition of a solution of 524 mg (2.0 mmol) PPh_3 in 8 mL toluene (or DME). The solvent was removed under reduced pressure. Addition of CH_2Cl_2 (4 mL) and pentane (5 mL) and storage of the solution at room temperature for 3 days produced colourless crystals. 0.54 g, yield 68%.

4.2.3 $[Cu_4\{Ar(\mu_2\text{-}S)_2P\text{-}O\text{-}P(\mu_2\text{-}S)_2Ar\}_2(dppa)_2]\cdot 3CH_2Cl_2$ (Ar = 4-anisyl) (3)

To a solution of 202 mg (0.5 mmol) Lawesson's reagent in toluene (12 mL) was added dropwise a solution of 136 mg (1.0 mmol) CuO^tBu in 10 mL toluene. The resulting yellow solution was refluxed for about 5 hours during this time a colour change to brown and the formation of a yellow precipitate was observed. The precipitate was dissolved upon addition of a solution of 385 mg (1.0 mmol) dppa in 10 mL toluene. The solvent was removed under reduced pressure. Addition of CH_2Cl_2 (3 mL) and pentane (5 mL) and storage of the solution at room temperature for one day produced colourless crystals. 0.42 g, yield 79%; m.p. 201ºC; found: C, 49.3; H, 3.8. $C_{76}H_{68}Cu_4N_2O_6P_8S_8$ (M = 1859.8) requires C, 48.9; H, 3.7%; ν_{max}/cm^{-1} (KBr) 3297w (N-H), 3051w, 1596s, 1435s (P-C), 1258s, 1107s, 880bs (P-O-P), 694s (P=S); δ_H (400 MHz, CD_2Cl_2, 25°C) 8.1-6.9 (24H, m, ArH), 5.4 (1H, s, *NH*, next to peak for CH_2Cl_2), 3.9-3.8 (3H, s, O*CH₃*); δ_C (100 MHz, CD_2Cl_2, 25°C): 162.2-113.5 (10 C, ar. C), 55.8 (1C, s, $O\underline{C}H_3$); δ_P (162 MHz, CD_2Cl_2, 25°C, 65% H_3PO_4): 89.1 (s, Ar*P*S_2O), 38.3 (br. s, N*P*Ph_2).

4.2.4 $[Cu_2(\mu_4\text{-}ArPS_3)(PPh_3)_2]_2\cdot 2CH_2Cl_2$ (Ar = 4-anisyl) (4)

a) A mixture of Lawesson's reagent (202 mg, 0.5 mmol) and CuO^tBu (136 mg, 1.0 mmol) was dissolved in 15 mL DME. The yellow-brown solution was heated to reflux for 4 hours during which time the formation of a yellow precipitate was observed. The precipitate dissolved upon addition of a solution of PPh_3 (524 mg, 2.0 mmol) in 8 mL DME. The solvent was removed under reduced pressure. Addition of CH_2Cl_2 (3 mL) and pentane (4 mL) and storage of the solution at room temperature for 2 days produced colourless crystals. 0.35 g, yield 79%; m.p. 197ºC; found: C, 53.8; H, 3.9. $C_{88}H_{78}Cl_4Cu_4P_6S_6$ requires C, 54.4; H, 4.0%; ν_{max}/cm^{-1}(KBr) 3051w, 1589s, 1430s (P-C), 1246s, 689s (P=S); δ_H (400 MHz, $CDCl_3$, 25°C) 8.0-7.9 (4H, dd, *J* = 7.6Hz, ArH), 7.4-7.3 (60H, m, ArH), 6.7 (4H, d, *J*

= 7.6Hz, ArH), 3.8 (3H, s, O*CH₃*); δ_C (100 MHz, $CDCl_3$, 25°C) 161.6-113.0 (8C, ar. C), 55.3 (1C, s, O$\underline{C}$H$_3$); δ_P (162 MHz, $CDCl_3$, 25°C, 65% H_3PO_4) 91.0 (s, Ar*P*S_3), -3.37 (s, *P*Ph_3).

b) A mixture of Lawesson's reagent (202 mg, 0.5 mmol) and CuS^{t}Bu (153 mg, 1.0 mmol) was dissolved in 15 mL toluene (or THF). The yellow solution was heated to reflux for 4 hours during which time the formation of a yellow precipitate was observed. The precipitate dissolved upon addition of a solution of PPh_3 (524 mg, 2.0 mmol) in 6 mL toluene (or THF). The solvent was removed under reduced pressure. Addition of CH_2Cl_2 (6 mL) and pentane (4 mL) and storage of the solution at room temperature for 2 days produced colourless crystals.

4.2.5 [Cu(ArP(S^{t}Bu)S$_2$)(PPh$_3$)$_2$] (Ar = 4-anisyl) (5)

A mixture of Lawesson's reagent (202 mg, 0.5 mmol) and CuS^{t}Bu (306 mg, 2.0 mmol) was dissolved in 8 mL THF. The yellow solution was stirred for about 3 hours at room temperature. The solvent was removed under reduced pressure, and the residue was redissolved by addition of a solution of PPh_3 (0.57 M in THF, 4 mL). The solution was layered with 50 mL hexane and storage of the solution at room temperature for 3 weeks produced colourless crystals. 0.25 g, yield 29%; m.p. 185-187°C; found: C, 64.00; H, 5.11. $C_{47}H_{46}CuOP_3S_3$ requires C, 64.18; H, 5.27%; ν_{max}/cm^{-1} (KBr) 3053m, 2957m, 2835w (CH_3O), 1592s, 1495s (P-C), 1249s, 692s (P=S); δ_H (400 MHz, $CDCl_3$, 25°C) 1.28 (9H, s, OC(*CH₃*)$_3$), 3.90 (3H, s, O*CH₃*), 6.86 (2H, m, ArH), 7.30 (30H, m, P*Ph₃*), 8.08 (2H, m, ArH); δ_C (100 MHz, $CDCl_3$, 25°C) 32.0, 52.4, 55.3, 128.2, 128.3, 129.2, 132.4, 132.6, 133.8, 133.9, 134.1; δ_P (162 MHz, $CDCl_3$, 25°C, 65% H_3PO_4) 74.9, -4.8 (br, s, *P*Ph_3).

4.2.6 $^1/_\infty$[Na{ArP(O^{t}Bu)S$_2$}(thf)]$_\infty$ (Ar = 4-anisyl) (6)

A mixture of Lawesson's reagent (606 mg, 1.5 mmol) and NaO^{t}Bu (288 mg, 3.0 mmol) was dissolved in 10 mL THF. The light yellow (almost colourless) solution was stirred overnight at room temperature and then the solution was layered with 50 mL hexane. Storage of the solution at room temperature for 5 days produced colourless crystals. 0.79 g, yield 71%; m.p. ~120°C (decomposition); found: C, 48.40; H, 6.31. $C_{15}H_{24}NaO_3PS_2$ requires C, 48.63; H, 6.53%; ν_{max}/cm^{-1} (KBr) 2973s, 2873s (OCH_3), 1592s, 1496s (P-C), 1237s, 1102s, 683s br (P=S); δ_H (400 MHz, $CDCl_3$, 25°C) 1.53

(9H, s, OC*(CH$_3$)$_3$*), 1.80 (4H, m, 2 x OCH$_2$*CH$_2$*), 3.63 (4H, m, 2 x O*CH$_2$*CH$_2$), 3.78 (3H, s, O*CH$_3$*), 6.78 (2H, m, ArH), 8.08 (2H, m, ArH); δ_P (162 MHz, CDCl$_3$, 25°C, 65% H$_3$PO$_4$) 96.7.

4.2.7 $[Na_2\{ArP(O^tBu)(\mu\text{-}S)S\}_2(dme)_2]$ (Ar = 4-anisyl) (7)

A mixture of Lawesson's reagent (606 mg, 1.5 mmol) and NaO^{t}Bu (288 mg, 3.0 mmol) was dissolved in 10 mL DME. The light yellow (almost colourless) solution was stirred overnight at room temperature and then the solution was layered with 80 mL hexane. Storage of the solution at room temperature for 2 weeks produced colourless crystals. 0.4 g, yield 34%; m.p. 127°C ; found: C, 46.20; H, 6.69. $C_{30}H_{52}Na_2O_8P_2S_4$ requires C, 46.38; H, 6.75%; ν_{max}/cm^{-1} (KBr) 2924s br, 2822s (OCH$_3$), 1590s, 1492s (P-C), 1231s, 1090s, 683s br (P=S).

4.2.8 $1/\infty[K_2\{ArP(O^tBu)(\mu\text{-}S)S\}_2(thf)_2]_\infty$ (Ar = 4-anisyl) (8)

A mixture of Lawesson's reagent (606 mg, 1.5 mmol) and KO^{t}Bu (336 mg, 3.0 mmol) was dissolved in 10 mL THF. The light yellow (almost colourless) solution was stirred overnight at room temperature and then the solution was layered with 50 mL hexane. Storage of the solution at room temperature for 4 days produced colourless crystals. 0.84 g, yield 72%; m.p. ~120°C (decomposition); found: C, 46.35; H, 6.02. $C_{15}H_{24}KO_3PS_2$ requires C, 46.61; H, 6.26%; ν_{max}/cm^{-1} (KBr) 2970s, 2840s (OCH$_3$), 1591s, 1493s (P-C), 1230s, 1096s, 678s br (P=S); δ_H (400 MHz, CDCl$_3$, 25°C) 1.49 (9H, s, OC*(CH$_3$)$_3$*), 1.79 (4H, m, 2 x OCH$_2$*CH$_2$*), 3.64 (4H, m, 2 x O*CH$_2$*CH$_2$), 3.77 (3H, s, O*CH$_3$*), 6.76 (2H, m, ArH), 8.13 (2H, m, ArH); δ_P (162 MHz, CDCl$_3$, 25°C, 65% H$_3$PO$_4$) 96.6.

4.2.9 $1/\infty[K_2\{ArP(O^tBu)(\mu\text{-}S)S\}_2(dme)_2]_\infty$ (Ar = 4-anisyl) (9)

A mixture of Lawesson's reagent (606 mg, 1.5 mmol) and KO^{t}Bu (336 mg, 3.0 mmol) was dissolved in 10 mL DME. The light yellow (almost colourless) solution was stirred overnight at room temperature and then the solution was layered with 60 mL hexane. Storage of the solution at room temperature for 5 days produced colourless crystals. 0.93 g, yield 77%; m.p. ~115°C (decomposition); found: C, 44.14; H, 6.22. $C_{15}H_{26}KO_4PS_2$ requires C, 44.53; H, 6.48%; ν_{max}/cm^{-1} (KBr) 2970s, 2840m (OCH$_3$), 1592s, 1496s (P-C), 1235s, 1101s, 677s (P=S).

4.2.10 1/∞[K_4\{ArP(S^tBu)(μ-S)S\}$_4$(thf)$_4$]$_\infty$ (Ar = 4-anisyl) (10)

A mixture of Lawesson's reagent (202 mg, 0.5 mmol) and KS^tBu (128 mg, 1.0 mmol) was dissolved in 8 mL THF. The colourless solution was stirred overnight at room temperature and then the solution was layered with 70 mL hexane. Storage of the solution at room temperature for 2 weeks produced colourless crystals. 0.32 g, yield 80%; m.p. 115ºC (decomposed); found: C, 44.33; H, 5.78. $C_{60}H_{96}K_4O_8P_4S_{12}$ requires C, 44.75; H, 6.01%; ν_{max}/cm^{-1} (KBr) 2955s, 2836m (OCH_3), 1590s, 1494s (P-C), 1238s, 1095s , 664s br (P=S).

4.2.11 [Cu_{14}(μ_6-ArP(O)S_2)$_6$(μ_3-ArP(O)(OAc)S)$_2$(PPh_3)$_6$)]•8THF (Ar=4-anisyl) (11)

A mixture of Lawesson's reagent (202 mg, 0.5 mmol) and CuOAc (246 mg, 2.0 mmol) was dissolved in 8 mL THF. The mixture was stirred for about 2 hours at room temperature, during which time the formation of a yellow precipitate was observed. The mixture was filtered and the residue dissolved by addition of a solution of PPh_3 (0.4 M in thf, 2.5 mL). Solvent diffusion within a double-Schlenck tube of Et_2O (0ºC) into the reaction mixture (room temperature) produced light yellow crystals after 4 days. 0.32 g, yield 60%; m.p. 193ºC (decomposition); found: C, 47.1; H, 3.6. $C_{168}H_{152}Cu_{14}O_{20}P_{14}S_{14}$ requires C, 47.3; H, 3.6%; ν_{max}/cm^{-1} (KBr) 3047w, 1755m (C=O), 1591s, 1433s (P-C), 1173s, 1094bs, 691s (P=S).

4.2.12 [Ag_4\{μ_4-ArP(O)S_2\}$_2$(dppm)$_4$]•2Et_2O•2THF (Ar = 4-anisyl) (12)

A mixture of Lawesson's reagent (202 mg, 0.5 mmol) and AgOAc (334 mg, 2.0 mmol) was dissolved in 10 mL THF. The mixture was stirred for about 3 hours at room temperature, during which time the formation of a grey-yellow precipitate was observed. The mixture was filtered and the residue was dissolved by addition of a solution of dppm (0.26 M in thf, 7.2 mL). Solvent diffusion within a double-Schlenck tube of Et_2O (0ºC) into the reaction mixture (room temperature) produced orange crystals after 7 days. 0.58 g, yield 51%; m.p. 149ºC (decomposed, black solid); found: C, 56.87; H, 4.63. $C_{114}H_{102}Ag_4O_4P_{10}S_4$ requires C, 56.92; H, 4.27%; ν_{max}/cm^{-1} (KBr) 3051s, 2859s (CH_3O), 1592s, 1431s (P-C), 1241s, 1090s and 692s (P=S); δ_H (400 MHz, $CDCl_3$, 25ºC) 1.25 (14H, t, *J* = 7.2 Hz, 4.7 x OCH_2CH_3), 1.90 (14H, m, 3.5 x OCH_2CH_2), 3.52 (17H, t and br, s, *J* = 7.2 Hz, 4.7 x OCH_2CH_3 and 4 x P-CH_2-P), 3.77-3.80 (14H, m, 3.5 x O*CH2*CH_2), 6.90-7.05 (84H, m, ArH), 8.54 (4H, m, ArH); δ_P (162 MHz, $CDCl_3$, 25ºC, 65% H_3PO_4) 66.7, -6.5 (br, s, dppm).

4.2.13 $[Ag_{28}(\mu_6\text{-}S)_2\{ArP(O)S_2\}_{12}(PPh_3)_{12}]\cdot 2Et_2O\cdot 13THF$ (Ar = 4-anisyl) (13)

A mixture of Lawesson's reagent (202 mg, 0.5 mmol) and AgOAc (334 mg, 2.0 mmol) was dissolved in 10 mL THF. The mixture was stirred for about 3 hours at room temperature, during which time the formation of a grey-yellow precipitate was observed. The mixture was filtered and the residue was dissolved by addition of a solution of PPh_3 (0.4 M in thf, 6 mL). Solvent diffusion within a double-Schlenck tube of Et_2O (0ºC) into the reaction mixture (room temperature) produced orange crystals after 7 days. 0.33g, yield 52; m.p. 140ºC (decomposed, black solid); found: C, 40.18; H, 2.95. $C_{300}H_{264}Ag_{28}O_{24}P_{24}S_{26}$ requires C, 40.71; H, 3.01%; ν_{max}/cm^{-1} (KBr) 3043m, 2830w (CH_3O), 1592s, 1433s (P-C), 1245s, 1093s and 691s (P=S); δ_H (400 MHz, $CDCl_3$, 25ºC) 1.25 (15H, t, *J* = 7.2 Hz, 5 x OCH_2*CH_3*), 1.90 (20H, m, 5 x OCH_2*CH_2*), 3.52 (12H, t, *J* = 7.2 Hz, 5 x O*CH_2*CH_3), 3.67-3.85 (56H, m, 5 x O*CH_2*CH_2 and 12 x O*CH_3*), 6.79-6.92 (24H, m, ArH), 7.26 (180H, br, P*Ph_3*) and 7.80-7.93 (24H, m, ArH); δ_P (162 MHz, $CDCl_3$, 25ºC, 65% H_3PO_4) 72.1, 68.7, 2.4 (br, s, *P*Ph_3).

Byproducts like Ac_2O or $[ArPOS]_3$ were found and characterised in similar reactions.

4.2.14 $[Fe_2(\mu\text{-}ArPS_3)(thf)_4]$ (Ar = 4-anisyl) (14)

A mixture of Lawesson's reagent (202 mg, 0.5 mmol) and anhydrous $Fe(OAc)_2$ (174 mg, 1.0 mmol) was dissolved in 10 mL THF. The brown solution was stirred for 5 hours at room temperature. The slightly cloudy solution was filtered and the filtrate layered with 15 mL Et_2O. Storage of the solution at room temperature for 4 days produced yellow crystals. 0.18 g, yield 83%; m.p. >300ºC; found: C, 39.5; H, 4.0. $[C_{30}H_{46}Fe_2O_6P_2S_6(\text{-}C_4H_8O)]$ requires C, 39.2; H, 4.8%; ν_{max}/cm^{-1} (KBr) 2936w, 1597s, 1439s (P-C), 1258s, 915bs, 658s (P=S).

4.2.15 $[Ni_2\{ArP(O)S_2\}_2(thf)_2(H_2O)_2]_2$ (Ar = 4-anisyl) (15)

A mixture of Lawesson's reagent (202 mg, 0.5 mmol) and $[Ni(OAc)_2{\cdot}4H_2O]$ (250 mg, 1.0 mmol) was dissolved in 8 mL THF. The resulting purple solution was stirred for about 5 hours at room temperature. The solution was layered with 15 mL Et_2O and stored at room temperature for 3 days producing purple crystals. 0.20 g, yield 54%;

m.p. > 300ºC (decomposition); found: C, 35.9; H, 4.5. $C_{44}H_{68}Ni_4O_{16}P_4S_8$ requires C, 36.0; H, 4.7%; UV (Nujol mull) λ_{max}/nm 253, 340, 652; ν_{max}/cm^{-1} (KBr) 3374s br (H_2O), 2962w, 1594s, 1440s (P-C), 878bw, 654s (P=S); δ_H (400 MHz, d_6-DMSO, 25°C) 8.3 (8H, s, br, ArH), 6.9 (8H, s, br, ArH), 3.8 (12H, s, O*CH₃*), 3.6 (16H, s, THF), 2.5 (16H, s, THF), 1.7 (8H, s, H_2O); δ_P (162 MHz, d_6-DMSO, 25°C, 65% H_3PO_4) 56.1 (s, Ar*P*S_2O).

4.2.16 [$Cd_2\{ArP(O^tBu)(\mu\text{-}S)S\}_4$] (Ar = 4-anisyl) (16)

To a mixture of KO^{t}Bu (224 mg, 2.0 mmol) and $CdCl_2$ (184 mg, 1.0 mmol) was added 10 mL DME. After the yellow cloudy solution was heated at 50ºC for 3 hours Lawesson's reagent 202 mg (0.50 mmol) was added. The precipitate was filtered off and the colourless solution layered with 25 mL hexane. Storage of mixture at room temperature for 2 weeks produced colourless crystals. 0.21 g, yield 63%; m.p. 126ºC (decomposed, mass change (differential thermal analysis) found -18.2%; mass change expected for $C_{44}H_{64}Cd_2O_8P_4S_8$ -2^{t}Bu$_2$O: -19.6%); found: C, 40.57; H, 4.57. $C_{44}H_{64}Cd_2O_8P_4S_8$ requires C, 39.85; H, 4.86%; ν_{max}/cm^{-1} (KBr) 2976s, 2834m (OCH_3), 1591s, 1497s (P-C), 1249s, 1106s, 672s (P=S).

4.2.17 [$Fe_2(\mu\text{-}ArPS_3)(thf)_4$] (Ar = 4-anisyl) (17)

A mixture of Lawesson's reagent (202 mg, 0.5 mmol) and NaS^{t}Bu (112 mg, 1.0 mmol) was dissolved in 8 mL THF. The colourless solution was stirred for about 4 hours at room temperature, and then added to $FeCl_2$ 64 mg (0.5 mmol). The filtrate was layered with 20 mL hexane. Storage of the solution at room temperature for 5 days produced yellow crystals. 0.13 g, yield 65%. Found: C, 39.2; H, 4.5. $[C_{30}H_{46}Fe_2O_6P_2S_6(-C_4H_8O)]_2$ requires C, 39.2; H, 4.8%.

4.2.18 [$Ni\{ArP(OH)S_2\}_2(thf)_2$] (Ar = 4-anisyl) (18)

A mixture of Lawesson's reagent (202 mg, 0.5 mmol) and NaS^{t}Bu (112 mg, 1.0 mmol) was dissolved in 8 mL THF. The colourless solution was stirred for about 5 hours at room temperature, and then added to $NiCl_2{\cdot}6H_2O$ 119 mg (0.5 mmol). The filtrate was layered with 20 mL hexane. Storage of the solution at room temperature for 2 weeks produced purple crystals. 0.19 g, yield 63%; m.p. 195ºC (decomposition); found: C, 39.56; H, 4.71. $[(C_{22}H_{32}NiO_6P_2S_4)_2\text{-}C_4H_8O]$ requires C, 39.68; H, 4.66%; ν_{max}/cm^{-1} (KBr), 2880w (CH_3O), 2293br, 1591m, 1497s (P-C), 1256s, 657s (P=S); δ_H (400 MHz, d_6-DMSO, 25ºC) 1.65 (8H, s, 4 x OCH_2*CH_2*), 3.53 (8H, s, 4 x O*CH_2*CH_2), 3.73 (6H, s, O*CH_3*), 3.81 (2H, s, 2 x O*H*), 6.87~7.11 (4H, m, ArH), 8.21~8.31 (4H, m, ArH); δ_P (162 MHz, d_6-DMSO, 25ºC, 65% H_3PO_4) 42.3, 56.9 (br).

4.2.19 1/∞[$K_2\{PhP(O^tBu)Se_2\}_2(thf)]_\infty$ (19)

A mixture of Woollins' reagent (798 mg, 1.5 mmol) and KO*^{t}*Bu (336 mg, 3.0 mmol) was dissolved in 15 mL THF. The yellow solution was stirred overnight at room temperature and then layered with 80 mL hexane. Storage of the solution at room temperature for 2 weeks produced yellow crystals. 0.43 g, yield 35%; m.p. 131°C (decomposed); found: C, 34.69; H, 4.40. $C_{24}H_{36}K_2O_3P_2Se_4$ (828.52) requires C, 34.79; H, 4.38%; ν_{max}/cm^{-1} (KBr) 3047m, 2970s, br, 1433s (P-C), 1304s, 1162s, 1091s, 928s br and 692s; δ_H (400 MHz, d_8-THF, 25°C) 1.60 (s, 18H, C*(CH3)3*), 1.78 (m, 4H), 3.64 (m, 4H), 7.22 (m, 6H, ArH), 8.26 (m, 4H, ArH); δ_C (100 MHz, d_8-THF, 25°C) 30.09, 30.14, 125.84, 125.97, 127.79, 129.70, 129.82, 147.48, 148.38; δ_P (162 MHz, d_8-THF, 25°C, 65% H_3PO_4): 60.37 (s+d satellites, $^1J_{P\text{-}Se}$ = 675 Hz; δ_{Se} (76 MHz, d_8-THF, 25°C) 151.2 (d, $^1J_{P\text{-}Se}$ = 675 Hz).

4.2.20 1/∞[$PhPSe_3Na_2(thf)_3]_\infty$ (20)

A mixture of Woollins' reagent (133 mg, 0.25 mmol) and NaS*^{t}*Bu (56 mg, 0.5 mmol) was dissolved in 10 mL THF. The yellow solution was stirred for 4h at room temperature. The slightly cloudy solution was filtered and the filtrate was layered with 40 mL hexane. Storage of this solution at room temperature for 4 weeks produced light yellow (almost colourless) crystals. 0.055 g, yield 44%; m.p. 90~92ºC (>100ºC decomposed); found: C, 28.76; H, 3.43. $C_{24}H_{34}Na_4O_3P_2Se_6$ requires C, 28.88; H, 3.43%; ν_{max}/cm^{-1} (KBr) 3044m, 1606s, 1432s (P-C), 1083s, 691s and 501s br; δ_H (400 MHz, d_8-THF, 25ºC) 1.80 (12H, m, 6 x OCH_2*CH_2*), 3.64 (12H, m, O*CH_2*CH_2), 7.06-7.21 (6H, m, ArH), 8.54 (4H, m, ArH); δ_P (162 MHz, d_8-THF, 25ºC, 65% H_3PO_4) 53.6, -29.4 (s+d satellites, $^1J_{P\text{-}Se}$ = -504 Hz); δ_{Se} (76 MHz, d_8-THF, 25ºC) 363.8 (d, $^1J_{P\text{-}Se}$= -504 Hz). Analysis of the mother liquor: All solvents were removed under reduced pressure. The yellow solid residue was redissolved in 0.8 mL deuterated chloroform and filtered. The filtrate was used for NMR and GC-MS studies. δ_H (400 MHz, $CDCl_3$, 25ºC) 1.56 (18H, s, C*$(CH_3)_3$*), 7.38-7.52 (3H, m, ArH), 8.28 (2H, m, ArH); δ_P (162 MHz, $CDCl_3$, 25ºC, 65% H_3PO_4) 43.7 (s+d satellites, $^1J_{P\text{-}Se}$ = -801 Hz); δ_{Se} (76

MHz, $CDCl_3$, 25ºC) -51.3 (d, $^1J_{P\text{-}Se}$ = -801 Hz); GC-MS retention time (min) 16.42; *m*/*z* (relative intensity) 286 (5, M^+-80), 230 (16, -C_4H_8), 174 (54, -C_4H_8), 141 (M_1^+, 20, -SH), 107 (16, M_1^+-SH_2), 77 (8, M_1^+-PSH), 57 (100) (M = $PhP(S^tBu)_2$, M_1 = PhPSH).

4.2.21 $1/\infty[(PhPSe_2Se\text{-}SeSe_2PPh)K_2(thf)_4]_\infty$ (21)

A mixture of Woollins' reagent (266 mg, 0.5 mmol) and KS^tBu (128 mg, 1.0 mmol) was dissolved in 10 mL THF. The yellow solution was stirred for 5h at room temperature. The slightly cloudy solution was filtered and the filtrate was layered with 35 mL hexane. Storage of this solution at room temperature for 3 weeks produced yellow crystals. 0.06 g, yield 24%; m.p. > 100ºC (decomposed, orange-red solid); found: C, 28.59; H, 3.28. $[(C_{14}H_{21}KO_2\ PSe_3)_8\text{-}5C_4H_8O]$ requires C, 28.58; H, 3.34%; ν_{max}/cm^{-1} (Nujol, selected) 1463s (P-C), 1376s, 1039w, 685s and 537m; δ_H (400 MHz, d_8-THF, 25ºC) 1.81 (8H, m, $OCH_2\mathit{CH_2}$), 3.64 (8H, m, $O\mathit{CH_2}CH_2$), 7.11-7.20 (3H, m, ArH), 8.44 (2H, m, ArH); δ_P (162 MHz, d_8-THF, 25ºC, 65% H_3PO_4) -27.7. Analysis of the mother liquor: All solvents were removed under reduced pressure. The yellow solid residue was redissolved in 0.8 mL deuterated chloroform and filtered. The filtrate was used for NMR and GC-MS studies. δ_H (400 MHz, $CDCl_3$, 25ºC) 1.55 (18H, s, 2 x $C(\mathit{CH_3})_3$), 7.52 (3H, m, ArH), 8.28 (2H, m, ArH); δ_P (162 MHz, $CDCl_3$, 25ºC, 65% H_3PO_4) 43.7 (s+d satellites, $^1J_{P\text{-}Se}$ = -801 Hz), 40.3; δ_{Se} (76 MHz, $CDCl_3$, 25ºC) -50.9 (d, $^1J_{P\text{-}Se}$ = -801 Hz); GC-MS retention time (min) 16.41; *m*/*z* (relative intensity) 286 (5, M^+-80), 230 (16, -C_4H_8), 174 (68, -C_4H_8), 141 (M_1^+, 23, -SH), 107 (17, M_1^+-SH_2), 77 (9, M_1^+-PSH), 57 (100) (M = $PhP(S^tBu)_2$, M_1 = PhPSH).

4.2.22 $1/\infty[(PhPSe_2Se\text{-}SeSe_2PPh)Rb_2(thf)_4]_\infty$ (22)

A mixture of Woollins' reagent (133 mg, 0.25 mmol) and RbO^tBu (79 mg, 0.50 mmol) was dissolved in 10 mL THF. The yellow solution was stirred for 5 hours at room temperature. The slightly cloudy solution was filtered and the filtrate was layered with 40 mL hexane. Storage of this solution at room temperature for 3 weeks produced yellow crystals. 0.05 g, yield 43%; m.p. >90ºC (decomposition); found: C, 20.68; H, 1.82. $[(C_{14}H_{21}RbO_2PSe_3)_2\text{-}3C_4H_8O]$ requires C, 20.60; H, 1.94%; ν_{max}/cm^{-1} (KBr) 3045m, 2959m, 1597m, 1432s (P-C), 1090s and 688s (P=Se), 530s; δ_H (400 MHz, d_8-THF, 25ºC) 1.80 (8H, m, $OCH_2\mathit{CH_2}$), 3.64 (8H, m, $O\mathit{CH_2}CH_2$), 7.21-7.23 (3H, m, ArH), 8.31 (2H, m, ArH); δ_P (162 MHz, d_8-THF, 25ºC, 65% H_3PO_4) 11.6.

4.2.23 $1/\infty[Na_2\{PhSe_2P\text{-}PSe_2Ph\}(thf)_3]_\infty$ (23)

To a mixture of Woollins' reagent (266 mg, 0.5 mmol) and $NaSe^tBu$ (159 mg, 1.0 mmol) was added 10 mL THF. The mixture was stirred at room temperature overnight. The reaction was filtered and the filtrate (yellow solution) was layered with 40 mL hexane. Storage of the solution at room temperature for 1 week produced yellow crystals. 0.1 g, yield 28%; m.p. 190ºC (grey), 215ºC (orange-brown); found: C, 33.19; H, 3.52. [$C_{24}H_{34}Na_2O_3P_2Se_4$-$C_4H_8O$] requires C, 33.26; H, 3.63%; ν_{max}/cm^{-1} (KBr) 3047m, 2958m, 1434s (P-C), 1084s, 689s and 523s; δ_H (400 MHz, d_8-THF; 25ºC) 1.76 (m, 8H), 3.60 (m, 8H), 7.10 (m, 6H, ArH), 8.16 (m, 4H, ArH); δ_C (100 MHz, d_8-THF, 25ºC) 25.13, 67.02, 124.39, 126.34, 126.78, 127.64, 130.14, 134.76; δ_P (162 MHz, d_8-THF, 25ºC, H_3PO_4) 46.8 (s+m, $^1J_{P\text{-}Se}$ = -659 Hz, $^2J_{P\text{-}Se}$ = 9 Hz, $^1J_{P\text{-}P}$ = 146 Hz); δ_{Se} (76 MHz, d_8-THF, 25ºC) -20.8 (dd, $^1J_{P\text{-}Se}$ = -658 Hz, $^2J_{P\text{-}Se}$ = 9 Hz, $^1J_{P\text{-}P}$ = 144 Hz).

4.2.24 $1/\infty[K_2(PhPSe_2Se\text{-}SeSe_2PPh)(thf)_2]_\infty$ (24)

To a mixture of Woollins' reagent (266 mg, 0.5 mmol) and KOAc (98 mg, 1.0 mmol) was added 8 mL THF. The mixture was heated to reflux for 5 hours. The reaction was filtered and the filtrate (yellow solution) was layered with 20 mL hexane. Storage of the solution at room temperature for 4 weeks produced orange crystals. 0.17 g yield 75%; m.p. 148- 150ºC (decomposed); found: C, 26.39; H 2.81. $C_{20}H_{26}K_2O_2P_2Se_6$ requires C, 26.33; H 2.87%; ν_{max}/cm^{-1} (KBr) 3045m, 2964m, 1433s (P-C), 1048s, 688s and 535s; δ_H (400 MHz, d_8-THF, 25ºC) 1.80 (m, 8H), 3.64 (m, 8H), 7.22 (m, 6H, ArH), 8.22 (m, 4H, ArH); δ_C (100 MHz, d_8-THF, 25ºC) 25.41, 67.24, 126.12, 126.26, 128.75, 130.27, 145.78; δ_P (162 MHz, d_8-THF, 25ºC, 65% H_3PO_4) 12.7 (s+d satellites, $^1J_{P\text{-}Se}$ = 655 Hz); δ_{Se} (76 MHz, d_8-THF, 25ºC) 138.0 (d, $^1J_{P\text{-}Se}$ = 655 Hz).

4.2.25 $1/\infty[Na_2(PhPSe_2O)(H_2O)_4(thf)]_\infty$ (25)

To a mixture of Woollins' reagent (266 mg, 0.5 mmol) and [$NaOAc\cdot 3H_2O$] (136 mg, 1.0 mmol) was added 8 mL THF. The mixture was heated for about 5 hours, and then the filtrate (yellow solution) was layered with 25 mL hexane. Storage of the solution at room temperature for 4 weeks produced colourless crystals. 0.2 g, yield 50%; m.p. 95-98ºC (decomposed); found: C, 23.81; H 3.32. [$C_{20}H_{42}Na_4O_{12}P_2Se_4$-$C_4H_8O$-$4H_2O$]

requires C, 24.02; H, 3.28%. ν_{max}/cm^{-1} (KBr) 3349s, br (H_2O), 3052m, 2968m, 1433s (P-C), 1040s and 689s.

4.2.26 [Cu_4(PhSeP-O-PSePh)$_2$(PPh_3)$_4$] (26)

A mixture of Woollins' reagent (177 mg, 0.33 mmol) and CuOAc (164 mg, 1.33 mmol) was dissolved in 10 mL THF. The mixture was stirred for 3 hours at room temperature, during which time the formation of a brown precipitate was observed. The mixture was filtered and the residue was added a solution of PPh_3 (0.57 M in THF, 5 mL). Solvent diffusion within a double-Schlenck tube of Et_2O into the filtrate produced brown crystals after 5 weeks. 0.04 g, yield 10%; despite repeated attempts correct analysis could not be obtained.

4.2.27 [Ni{PhP(OH)Se_2}$_2$(thf)$_2$] (27)

A mixture of Woollins' reagent (266 mg, 0.5 mmol) and NaS^{t}Bu (112 mg, 1.0 mmol) was dissolved in 10 mL THF. The colourless solution was stirred for about 5 hours at room temperature, and then added to $NiCl_2{\cdot}6H_2O$ 119 mg (0.5 mmol). The filtrate was layered with 20 mL hexane. Storage of the solution at room temperature for 2 weeks produced brown crystals. (or: A mixture of Woollins' reagent 266 mg (0.5 mmol) and $Ni(OAc)_2{\cdot}4H_2O$ 125 mg (0.5 mmol) was dissolved in 8 mL THF. The brown solution was stirred overnight at room temperature, and then the filtrate was layered with 40 mL hexane. Storage of the solution at room temperature for 2 weeks produced brown crystals. 0.23 g, yield 60%; m.p. 180ºC (decomposition); found: C, 30.88; H, 3.49. $C_{20}H_{28}NiO_4P_2Se_4$ requires C, 31.24; H, 3.67%; ν_{max}/cm^{-1} (KBr) 3129br, 1478m (P-C),1434s, 1110s, 900s br, 685s (P=S); δ_H (400 MHz; d_8-THF, 25ºC) 1.80 (8H, s, 4 x $OCH_2\mathit{CH_2}$), 3.65 (8H, s, 4 x $O\mathit{CH_2}CH_2$), 7.54 (6H, m, ArH), 8.17 (4H, m, ArH), 12.19 (2H, br, s, 2 x OH); δ_P (162 MHz, d_8-THF, 25ºC, 65% H_3PO_4) 37.9 (s+d satellites, $J_{P\text{-}Se}$ = 520 Hz).

4.2.28 [Mg{PhP(Se,O)Se-Se(O,Se)PPh}(thf)$_4$(H_2O)$_2$]·[Mg{PhP(Se,O)Se-Se (O,Se)PPh}(thf)$_3$(H_2O)] (28)

A mixture of Woollins' reagent (266 mg, 0.5 mmol) and $Mg(OAc)_2{\cdot}4H_2O$ (107 mg, 0.5 mmol) was dissolved in 8 mL THF. The yellow solution was heated to about 50ºC for 5 hours and stirred overnight at room temperature, and then the filtrate was layered with 50 mL hexane. Storage of the solution at room temperature for 4 weeks produced yellow crystals. 0.26 g, yield 60% (based on $[Mg(OAc)_2(H_2O)_4]$ supplied); m.p. 130°C (decomposition); found: C, 32.79; H, 4.17. $C_{44}H_{66}Mg_2O_{12}P_4Se_8$ requires C, 33.21; H, 4.18%; ν_{max}/cm^{-1} (Nujol, NaCl) 3321br (H_2O), 1608m, 1430s (P-C), 1036m, 880m, 692m; δ_H (400 MHz, d_6-DMSO, 25°C) 8.1 (4H, m, ArH), 7.4 (4H, m, ArH), 3.6 (10H, m, O*CH₂*CH₂), 3.3 (s, H_2O), 1.8 (10H, m, OCH₂*CH₂*); δ_C (100 MHz, d_6-DMSO, 25°C) 130.9, 130.8, 129.8, 126.8, 126.7, 67.0, 25.2; δ_P (162 MHz, d_6-DMSO, 25°C, 65% H_3PO_4) 32.9 (s+2d satellites, $^1J_{P\text{-}Se}$ = -396 Hz, -698 Hz); δ_{Se} (76 MHz, d_6-DMSO, 25°C, Me_2Se) 40.5 (d, $^1J_{P\text{-}Se}$ = -698 Hz).

4.2.29 [Mg{PhP(Se,O)Se-Se(O,Se)PPh}(thf)$_3$(H$_2$O)] (29)

A mixture of Woollins' reagent (266 mg, 0.5 mmol) and $Mg(OAc)_2{\cdot}4H_2O$ (107 mg, 0.5 mmol) was dissolved in 8 mL THF. The yellow solution was stirred overnight at room temperature, and then the filtrate was layered with 50 mL hexane. Storage of the solution at room temperature for 4 weeks produced yellow crystals. 0.25 g, yield 60%; m.p. 125-128°C (decomposition); found: C, 35.94; H, 4.41. $C_{24}H_{36}MgO_6P_2Se_4$ requires C, 35.04; H, 4.41%; ν_{max}/cm^{-1} (KBr) 3306br (H_2O), 2970m, 1610s, 1436s (P-C), 1036s, 888s br, 690s. δ_H (400 MHz, d_6-DMSO, 25°C) 8.1-6.9 (10H, 6 x m, ArH), 3.6 (10H, m, O*CH₂*CH₂), 3.3 (s, H_2O), 1.7 (10H, m, OCH₂*CH₂*); δ_C (100 MHz, d_6-DMSO, 25°C) 126.2-130.9 (8C, ar. C), 67.0, 25.2; δ_P (162 MHz, d_6-DMSO, 25°C, 65% H_3PO_4) 32.9 (s+2d satellites, $^1J_{P\text{-}Se}$ = -395 Hz, -697 Hz), 43.6 (m, slow decomposition in d_6-DMSO into a yet unknown compound); δ_P (162 MHz, d_8-THF, 25°C, 65% H_3PO_4) 37.3 (s+2d satellites, $^1J_{P\text{-}Se}$ = -392 Hz, -704 Hz); δ_{Se} (76 MHz, d_6-DMSO, 25°C, Me_2Se) 40.5 (d, $^1J_{P\text{-}Se}$ = 698 Hz), 131.0 (d, $^1J_{P\text{-}Se}$ = -710 Hz).

4.2.30 [Mn{PhP(Se,O)Se-Se(O,Se)PPh}(thf)$_3$(H$_2$O)] (30)

A mixture of Woollins' reagent (266 mg, 0.5 mmol) and $Mn(OAc)_2{\cdot}4H_2O$ (123 mg, 0.5 mmol) was dissolved in 8 mL THF. The yellow solution was stirred overnight at room temperature, and then the filtrate was layered with 60 mL hexane. Storage of the solution at room temperature for 2 weeks produced yellow crystals. 0.28 g, yield 60%; m.p. 105ºC (decomposition); found: C, 33.25; H, 4.18. $C_{24}H_{36}MnO_6P_2Se_4$ requires C, 33.78; H, 4.25%; ν_{max}/cm^{-1} (KBr) 3306br (H_2O), 2973m, 1601m, 1435s (P-C), 1027s, 870s br, 687s.

4.2.31 [{PhPSe$_2$(μ_2-Se)Na(thf)$_3$}$_2$Ni] (31)

a) A mixture of Woollins' reagent (266 mg, 0.5 mmol) and NaSe^{t}Bu (159 mg, 1.0 mmol) was dissolved in 10 mL THF. The yellow solution was stirred for about 3h at room temperature and then added to NiCl$_2$ 65 mg (0.5 mmol). The resulting mixture was heated to 60^{o}C for about 3h. The filtrate was layered with 20 mL hexane. Storage of this solution at room temperature for 3 weeks produced brown crystals. 0.17 g, yield 70%; m.p. > 300ºC (decomposed, black solid); found: C, 25.55; H, 2.64. [$C_{36}H_{58}Na_2NiO_6P_2Se_6$(−4thf)] requires C, 25.59; H, 2.79%; ν_{max}/cm^{-1} (KBr) 3040m, 2957m, 1601m, 1433s (P-C), 1083s, 683s and 520s; δ_H (400 MHz, d$_8$-THF, 25ºC) 1.64 (24H, m, OCH$_2$*CH$_2$*), 3.48 (24H, m, O*CH$_2$*CH$_2$), 7.11-7.20 (6H, m, ArH), 8.32 (4H, m, ArH); δ_P (400 MHz, d$_8$-THF, 25ºC, 65% H$_3$PO$_4$) -12.73 ($J_{P\text{–}Se}$ = −350 Hz, −390 Hz).

b) A mixture of Woollins' reagent (266 mg, 0.5 mmol) and NaS^{t}Bu (112 mg, 1.0 mmol) was dissolved in 8 mL THF. The yellow solution was stirred for about 4h at room temperature and then added to NiCl$_2$ 65 mg (0.5 mmol). The resulting mixture was stirred overnight at room temperature. The filtrate was layered with 25 mL hexane. Storage of this solution at room temperature for 3 weeks produced brown crystals. 0.10 g, yield 41%.

4.2.32 1/∞[Ni{Na(PhPSe$_3$)(thf)$_2$]$_\infty$ (32)

A mixture of Woollins' reagent (266 mg, 0.5 mmol) and NaS^{t}Bu (112 mg, 1.0 mmol) was dissolved in THF (10 mL). The yellow, cloudy solution was stirred for about 5h at room temperature, and then added to Ni(OAc)$_2$ (177 mg, 1.0 mmol). The mixture was stirred overnight and the filtrate was layered with 40 mL hexane. Storage of this solution at room temperature for 2 weeks produced brown crystals. Spectroscopic and analytical data are same as 3.2.31.

4.2.33 [Cu$_3${PS$_2$(OPS$_2$O^{t}Bu)$_2$}(PPh$_3$)$_4$] (33)

A mixture of P$_2$S$_5$ (111 mg, 0.5 mmol), CuO^{t}Bu (137 mg, 1.0 mmol) and PPh$_3$ (524 mg, 2.0 mmol) was dissolved in 10 mL toluene. The resulting yellow solution was heated to 40~50ºC for about 3 hours. Storage of the yellow solution at 0ºC for 4 weeks produced colourless crystals. 0.05 g, yield 17%; m.p. 134ºC (decomposed, brown solid); found: C, 58.01; H, 4.65. [$C_{80}H_{78}Cu_3O_4P_7S_6(+C_7H_8O)$] requires C, 57.68; H, 4.79%; ν_{max}/cm^{-1} (KBr) 3047m, 2970w, 1584w, 1433s (P-C), 1093s, 868s (P-O-P) and 689s (P=S); δ_H (400 MHz, d_8-toluene, 25ºC) 1.60 (18H, s, 2 x OC*(CH$_3$)$_3$*), 6.96-7.46 (60H, m, ArH); δ_P (162 MHz, $CDCl_3$, 25ºC, 65% H_3PO_4) 59.9, 42.6, -2.9 (br, s, *P*Ph$_3$).

4.2.34 [$Cu_4\{\mu_3\text{-}P(O^tBu)S_3\}_2(PPh_3)_4$] (34a,b)

A mixture of CuO^{t}Bu (137 mg, 1.0 mmol), P_2S_3 (79 mg, 0.5 mmol) and PPh_3 (524 mg, 2.0 mmol) was dissolved in 15 mL toluene. The mixture was stirred for 7h. Solvent concentration within a double-Schlenk tube produced very light yellow (almost colourless) crystals after 4 days together with a colourless amorphous precipitate. 0.08 g, yield 19%; m.p. 175ºC (decomposed, brown solid); found: C, 55.52; H, 4.52. $C_{80}H_{78}Cu_4O_2P_6S_6$ requires C, 56.39; H, 4.61% (despite repeated attempts a more accurate analysis could not be obtained, indicating that solid samples are contaminated by amorphous byproducts); ν_{max}/cm^{-1} (KBr) 3049m, 2971m, 1434s (P-C), 1241s, 1092s, 692s (P=S).

b was synthesized by using 15 mL THF instead of 15 mL toluene. 0.2 g, yield 47%.

4.2.35 $^1/_\infty[Na_2(S_3PS^tBu)(dme)]_\infty$ (35)

A mixture of P_2S_5 (222 mg, 1.0 mmol) and NaS^{t}Bu (448 mg, 4.0 mmol) was dissolved in DME (12 mL). The mixture was stirred overnight and the filtrate was layered with 60 mL hexane. Storage of this solution at room temperature for one week produced colourless crystals. 0.48 g, yield 68% (based on NaS^{t}Bu supplied); m.p. >120ºC (decomposition) > 220ºC (black); found: C, 25.70; H, 4.89. [$2(C_{16}H_{38}Na_4O_4P_2S_8)$-$C_4H_{10}O_2$] requires C, 25.48; H, 5.04%; ν_{max}/cm^{-1} (Nujol) 1456s, 1377s, 1034m, 855m, 722m; δ_H (400 MHz, d_8-THF, 25ºC) 1.63 (9H, s+s, SC(*CH$_3$*)$_3$), 3.31 (6H, s, 2 x CH$_2$O*CH$_3$*), 3.46 (4H, s, 2 x *CH$_2$*OCH$_3$); δ_C (100 MHz; d_8-THF, 25ºC) 31.48, 31.52, 49.21, 49.27, 57.98, 71.76; δ_P (162 MHz, d_8-THF, 25ºC, 65% H_3PO_4) 93.3.

4.2.36 [$Ni\{P(OH)_2S_2\}_2(thf)_2$] (36)

A mixture of P_2S_5 (111 mg, 0.5 mmol) and NaS^{t}Bu (112 mg, 1.0 mmol) was dissolved in 7 mL THF. The yellow solution was stirred for about 5 hours at room temperature, and then added to $NiCl_2 \cdot 6H_2O$ 119 mg (0.5 mmol). The filtrate was layered with 20 mL hexane. Storage of the solution at room temperature for 2 weeks produced purple crystals. 0.09 g, yield 39% (based on NaS^{t}Bu supplied); m.p. 250ºC (decomposition); found: C, 20.62; H, 4.17. $C_8H_{20}NiO_6P_2S_4$ requires C, 20.84; H, 4.37%; δ_H (400 MHz, d_6-DMSO, 25ºC) 1.75 (4H, s, 2 x $OCH_2\mathit{CH_2}$), 3.59 (4H, s, 2 x $O\mathit{CH_2}CH_2$), 3.91 (4H, br, 4 x O*H*); δ_c (100 MHz, d_6-DMSO, 25ºC) 25.1, 67.0; δ_P (162 MHz, d_6-DMSO, 25ºC, 65% H_3PO_4) -0.8.

4.2.37 [ArPS(μ-S)(μ-NPh)SPAr] (Ar = 4-anisyl) (37)

Lawesson's reagent (5.0 g, 12.4 mmol) and phenyl isocyanate (2.0 g, 16.8 mmol) are heated in 50 mL xylene for 2h, and then the xylene and excess of phenyl isocyanate are subsequently distilled off. The colourless substance that crystallizes is filtered off from the distillation residue and recrystallized from the mixture of THF and hexane. Found: C, 50.56; H, 4.07. $C_{20}H_{19}NO_2P_2S_3$ requires C, 51.82; H, 4.13%.

5. Crystallographic Data

5.1 General Information

Crystallographic data were collected with a STOE IPDS II diffractometer using graphite-monochromated Mo-K_α radiation (λ = 0.71073 Å) or STOE STADI diffractometer with CCD-detector. The structures were solved by direct methods and refined by full-matrix least squares on F^2 (all data) using the SHELXTL program package.[172-175] Data reduction used the software supplied by the diffractometer manufacturers with R_{int} values defined as:

$$R_{int} = \sqrt{\frac{\sum \left| \mathrm{F}_0^2 - \mathrm{F}_0^2(mean) \right|}{\sum \mathrm{F}_0^2}}$$

The equations for the R-factors and goodness of fit S used in the structure refinement are:

$$wR_2 = \sqrt{\frac{\sum w\left(F_0^2 - F_C^2\right)^2}{\sum w\left(F_0^2\right)^2}}; \quad S = \sqrt{\frac{\sum w\left(F_0^2 - F_C^2\right)^2}{(n-p)}}; \quad R_1 = \frac{\sum \left\| F_0 \right| - \left| F_C \right\|}{\sum \left| F_0 \right|}$$

When F_o and F_c are the observed and calculated structure factors for each reflection, while n and p are the number of unique reflections (omitting systematic absences) and the total number of parameters, respectively. The weighting factor, w, is defined as

$$\frac{1}{w} = \sigma^2 F_0^2 + (aP)^2 + bP$$

Where

$$P = \frac{\max\left(F_0^2, 0\right) + 2F_C^2}{3}$$

wR_2 is the function minimized during the refinement process, and all reflections (except those having large negative values or that have been flagged manually using OMIT as ‘‘bad reflections’’) were used in the refinement, and for the calculation of S. R_1 was only calculated after the refinement process, and only used the stronger reflections with $F_o \geqslant 4\sigma(F_o)$, which corresponds to $I \geqslant 2\sigma(I)$, for comparison with R-factors for structures refined against F_o.

5.2 Crystallographic Data

5.2.1 $[Cu_2(\textit{o}\text{-}CO_2C_6H_4SO_3)(dppm)_2]\cdot 3CH_2Cl_2$ (1)

Empirical formula	$C_{60}H_{54}Cl_6Cu_2O_5P_4S$
Molecular weight /[g•mol^{-1}]	1350.75
Temperature /[K]	200(2)
λ/[Å]	0.71073
Crystal system	Monoclinic
space group	$P2_1/c$
Unit cell /[Å]; [deg.]	a = 12.861(3) b = 20.043(4) β = 100.65(3) c = 23.815(5)
Volume /[Å^3]	6033(2)
Z, Calculated density /[g•cm^{-3}]	4, 1.487
μ/[mm^{-1}]	1.159
F(000)	2760
2θ range	7.54-63.54
Reflections collected / unique	12873 / 10218; [R_{int} = 0.0188]
parameters	703
R_1[I>2σ(I)]	0.0513
wR_2(all data)	0.1721
Largest diff. peak and hole /[eÅ^{-3}]	0.719 / -0.884

Atomic coordinates (x10^4) and equivalent isotropic displacement parameters (A^2 x10^3)

Atom	x	y	z	U(eq)
S(1)	-607(1)	2897(1)	7164(1)	30(1)
Cu(1)	474(1)	4286(1)	7161(1)	25(1)
Cu(2)	2328(1)	4354(1)	7946(1)	27(1)
P(1)	-23(1)	5305(1)	7370(1)	25(1)
P(2)	2096(1)	5421(1)	8168(1)	25(1)
P(3)	1617(1)	4020(1)	6588(1)	27(1)
P(4)	3328(1)	3637(1)	7568(1)	29(1)
Cl(1)	2665(1)	1676(1)	5174(1)	89(1)
Cl(2)	3959(1)	2853(1)	5174(1)	85(1)
Cl(3)	6700(2)	1147(1)	10638(1)	110(1)
Cl(4)	7005(1)	2419(1)	10125(1)	90(1)
Cl(5)	6324(2)	4042(2)	9501(1)	138(1)
Cl(6)	4176(2)	4436(2)	9243(2)	140(1)
O(1)	468(2)	2650(2)	7237(2)	40(1)
O(2)	-1384(2)	2455(2)	6837(2)	47(1)
O(3)	-729(2)	3582(2)	6950(1)	31(1)
O(4)	971(2)	3857(2)	7985(1)	33(1)
O(5)	1576(2)	3251(2)	8742(2)	45(1)
C(1)	-924(3)	2929(2)	7853(2)	28(1)
C(2)	-1946(3)	2704(3)	7913(3)	45(1)
C(3)	-2274(4)	2739(3)	8426(3)	57(2)
C(4)	-1603(4)	2984(3)	8914(3)	55(2)
C(5)	-581(4)	3190(3)	8858(2)	42(1)
C(6)	-236(3)	3162(2)	8345(2)	29(1)
C(7)	875(3)	3428(2)	8358(2)	27(1)
C(8)	-897(3)	5415(2)	7894(2)	29(1)
C(9)	-1248(3)	4870(3)	8134(2)	40(1)
C(10)	-1900(4)	4937(3)	8522(3)	55(2)
C(11)	-2212(4)	5549(3)	8673(3)	54(2)
C(12)	-1863(4)	6106(3)	8425(3)	53(1)
C(13)	-1208(3)	6046(3)	8037(2)	42(1)
C(14)	-717(3)	5704(2)	6724(2)	26(1)
C(15)	-630(3)	6374(2)	6591(2)	32(1)
C(16)	-1151(3)	6625(3)	6070(2)	40(1)
C(17)	-1759(3)	6204(3)	5687(2)	43(1)
C(18)	-1864(3)	5540(3)	5815(2)	43(1)
C(19)	-1347(3)	5284(2)	6334(2)	33(1)
C(20)	3237(3)	5984(2)	8238(2)	31(1)
C(21)	3754(4)	6179(3)	8774(3)	58(2)
C(22)	4691(5)	6544(4)	8821(3)	79(2)
C(23)	5089(4)	6715(4)	8352(4)	72(2)

Atom	x	y	z	U(eq)
C(24)	4571(4)	6530(3)	7814(3)	62(2)
C(25)	3646(3)	6152(3)	7765(2)	45(1)
C(26)	1632(3)	5504(2)	8835(2)	31(1)
C(27)	1627(3)	4944(3)	9183(2)	38(1)
C(28)	1294(4)	5005(3)	9709(2)	54(1)
C(29)	990(4)	5606(3)	9887(2)	55(2)
C(30)	984(4)	6164(3)	9541(2)	53(1)
C(31)	1297(3)	6117(3)	9025(2)	43(1)
C(32)	1109(3)	5860(2)	7629(2)	26(1)
C(33)	877(3)	3698(3)	5917(2)	35(1)
C(34)	955(4)	3055(3)	5722(2)	47(1)
C(35)	322(5)	2864(4)	5211(3)	64(2)
C(36)	−378(4)	3297(4)	4899(3)	62(2)
C(37)	−466(4)	3939(4)	5091(3)	68(2)
C(38)	171(4)	4139(3)	5594(3)	56(2)
C(39)	2419(3)	4653(3)	6321(2)	35(1)
C(40)	2110(4)	5309(3)	6331(2)	44(1)
C(41)	2662(5)	5811(3)	6097(3)	65(2)
C(42)	3535(5)	5636(4)	5851(3)	76(2)
C(43)	3830(5)	4983(5)	5834(3)	75(2)
C(44)	3268(4)	4476(3)	6070(3)	57(2)
C(45)	4573(3)	3937(3)	7403(2)	39(1)
C(46)	5262(4)	3519(3)	7184(3)	55(2)
C(47)	6192(4)	3787(5)	7052(3)	72(2)
C(48)	6423(4)	4447(5)	7138(3)	75(2)
C(49)	5768(5)	4851(4)	7369(3)	77(2)
C(50)	4833(4)	4596(3)	7502(3)	53(2)
C(51)	3688(3)	2858(2)	7951(2)	31(1)
C(52)	4636(3)	2827(3)	8351(2)	45(1)
C(53)	4872(3)	2255(3)	8684(3)	51(1)
C(54)	4199(4)	1711(3)	8608(3)	53(2)
C(55)	3266(4)	1730(3)	8210(3)	51(2)
C(56)	3016(3)	2305(3)	7895(2)	42(1)
C(57)	2543(3)	3364(2)	6883(2)	33(1)
C(58)	3277(5)	2202(3)	4769(3)	68(2)
C(59)	7419(7)	1910(5)	10706(4)	104(3)
C(60)	5413(6)	4617(5)	9167(5)	111(3)

5.2.2 $[Cu_2(\mu_2\text{-}ArS_2P\text{-}O\text{-}PS_2Ar)(PPh_3)_4]\cdot CH_2Cl_2$ (Ar = 4-anisyl) (2)

Empirical formula	$C_{87}H_{76}Cl_2Cu_2O_3P_6S_4$
Molecular weight /[g•mol^{-1}]	1681.52
Temperature /[K]	100(2)
λ/[Å]	0.71073
Crystal system	Monoclinic
space group	*C*2/*c*
Unit cell /[Å]; [deg.]	a = 22.431(5) b = 13.711(3) β = 104.20(3) c = 26.435(5)
Volume /[Å^3]	7882(3)
Z, Calculated density /[g•cm^{-3}]	4, 1.417
μ/[mm^{-1}]	0.886
F(000)	3472
2θ range	3.18-54.04
Reflections collected / unique	29604 / 8548; [R_{int} = 0.0485]
parameters	238
R_1[I>2σ(I)]	0.0742
wR_2(all data)	0.2063
Largest diff. peak and hole /[eÅ^{-3}]	2.446 / -1.145
CCDC number	263199

5.2.3 [Cu_4{Ar(μ_2-S)$_2$P-O-P(μ_2-S)$_2$Ar}$_2$(dppa)$_2$]•3CH_2Cl_2 (Ar = 4-anisyl) (3)

Empirical formula	$C_{79}H_{74}Cl_6Cu_4N_2O_6P_8S_8$
Molecular weight /[g•mol^{-1}]	2118.65
Temperature /[K]	100(2)
λ/[Å]	0.71073
Crystal system	Monoclinic
space group	*C2/c*
Unit cell /[Å]; [deg.]	a = 18.457(4) b = 19.747(4) β = 93.66(3) c = 24.311(5)
Volume /[Å^3]	8843(3)
Z, Calculated density /[g•cm^{-3}]	4, 1.600
μ/[mm^{-1}]	1.516
F(000)	4328
2θ range	3.36-53.86
Reflections collected / unique	13293 / 7876; [R_{int} = 0.0460]
parameters	509
R_1[I>2σ(I)]	0.0682
wR_2(all data)	0.2042
Largest diff. peak and hole /[eÅ^{-3}]	0.995 / -1.633
CCDC number	263200

5.2.4 $[Cu_2(\mu_4\text{-}ArPS_3)(PPh_3)_2]_2\cdot 2CH_2Cl_2$ (Ar = 4-anisyl) (4)

Empirical formula	$C_{88}H_{78}Cl_4Cu_4O_2P_6S_6$
Molecular weight /[g•mol^{-1}]	1941.64
Temperature /[K]	173(2)
λ/[Å]	0.71073
Crystal system	Monoclinic
space group	$P2_1/c$
Unit cell /[Å]; [deg.]	a = 12.960(3) b = 22.853(5) β = 113.02(3) c = 15.976(3)
Volume /[Å^3]	4354.9(15)
Z, Calculated density /[g•cm^{-3}]	2, 1.481
μ/[mm^{-1}]	1.387
F(000)	1984
2θ range	7.50-63.64
Reflections collected / unique	28160 / 10288; [R_{int} = 0.0364]
parameters	506
R_1[I>2σ(I)]	0.0437
wR_2(all data)	0.1555
Largest diff. peak and hole /[eÅ^{-3}]	1.165 / -0.827
CCDC number	276586

5.2.5 [Cu(ArP(S^{t}Bu)S$_2$)(PPh$_3$)$_2$] (Ar = 4-anisyl) (5)

Empirical formula	$C_{47}H_{46}CuOP_3S_3$
Molecular weight /[g•mol^{-1}]	879.47
Temperature /[K]	150(2)
λ/[Å]	0.71073
Crystal system	Triclinic
space group	$P\bar{1}$
Unit cell /[Å]; [deg.]	a = 11.4902(4) α = 74.107(3) b = 13.0272(5) β = 71.686(3) c = 15.6664(5) γ = 83.651(3)
Volume /[Å^3]	2140.38(13)
Z, Calculated density /[g•cm^{-3}]	2, 1.365
μ/[mm^{-1}]	0.804
F(000)	916
2θ range	5.78-63.58
Reflections collected / unique	17126 / 9353; [R_{int} = 0.0282]
parameters	496
R_1[I>2σ(I)]	0.0398
wR_2(all data)	0.1452
Largest diff. peak and hole /[eÅ^{-3}]	1.079 / -1.021
CCDC number	601694

5.2.6 1/∞[Na{ArP(O^{t}Bu)S$_2$}(thf)]$_\infty$ (Ar = 4-anisyl) (6)

Empirical formula	$C_{15}H_{24}NaO_3PS_2$
Molecular weight /[g•mol^{-1}]	370.42
Temperature /[K]	150(2)
λ/[Å]	0.71073
Crystal system	Monoclinic
space group	*P*2$_1$/*n*
Unit cell /[Å]; [deg.]	a = 13.0592(11) b = 8.7781(9) β = 102.117(7) c = 16.8189(15)
Volume /[Å^3]	1885.1(3)
Z, Calculated density /[g•cm^{-3}]	4, 1.305
μ/[mm^{-1}]	0.398
F(000)	784
2θ range	7.90-63.50
Reflections collected / unique	10946 / 4416; [R_{int} = 0.0570]
Parameters	195
R_1[I>2σ(I)]	0.0957
wR_2(all data)	0.3278
Largest diff. peak and hole /[eÅ^{-3}]	1.538 / -1.040
CCDC number	601695

5.2.7 [Na_2{ArP(O^{t}Bu)(μ-S)S}$_2$(dme)$_2$] (Ar = 4-anisyl) (7)

Empirical formula	$C_{30}H_{52}Na_2O_8P_2S_4$
Molecular weight /[g•mol^{-1}]	776.88
Temperature /[K]	150(2)
λ/[Å]	0.71073
Crystal system	Monoclinic
space group	*P*2$_1$/*c*
Unit cell /[Å]; [deg.]	a = 8.2730(17) b = 11.841(2) β = 98.61(3) c = 20.614(4)
Volume /[Å^3]	1996.6(7)
Z, Calculated density /[g•cm^{-3}]	2, 1.292
μ/[mm^{-1}]	0.382
F(000)	824
2θ range	6.88-63.62
Reflections collected / unique	15549 / 4733; [R_{int} = 0.0588]
Parameters	202
R_1[I>2σ(I)]	0.0651
wR_2(all data)	0.2077
Largest diff. peak and hole /[eÅ^{-3}]	1.103 / -0.651
CCDC number	601696

5.2.8 1/∞[K_2\{ArP(O^tBu)(μ-S)S\}$_2$(thf)$_2$]$_\infty$ (Ar = 4-anisyl) (8)

Empirical formula	$C_{15}H_{24}KO_3PS_2$
Molecular weight /[g•mol^{-1}]	386.53
Temperature /[K]	150(2)
λ/[Å]	0.71073
Crystal system	Triclinic
space group	$P\bar{1}$
Unit cell /[Å]; [deg.]	a = 8.264(6) α = 96.849(6) b = 11.2990(9) β = 102.612(6) c = 11.3100(8) γ = 111.286(7)
Volume /[Å^3]	937.1(7)
Z, Calculated density /[g•cm^{-3}]	2, 1.370
μ/[mm^{-1}]	0.600
F(000)	408
2θ range	7.72-63.66
Reflections collected / unique	7578 / 4099; [R_{int} = 0.0314]
parameters	203
R_1[I>2σ(I)]	0.0327
wR_2(all data)	0.1430
Largest diff. peak and hole /[eÅ^{-3}]	0.777 / -0.734
CCDC number	601697

5.2.9 1/∞[K_2{ArP(O^tBu)(μ-S)S}$_2$($dme)_2$]$_\infty$ (Ar = 4-anisyl) (9)

Empirical formula	$C_{15}H_{26}KO_4PS_2$
Molecular weight /[g•mol^{-1}]	404.55
Temperature /[K]	150(2)
λ/[Å]	0.71073
Crystal system	Monoclinic
space group	*P*2$_1$/*n*
Unit cell /[Å]; [deg.]	a = 10.6833(9) b = 10.9392(8) β = 106.174(7) c = 17.6404(14)
Volume /[Å^3]	1980.0(3)
Z, Calculated density /[g•cm^{-3}]	4, 1.357
μ/[mm^{-1}]	0.574
F(000)	856
2θ range	7.46-64.10
Reflections collected / unique	15474 / 4755; [R_{int} = 0.0885]
parameters	214
R_1[I>2σ(I)]	0.0488
wR_2(all data)	0.1637
Largest diff. peak and hole /[eÅ^{-3}]	1.289 / -0.737
CCDC number	601698

5.2.10 1/∞$[K_4\{ArP(S^tBu)(\mu\text{-}S)S\}_4(thf)_4]_\infty$ (Ar = 4-anisyl) (10)

Empirical formula	$C_{60}H_{96}K_4O_8P_4S_{12}$
Molecular weight /[g•mol^{-1}]	1610.37
Temperature /[K]	110(2)
λ/[Å]	0.71073
Crystal system	Tetragonal
space group	$I4_1/a$
Unit cell /[Å]; [deg.]	a = 26.4622(16) b = 26.4622(16) c = 11.2432(6)
Volume /[Å^3]	7873.0(8)
Z, Calculated density /[g•cm^{-3}]	4, 1.359
μ/[mm^{-1}]	0.672
F(000)	3392
2θ range	3.94-54.04
Reflections collected / unique	11638 / 4276; [R_{int} = 0.0827]
parameters	199
R_1[I>2σ(I)]	0.0917
wR_2(all data)	0.2778
Largest diff. peak and hole /[eÅ^{-3}]	2.100 / -0.468
CCDC number	601700

5.2.11 [Cu_{14}(μ_6-ArP(O)S_2)$_6$(μ_3-ArP(O)(OAc)S)$_2$(PPh_3)$_6$)]•8THF (Ar = 4-anisyl) (11)

Empirical formula	$C_{200}H_{216}Cu_{14}O_{28}P_{14}S_{14}$
Molecular weight /[g•mol^{-1}]	4839.71
Temperature /[K]	120(2)
λ/[Å]	0.71073
Crystal system	Triclinic
space group	$P\bar{1}$
Unit cell /[Å]; [deg.]	a = 17.1353(9) α = 95.756(4) b = 19.6186(10) β = 111.961(4) c = 20.0847(20) γ = 113.646(4)
Volume /[Å^3]	5481.6(5)
Z, Calculated density /[g•cm^{-3}]	1, 1.466
μ/[mm^{-1}]	1.625
F(000)	2480
2θ range	3.74-54.32
Reflections collected / unique	42933 / 21979; [R_{int} = 0.0589]
parameters	1098
R_1[I>2σ(I)]	0.0799
wR_2(all data)	0.2526
Largest diff. peak and hole /[eÅ^{-3}]	2.970 / -1.089
CCDC number	276587

5.2.12 [$Ag_4\{\mu_4$-ArP(O)$S_2\}_2$(dppm)$_4$]•2Et_2O•2THF (Ar = 4-anisyl) (12)

Empirical formula	$C_{130}H_{138}Ag_4O_8P_{10}S_4$
Molecular weight /[g•mol^{-1}]	2697.82
Temperature /[K]	100(2)
λ/[Å]	0.71073
Crystal system	Monoclinic
space group	*C*2/*c*
Unit cell /[Å]; [deg.]	a = 25.1473(9) b = 20.5188(4) β = 113.361(3) c = 26.3469(10)
Volume /[Å^3]	12480.4(7)
Z, Calculated density /[g•cm^{-3}]	4, 1.449
μ/[mm^{-1}]	0.869
F(000)	5636
2θ range	2.74-55.72
Reflections collected / unique	48865 / 13532; [R_{int} = 0.0363]
parameters	705
R_1[I>2σ(I)]	0.0408
wR_2(all data)	0.1186
Largest diff. peak and hole /[eÅ^{-3}]	0.646 / -1.063
CCDC number	283238

5.2.13 $[Ag_{28}(\mu_6\text{-}S)_2\{ArP(O)S_2\}_{12}(PPh_3)_{12}]\bullet 2Et_2O\bullet 13THF$ (Ar = 4-anisyl) (13)

Empirical formula	$C_{360}H_{388}Ag_{28}O_{39}P_{24}S_{26}$
Molecular weight /[g•mol^{-1}]	9935.90
Temperature /[K]	100(3)
λ/[Å]	0.71073
Crystal system	Triclinic
space group	$P\bar{1}$
Unit cell /[Å]; [deg.]	a = 22.8410(6) α = 118.290(2) b = 23.4102(7) β = 96.031(2) c = 23.8337(6) γ = 113.295(2)
Volume /[Å^3]	9609.6(5)
Z, Calculated density /[g•cm^{-3}]	1, 1.730
μ/[mm^{-1}]	1.692
F(000)	4996
2θ range	2.62-54.30
Reflections collected / unique	77691 / 39248; [R_{int} = 0.0458]
parameters	1943
R_1[I>2σ(I)]	0.0630
wR_2(all data)	0.1946
Largest diff. peak and hole /[eÅ^{-3}]	2.651 / -2.750
CCDC number	283239

5.2.14 [Fe_2(μ-$ArPS_3$)$(thf)_4$] (Ar = 4-anisyl) (14)

Empirical formula	$C_{30}H_{46}Fe_2O_6P_2S_6$
Molecular weight /[g•mol^{-1}]	868.67
Temperature /[K]	205(2)
λ/[Å]	0.71073
Crystal system	Monoclinic
space group	$P2_1/c$
Unit cell /[Å]; [deg.]	a = 10.760(1) b = 17.020(2) β = 109.91(1) c = 11.300(1)
Volume /[Å^3]	1945.7(1)
Z, Calculated density /[g•cm^{-3}]	2, 1.483
μ/[mm^{-1}]	1.188
F(000)	904
2θ range	4.68-51.76
Reflections collected / unique	8829 / 3680; [R_{int} = 0.1237]
parameters	208
R_1[I>2σ(I)]	0.0687
wR_2(all data)	0.2225
Largest diff. peak and hole /[eÅ^{-3}]	0.617 / -0.739
CCDC number	276588

5.2.15 $[Ni_2\{ArP(O)S_2\}_2(thf)_2(H_2O)_2]_2$ (Ar = 4-anisyl) (15)

Empirical formula	$C_{44}H_{68}Ni_4O_{16}P_4S_8$
Molecular weight /[g•mol^{-1}]	1468.18
Temperature /[K]	120(2)
λ/[Å]	0.71073
Crystal system	Orthorhombic
space group	*Pna*2$_1$
Unit cell /[Å]; [deg.]	a = 26.921(5) b = 13.001(3) c = 18.206(4)
Volume /[Å^3]	6372(2)
Z, Calculated density /[g•cm^{-3}]	4, 1.530
μ/[mm^{-1}]	1.585
F(000)	3040
2θ range	3.02-54.08
Reflections collected / unique	35061 / 13469; [R_{int} = 0.1692]
parameters	657
R_1[I>2σ(I)]	0.1262
wR_2(all data)	0.3167
Largest diff. peak and hole /[eÅ^{-3}]	3.370 / -0.871
CCDC number	276589

5.2.16 [Cd_2{ArP(O^{t}Bu)(μ-S)S}$_4$] (Ar = 4-anisyl) (16)

Empirical formula	$C_{44}H_{64}Cd_2O_8P_4S_8$
Molecular weight /[g•mol^{-1}]	1326.11
Temperature /[K]	120(2)
λ/[Å]	0.71073
Crystal system	Triclinic
space group	$P\bar{1}$
Unit cell /[Å]; [deg.]	a = 11.3883(9) α = 74.356(6) b = 11.8699(9) β = 65.181(5) c = 12.2242(9) γ = 77.253(6)
Volume /[Å^3]	1433.30(19)
Z, Calculated density /[g•cm^{-3}]	1, 1.536
μ/[mm^{-1}]	1.190
F(000)	676
2θ range	3.60-56.46
Reflections collected / unique	12818 / 6527; [R_{int} = 0.0408]
parameters	291
R_1[I>2σ(I)]	0.0313
wR_2(all data)	0.0763
Largest diff. peak and hole /[eÅ^{-3}]	1.038 / -0.543
CCDC number	601699

5.2.17 [Fe_2(*µ*-$ArPS_3$)(thf)$_4$]$_2$ (Ar = 4-anisyl) (17)

Empirical formula	$C_{60}H_{92}Fe_4O_{12}P_4S_{12}$
Molecular weight /[g•mol^{-1}]	1737.34
Temperature /[K]	293(2)
λ/[Å]	0.71073
Crystal system	Triclinic
space group	$P\bar{1}$
Unit cell /[Å]; [deg.]	a = 10.829(2) α = 91.71(3) b = 11.275(2) β = 96.53(3) c = 16.737(3) γ = 110.24(3)
Volume /[Å^3]	1899.7(7)
Z, Calculated density /[g•cm^{-3}]	1, 1.519
µ/[mm^{-1}]	1.217
F(000)	904
2θ range	3.86-56.24
Reflections collected / unique	11260 / 7920; [R_{int} = 0.0578]
parameters	410
R_1[I>2σ(I)]	0.0855
wR_2(all data)	0.2721
Largest diff. peak and hole /[eÅ^{-3}]	1.805 / -1.020

Atomic coordinates (x10^4) and equivalent isotropic displacement parameters (A^2 x10^3)

Atom	x	y	z	U(eq)
Fe(1)	5225(1)	5421(1)	3958(1)	32(1)
Fe(2)	5193(1)	10308(1)	1103(1)	30(1)
P(1)	4091(2)	6745(2)	5186(1)	29(1)
P(2)	5930(2)	8260(2)	182(1)	30(1)
S(1)	5246(2)	7625(2)	4359(1)	38(1)
S(2)	3261(2)	4856(2)	4801(1)	33(1)
S(3)	5057(2)	6859(2)	6312(1)	36(1)
S(4)	6739(2)	10179(2)	65(1)	30(1)
S(5)	5049(2)	8020(2)	1195(1)	34(1)
S(6)	4704(2)	7471(2)	-855(1)	35(1)
O(1)	67(6)	9117(6)	5730(4)	42(1)
O(2)	4046(9)	5397(9)	2828(4)	63(2)
O(3)	6948(7)	6225(6)	3346(5)	50(2)
O(4)	10148(7)	5968(7)	722(8)	84(3)
O(5)	3895(6)	10052(6)	2001(3)	38(1)
O(6)	6821(6)	10947(6)	2083(3)	37(1)
C(1)	2794(8)	7418(7)	5253(4)	30(1)
C(2)	1472(8)	6656(7)	5250(5)	37(2)
C(3)	522(8)	7197(8)	5388(5)	36(2)
C(4)	900(8)	8493(8)	5548(5)	34(2)
C(5)	2226(8)	9272(7)	5539(5)	34(2)
C(6)	3179(8)	8744(7)	5393(4)	32(2)
C(7)	-1317(9)	8387(9)	5641(6)	48(2)
C(8)	3018(15)	5909(15)	2701(9)	28(3)
C(9)	1880(17)	4656(16)	2405(10)	37(3)
C(10)	2538(17)	3852(18)	1967(11)	41(3)
C(11)	3910(20)	4580(20)	2115(15)	37(2)
C(8A)	2500(30)	5280(30)	2796(15)	65(6)
C(9A)	2090(30)	5310(30)	1940(16)	69(6)
C(10A)	2690(30)	4370(30)	1582(16)	66(6)
C(11A)	4120(20)	4800(20)	2075(15)	37(2)
C(12)	7273(11)	7368(11)	2979(8)	59(3)
C(13)	8579(12)	7680(11)	2713(9)	64(3)
C(14)	9051(13)	6592(13)	2943(9)	67(3)
C(15)	7781(16)	5560(12)	3105(10)	86(5)
C(16)	7255(8)	7607(7)	313(5)	33(2)
C(17)	6938(8)	6340(8)	524(7)	45(2)
C(18)	7920(11)	5831(10)	641(9)	63(3)
C(19)	9235(10)	6557(9)	553(8)	57(3)
C(20)	9561(10)	7795(9)	332(6)	46(2)

Atom	x	y	z	U(eq)
C(21)	8560(8)	8305(8)	220(5)	37(2)
C(22)	11474(11)	6639(11)	528(14)	107(7)
C(23)	2816(10)	10507(11)	2003(6)	51(2)
C(24)	2010(13)	9764(17)	2593(8)	78(4)
C(25)	2903(13)	9394(13)	3173(7)	63(3)
C(26)	4091(12)	9503(11)	2765(5)	52(2)
C(27)	7253(9)	12203(9)	2503(5)	43(2)
C(28)	8576(11)	12883(10)	2225(7)	55(2)
C(29)	9140(10)	11819(10)	2087(7)	52(2)
C(30)	8002(9)	10605(9)	2166(5)	38(2)

5.2.18 [Ni{ArP(OH)S$_2$}$_2$(thf)$_2$] (Ar = 4-anisyl) (18)

Empirical formula	$C_{22}H_{32}NiO_6P_2S_4$
Molecular weight /[g•mol^{-1}]	641.37
Temperature /[K]	173(2)
λ/[Å]	0.71073
Crystal system	Triclinic
space group	$P\bar{1}$
Unit cell /[Å]; [deg.]	a = 8.3593(6) α = 64.376(13) b = 9.4774(12) β = 75.010(9) c = 10.4564(14) γ = 71.497(9)
Volume /[Å^3]	701.14(14)
Z, Calculated density /[g•cm^{-3}]	1, 1.519
μ/[mm^{-1}]	1.139
F(000)	334
2θ range	7.72-62.88
Reflections collected / unique	5271 / 3044; [R_{int} = 0.0302]
parameters	161
R_1[I>2σ(I)]	0.0419
wR_2(all data)	0.1653
Largest diff. peak and hole /[eÅ^{-3}]	1.067 / -1.294
CCDC number	614760

5.2.19 1/∞[$K_2\{PhP(O^tBu)Se_2\}_2$(thf)]$_\infty$ (19)

Empirical formula	$C_{24}H_{36}K_2O_3P_2Se_4$
Molecular weight /[g•mol^{-1}]	828.51
Temperature /[K]	150(2)
λ/[Å]	0.71073
Crystal system	Monoclinic
space group	$P2_1/n$
Unit cell /[Å]; [deg.]	a = 17.0055(10) b = 10.0063(3) β = 101.019(4) c = 19.1984(11)
Volume /[Å^3]	3206.6(3)
Z, Calculated density /[g•cm^{-3}]	4, 1.716
μ/[mm^{-1}]	4.959
F(000)	1632
2θ range	3.56-56.48
Reflections collected / unique	14199 / 7442; [R_{int} = 0.0751]
parameters	316
R_1[I>2σ(I)]	0.0634
wR_2(all data)	0.1874
Largest diff. peak and hole /[eÅ^{-3}]	1.484 / -1.403
CCDC number	603361

5.2.20 1/∞[PhPSe$_3$Na$_2$(thf)$_3$]$_\infty$ (20)

Empirical formula	$C_{24}H_{34}Na_4O_3P_2Se_6$
Molecular weight /[g•mol^{-1}]	998.17
Temperature /[K]	100(2)
λ/[Å]	0.71073
Crystal system	Triclinic
space group	$P\bar{1}$
Unit cell /[Å]; [deg.]	a = 9.7746(8) α = 71.905(6) b = 11.4669(10) β = 78.473(6) c = 16.7949(14) γ = 85.510(7)
Volume /[Å^3]	1753.0(3)
Z, Calculated density /[g•cm^{-3}]	2, 1.891
μ/[mm^{-1}]	6.428
F(000)	960
2θ range	3.74-56.36
Reflections collected / unique	15513 / 7931; [R_{int} = 0.0472]
parameters	345
R_1[I>2σ(I)]	0.0386
wR_2(all data)	0.1026
Largest diff. peak and hole /[eÅ^{-3}]	1.991 / -1.440
CCDC number	292989

5.2.21 1/∞[($PhPSe_2Se$-$SeSe_2PPh$)K_2(thf)$_4$]$_\infty$ (21)

Empirical formula	$C_{28}H_{42}K_2O_4P_2Se_6$
Molecular weight /[g•mol^{-1}]	1056.52
Temperature /[K]	150(2)
λ/[Å]	0.71073
Crystal system	Monoclinic
space group	*P*2$_1$/*c*
Unit cell /[Å]; [deg.]	a = 12.6326(7) b = 19.9940(10) β = 93.654(5) c = 15.4290(10)
Volume /[Å^3]	3889.1(4)
Z, Calculated density /[g•cm^{-3}]	4, 1.804
μ/[mm^{-1}]	5.971
F(000)	2056
2θ range	7.56-63.68
Reflections collected / unique	29272 / 8957; [R_{int} = 0.0804]
parameters	373
R_1[I>2σ(I)]	0.0519
wR_2(all data)	0.1743
Largest diff. peak and hole /[eÅ^{-3}]	1.528 / -1.221
CCDC number	292992

5.2.22 $1/\infty[(\mathrm{PhPSe_2Se\text{-}SeSe_2PPh})\mathrm{Rb_2(thf)_4}]_\infty$ (22)

Empirical formula	$C_{28}H_{42}Rb_2O_4P_2Se_6$
Molecular weight /[g•mol^{-1}]	1149.26
Temperature /[K]	173(2)
λ/[Å]	0.71073
Crystal system	Monoclinic
space group	*C*2/*c*
Unit cell /[Å]; [deg.]	a = 14.0598(12) b = 23.1403(15) β = 112.154(6) c = 13.4145(10)
Volume /[Å^3]	4042.2(5)
Z, Calculated density /[g•cm^{-3}]	4, 1.888
μ/[mm^{-1}]	7.932
F(000)	2200
2θ range	3.52-54.16
Reflections collected / unique	13034 / 4419; [R_{int} = 0.0609]
parameters	159
R_1[I>2σ(I)]	0.0490
wR_2(all data)	0.1196
Largest diff. peak and hole /[eÅ^{-3}]	0.674 / -0.624
CCDC number	292993

5.2.23 1/∞[Na_2\{$PhSe_2P$-PSe_2Ph\}(thf)$_3$]$_\infty$ (23)

Empirical formula	$C_{24}H_{34}Na_2O_3P_2Se_4$
Molecular weight /[g•mol^{-1}]	794.27
Temperature /[K]	120(2)
λ/[Å]	0.71073
Crystal system	Monoclinic
space group	*P*2$_1$/*n*
Unit cell /[Å]; [deg.]	a = 11.5501(8) b = 24.8978(15) β = 116.901(5) c = 11.7555(9)
Volume /[Å^3]	3014.7(4)
Z, Calculated density /[g•cm^{-3}]	4, 1.750
μ/[mm^{-1}]	5.027
F(000)	1560
2θ range	3.28-54.14
Reflections collected / unique	23625 / 6591; [R_{int} = 0.0664]
parameters	316
R_1[I>2σ(I)]	0.0424
wR_2(all data)	0.1036
Largest diff. peak and hole /[eÅ^{-3}]	0.758 / -1.042
CCDC number	603362

5.2.24 1/∞[$K_2(PhPSe_2Se\text{-}SeSe_2PPh)(thf)_2]_\infty$ (24)

Empirical formula	$C_{20}H_{26}K_2O_2P_2Se_6$
Molecular weight /[g•mol^{-1}]	912.31
Temperature /[K]	100(2)
λ/[Å]	0.71073
Crystal system	Monoclinic
space group	*P*2$_1$/*n*
Unit cell /[Å]; [deg.]	a = 12.0394(6) b = 23.4696(10) β = 116.301(4) c = 12.0063(6)
Volume /[Å^3]	3041.3(3)
Z, Calculated density /[g•cm^{-3}]	4, 1.992
μ/[mm^{-1}]	7.614
F(000)	1736
2θ range	3.48-56.56
Reflections collected / unique	26890 / 7497; [R_{int} = 0.0431]
parameters	289
R_1[I>2σ(I)]	0.0293
wR_2(all data)	0.0701
Largest diff. peak and hole /[eÅ^{-3}]	0.615 / -0.909
CCDC number	603363

5.2.25 1/∞[$Na_2(PhPSe_2O)(H_2O)_4(thf)]_\infty$ (25)

Empirical formula	$C_{10}H_{21}Na_2O_6PSe_2$
Molecular weight /[g•mol^{-1}]	472.14
Temperature /[K]	150(2)
λ/[Å]	0.71073
Crystal system	Triclinic
space group	$P\bar{1}$
Unit cell /[Å]; [deg.]	a = 6.839(1) α = 101.55(1) b = 7.748(1) β = 93.41(1) c = 18.691(3) γ = 103.92(1)
Volume /[Å^3]	935.8(2)
Z, Calculated density /[g•cm^{-3}]	2, 1.676
μ/[mm^{-1}]	4.100
F(000)	468
2θ range	8.16-52.00
Reflections collected / unique	6604 / 3591; [R_{int} = 0.0703]
parameters	209
R_1[I>2σ(I)]	0.0792
wR_2(all data)	0.2344
Largest diff. peak and hole /[eÅ^{-3}]	2.906 / -2.136
CCDC number	603364

5.2.26 [Cu_4(PhSeP-O-PSePh)$_2$(PPh_3)$_4$] (26)

Empirical formula	$C_{104}H_{96}Cu_4O_4P_8Se_4$
Molecular weight /[g•mol^{-1}]	2227.57
Temperature /[K]	100(2)
λ/[Å]	0.71073
Crystal system	Triclinic
space group	$P\bar{1}$
Unit cell /[Å]; [deg.]	a = 14.0222(6) α = 78.144(3) b = 14.2408(6) β = 87.007(3) c = 24.6917(11) γ = 82.187(3)
Volume /[Å^3]	4779.1(4)
Z, Calculated density /[g•cm^{-3}]	2, 1.548
μ/[mm^{-1}]	2.587
F(000)	2248
2θ range	3.34-56.42
Reflections collected / unique	42640 / 21721; [R_{int} = 0.0439]
parameters	486
R_1[I>2σ(I)]	0.0626
wR_2(all data)	0.1738
Largest diff. peak and hole /[eÅ^{-3}]	1.344 / -1.036
CCDC number	603365

5.2.27 [Ni{PhP(OH)Se$_2$}$_2$(thf)$_2$] (27)

Empirical formula	$C_{20}H_{28}NiO_4P_2Se_4$
Molecular weight /[g•mol^{-1}]	768.91
Temperature /[K]	150(2)
λ/[Å]	0.71073
Crystal system	Monoclinic
space group	*P*2$_1$/*c*
Unit cell /[Å]; [deg.]	a = 9.905(2) b = 22.466(3) β = 92.90(2) c = 11.906(4)
Volume /[Å^3]	2646.2(2)
Z, Calculated density /[g•cm^{-3}]	4, 1.930
μ/[mm^{-1}]	6.380
F(000)	1496
2θ range	3.88-53.92
Reflections collected / unique	7506 / 5157; [R_{int} = 0.0577]
parameters	280
R_1[I>2σ(I)]	0.0486
wR_2(all data)	0.1053
Largest diff. peak and hole /[eÅ^{-3}]	1.147 / -0.678
CCDC number	614761

5.2.28 [Mg{PhP(O,Se)Se-Se(O,Se)PPh}(thf)$_4$(H$_2$O)$_2$]•[Mg{PhP(O,Se)Se-Se (O,Se)PPh}(thf)$_3$(H$_2$O)] (28)

Empirical formula	$C_{52}H_{82}Mg_2O_{14}P_4Se_8$
Molecular weight /[g•mol^{-1}]	1735.36
Temperature /[K]	170(2)
λ/[Å]	0.71073
Crystal system	Orthorhombic
space group	*P*ca2$_1$
Unit cell /[Å]; [deg.]	a = 42.900(9) b = 15.650(3) c = 10.115(2)
Volume /[Å^3]	6791(2)
Z, Calculated density /[g•cm^{-3}]	4, 1.653
μ/[mm^{-1}]	4.474
F(000)	3448
2θ range	7.44-63.86
Reflections collected / unique	45508 / 15777; [R_{int} = 0.0843]
parameters	739
R_1[I>2σ(I)]	0.0661
wR_2(all data)	0.1928
Largest diff. peak and hole /[eÅ^{-3}]	1.508 / -2.661
CCDC number	624864

5.2.29 [Mg{PhP(O,Se)Se-Se(O,Se)PPh}(thf)$_3$(H$_2$O)] (29)

Empirical formula	$C_{24}H_{36}MgO_6P_2Se_4$
Molecular weight /[g•mol^{-1}]	822.62
Temperature /[K]	150(2)
λ/[Å]	0.71073
Crystal system	Monoclinic
space group	*P*2$_1$/*c*
Unit cell /[Å]; [deg.]	a = 15.527(3) b = 41.777(8) β = 91.38(3) c = 9.782(2)
Volume /[Å^3]	6343(2)
Z, Calculated density /[g•cm^{-3}]	8, 1.769
μ/[mm^{-1}]	4.893
F(000)	3264
2θ range	2.62-52.10
Reflections collected / unique	19615 / 10383; [R_{int} = 0.0684]
parameters	651
R_1[I>2σ(I)]	0.0997
wR_2(all data)	0.2967
Largest diff. peak and hole /[eÅ^{-3}]	2.513 / -1.229
CCDC number	624865

5.2.30 [Mn{PhP(O,Se)Se-Se(O,Se)PPh}(thf)$_3$(H_2O)] (30)

Empirical formula	$C_{24}H_{36}MnO_6P_2Se_4$
Molecular weight /[g•mol^{-1}]	853.25
Temperature /[K]	105(2)
λ/[Å]	0.71073
Crystal system	Monoclinic
space group	$P2_1/c$
Unit cell /[Å]; [deg.]	a = 9.6810(19) b = 15.539(3) β = 95.33(3) c = 42.003(8)
Volume /[Å^3]	6291(2)
Z, Calculated density /[g•cm^{-3}]	8, 1.802
μ/[mm^{-1}]	5.185
F(000)	3352
2θ range	2.80-52.16
Reflections collected / unique	38688 / 12175; [R_{int} = 0.0968]
parameters	673
R_1[I>2σ(I)]	0.0660
wR_2(all data)	0.1901
Largest diff. peak and hole /[eÅ^{-3}]	1.157 / -1.346
CCDC number	624866

5.2.31 [{PhPSe$_2$(μ_2-Se)Na(thf)$_3$}$_2$Ni] (31)

Empirical formula	$C_{36}H_{58}Na_2NiO_6P_2Se_6$
Molecular weight /[g•mol^{-1}]	1227.21
Temperature /[K]	203(2)
λ/[Å]	0.71073
Crystal system	Monoclinic
space group	$P2_1/n$
Unit cell /[Å]; [deg.]	a = 15.440(6) b = 10.313(3) β = 116.31(4) c = 16.676(6)
Volume /[Å^3]	2380.2(14)
Z, Calculated density /[g•cm^{-3}]	2, 1.712
μ/[mm^{-1}]	5.119
F(000)	1212
2θ range	4.96-51.94
Reflections collected / unique	11125 / 4458; [R_{int} = 0.0864]
parameters	230
R_1[I>2σ(I)]	0.0566
wR_2(all data)	0.1651
Largest diff. peak and hole /[eÅ^{-3}]	0.658 / -0.803
CCDC number	292991

5.2.32 1/∞[Ni{Na(PhPSe$_3$)(thf)$_2$]$_\infty$ (32)

Empirical formula	$C_{20}H_{26}Na_2NiO_2P_2Se_6$
Molecular weight /[g•mol^{-1}]	938.80
Temperature /[K]	120(2)
λ/[Å]	0.71073
Crystal system	Monoclinic
space group	*P*2$_1$/*c*
Unit cell /[Å]; [deg.]	a = 7.6892(9) b = 24.398(3) β = 91.937(10) c = 7.8155(9)
Volume /[Å^3]	1465.3(3)
Z, Calculated density /[g•cm^{-3}]	2, 2.128
μ/[mm^{-1}]	8.270
F(000)	892
2θ range	3.34-54.08
Reflections collected / unique	8354 / 3175; [R_{int} = 0.1196]
parameters	134
R_1[I>2σ(I)]	0.1345
wR_2(all data)	0.4385
Largest diff. peak and hole /[eÅ^{-3}]	4.822 / -1.941
CCDC number	606341

5.2.33 [$Cu_3\{PS_2(OPS_2O^tBu)_2\}(PPh_3)_4$] (33)

Empirical formula	$C_{122}H_{126}Cu_3O_4P_7S_6$	
Molecular weight /[g•mol^{-1}]	2256.00	
Temperature /[K]	100(3)	
λ/[Å]	0.71073	
Crystal system	Triclinic	
space group	$P\bar{1}$	
Unit cell /[Å]; [deg.]	a = 14.0332(4)	α = 106.226(2)
	b = 16.4359(5)	β = 102.598(2)
	c = 26.1064(8)	γ = 91.228(3)
Volume /[Å^3]	5620.5(3)	
Z, Calculated density /[g•cm^{-3}]	2, 1.333	
μ/[mm^{-1}]	0.826	
F(000)	2356	
2θ range	2.98-54.12	
Reflections collected / unique	45184 / 22875; [R_{int} = 0.0389]	
parameters	1285	
R_1[I>2σ(I)]	0.0446	
wR_2(all data)	0.1118	
Largest diff. peak and hole /[eÅ^{-3}]	0.532 / -0.493	
CCDC number	283240	

5.2.34a [$Cu_4\{\mu_3$-$P(O^tBu)S_3\}_2(PPh_3)_4$] (34a)

Empirical formula	$C_{80}H_{78}Cu_4O_2P_6S_6$
Molecular weight /[g•mol^{-1}]	1703.76
Temperature /[K]	100(2)
λ/[Å]	0.71073
Crystal system	Triclinic
space group	$P\bar{1}$
Unit cell /[Å]; [deg.]	a = 13.420(2) α = 78.256(16) b = 16.052(3) β = 86.306(15) c = 19.785(4) γ = 65.845(14)
Volume /[Å^3]	3806.7(13)
Z, Calculated density /[g•cm^{-3}]	2, 1.486
μ/[mm^{-1}]	1.440
F(000)	1752
2θ range	2.84-56.54
Reflections collected / unique	34222 / 17354; [R_{int} = 0.0483]
parameters	883
R_1[I>2σ(I)]	0.0488
wR_2(all data)	0.1445
Largest diff. peak and hole /[eÅ^{-3}]	1.387 / -0.949
CCDC number	601692

5.2.34b [$Cu_4\{\mu_3$-$P(O^tBu)S_3\}_2(PPh_3)_4$] (34b)

Empirical formula	$C_{80}H_{78}Cu_4O_2P_6S_6$
Molecular weight /[g•mol^{-1}]	1703.76
Temperature /[K]	150(2)
λ/[Å]	0.71073
Crystal system	Triclinic
space group	$P\bar{1}$
Unit cell /[Å]; [deg.]	a = 11.8442(10) α = 101.538(7) b = 13.4796(12) β = 101.470(7) c = 13.6857(12) γ = 109.779(6)
Volume /[Å^3]	1928.5(3)
Z, Calculated density /[g•cm^{-3}]	1, 1.467
μ/[mm^{-1}]	1.421
F(000)	876
2θ range	3.18-56.32
Reflections collected / unique	16967 / 8709; [R_{int} = 0.0585]
parameters	442
R_1[I>2σ(I)]	0.0524
wR_2(all data)	0.1323
Largest diff. peak and hole /[eÅ^{-3}]	1.491 / -0.655
CCDC number	601693

5.2.35 1/∞[Na_2\{P(S^{t}Bu)S_3\}(dme)]$_\infty$ (35)

Empirical formula	$C_{16}H_{38}Na_4O_4P_2S_8$
Molecular weight /[g•mol^{-1}]	704.84
Temperature /[K]	100(2)
λ/[Å]	0.71073
Crystal system	Triclinic
space group	$P\bar{1}$
Unit cell /[Å]; [deg.]	a = 10.8600(6) α = 89.670(4) b = 11.8116(7) β = 82.780(4) c = 13.6914(7) γ = 83.450(5)
Volume /[Å^3]	1730.89(17)
Z, Calculated density /[g•cm^{-3}]	2, 1.352
μ/[mm^{-1}]	0.679
F(000)	736
2θ range	3.00-54.00
Reflections collected / unique	13736 / 7000; [R_{int} = 0.0303]
parameters	317
R_1[I>2σ(I)]	0.0235
wR_2(all data)	0.0549
Largest diff. peak and hole /[eÅ^{-3}]	0.540 / -0.318
CCDC number	623842

5.2.36 [Ni{P(OH)S_2}$_2$(thf)$_4$] (36)

Empirical formula	$C_{16}H_{36}NiO_8P_2S_4$
Molecular weight /[g•mol^{-1}]	605.34
Temperature /[K]	200(2)
λ/[Å]	0.71073
Crystal system	Triclinic
space group	$P\bar{1}$
Unit cell /[Å]; [deg.]	a = 8.059(2) α = 71.86(4) b = 9.431(3) β = 77.80(4) c = 10.392(3) γ = 65.62(4)
Volume /[Å^3]	680.5(4)
Z, Calculated density /[g•cm^{-3}]	1, 1.477
μ/[mm^{-1}]	1.173
F(000)	318
2θ range	4.14-51.68
Reflections collected / unique	5318 / 2430; [R_{int} = 0.0675]
parameters	145
R_1[I>2σ(I)]	0.0475
wR_2(all data)	0.1409
Largest diff. peak and hole /[eÅ^{-3}]	0.441 / -0.727
CCDC number	614762

5.2.37 [ArPS(*μ*-S){*μ*-N(Ph)}SPAr] (Ar = 4-anisyl) (37)

Empirical formula	$C_{20}H_{19}NO_2P_2S_3$
Molecular weight /[g•mol^{-1}]	463.48
Temperature /[K]	120(2)
λ/[Å]	0.71073
Crystal system	Monoclinic
space group	$P2_1/c$
Unit cell /[Å]; [deg.]	a = 10.406(2) b = 15.895(3) β = 97.32(3) c = 13.005(3)
Volume /[Å^3]	2133.5(7)
Z, Calculated density /[g•cm^{-3}]	4, 1.443
μ/[mm^{-1}]	0.514
F(000)	960
2θ range	4.06-53.98
Reflections collected / unique	7973 / 4423; [R_{int} = 0.0794]
parameters	253
R_1[I>2σ(I)]	0.0548
wR_2(all data)	0.1747
Largest diff. peak and hole /[eÅ^{-3}]	0.606 / -0.773

6. Conclusion

The results here demonstrate that a broad variety of novel architectures can be obtained by one-pot syntheses using P/S or P/Se precursors and metal salts.

At first, in the systematic studies of the reactions of Lawesson's reagent and metal alkoxides, carboxylates and thiolates, a number of new metal complexes (**1-18**) (Scheme 6.1) containing different kinds of P/S ligands-$[ArS_2P\text{-}O\text{-}PS_2Ar]^{2-}$, $[ArPS_3]^{2-}$, $[ArP(O^tBu)S_2]^-$, $[ArP(S^tBu) S_2]^-$, $[ArP(O)S_2]^{2-}$, $[ArP(O)(OAc)S]^-$ and $[ArP(OH)S_2]^-$ were prepared (Scheme 6.2). In addition, the mechanism of the ring-opening reaction of Lawesson's reagent is basically proved by NMR investigations, whilst the differential thermal analysis of some complexes is in fairly good agreement for the expected theoretical value. Among these complexes, $[Ag_{28}(\mu_6\text{-}S)_2\{ArP(O)S_2\}_{12}(PPh_3)_{12}]$ (**13**) is the biggest metal cluster, and its theoretical calculations are currently performed.

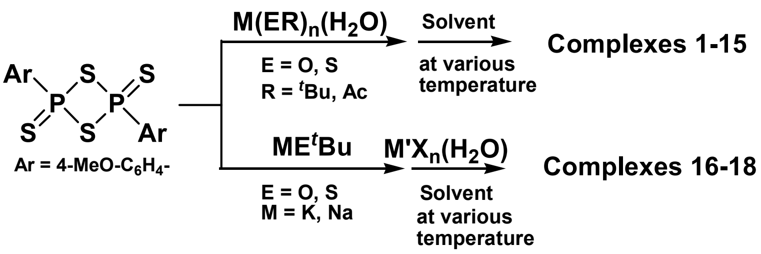

Scheme 6.1 Reactions of Lawesson's reagent and metal salts

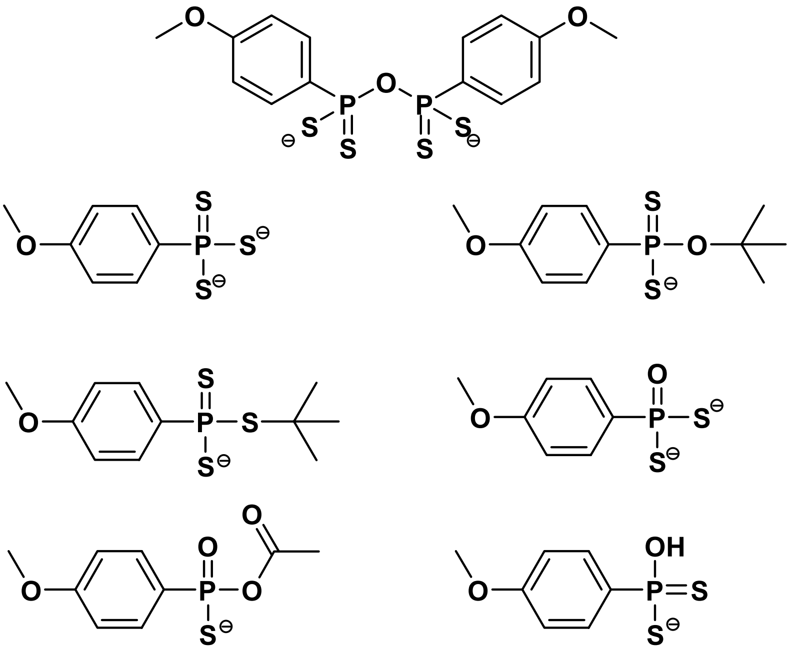

Scheme 6.2 Different P/S ligands generated from Lawesson's reagent

Secondly, the ring-opening reactions of Woollins' reagent with metal salts offer a new approach to the coordination chemistry of P-Se based ligands and thereby complexes **19-32** are synthesized (Scheme 6.3). One-dimensional coordination polymers are formed in the case of alkali metal salts are used. Different kinds of P/Se ligands obtained from Woollins' reagent are shown in scheme 6.4.

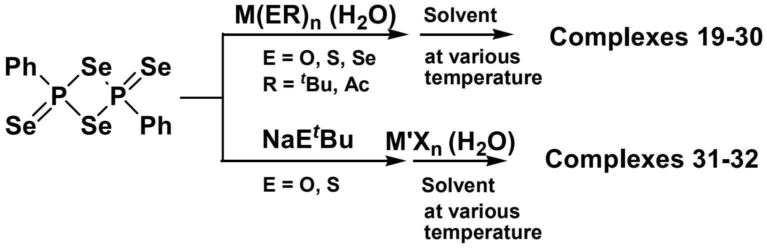

Scheme 6.3 Reactions of Woollins' reagent and metal salts

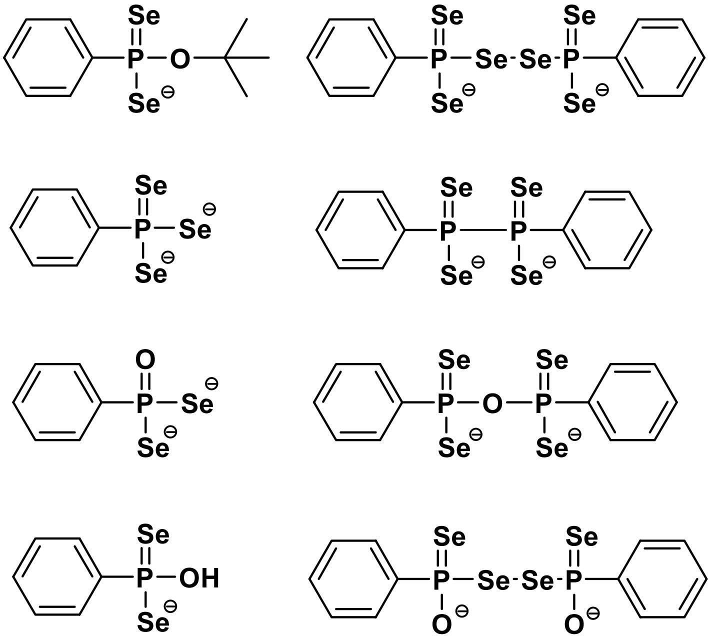

Scheme 6.4 Different P/Se ligands generated from Woollins' reagent

Finally, the unusual break-up of P_4S_6 and P_4S_{10} by metal alkoxides is presented and complexes **33-36** are obtained (Scheme 6.5 and 6.6). Because of the complexity of the reactions, the mechanism is still under surface. A honeycomb-like architecture of 2D-polymer is observed when the reaction of NaS^{t}Bu and P_4S_{10} is performed in DME.

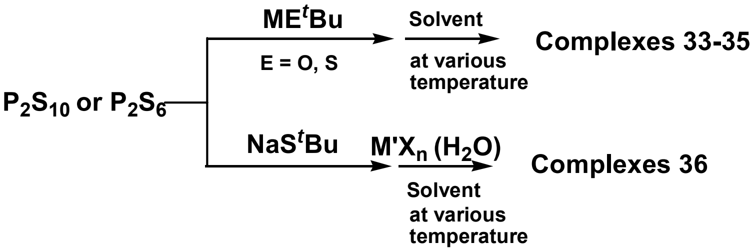

Scheme 6.5 Reactions of P_4S_n and metal salts (n = 6 or 10)

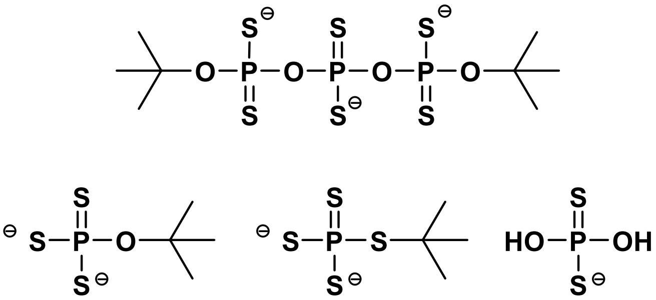

Scheme 6.6 Different P/S ligands generated from P_4S_n (n = 6 or 10)

Reaction mechanisms of Woollins' reagent and P_4S_6 (P_4S_{10}), together with the physical properties of these new metal complexes, *e.g.*, magnetic behavior, thermal decomposition and the development of thermolabile precursors for MOCVD, will be the subjects of future investigations.

7. Literature

1. J. Bjernemose, R. P. Davies, A. P. S. Jurd, M. G. Martinelli, P. R. Raithby and A. J. P. White, *Dalton Trans.*, **2004**, 3169.
2. C. W. Liu, B.-J. Liaw, L.-S. Liou and J.-C. Wang, *Chem. Commun.*, **2005**, 1983.
3. A. Clearfield, *Prog. Inorg. Chem.*, **1998**, *47*, 371.
4. M. Walawalker, H. W. Roesky and R. Murugavel, *Acc. Chem. Res.*, **1999**, *32*, 117.
5. G. Yucesan, V. Golub, C. J. O'Connor and J. Zubieta, *Dalton Trans.*, **2005**, 2241.
6. S. Langley, M. Helliwell, J.Raftery, E. I. Tolis and R. E. P. Winpenny, *Chem. Commun.*, **2004**, 142.
7. I. Haiduc, *J. Organomet. Chem.*, **2001**, *623*, 29, and references therein.
8. G. A. Zank and T. B. Rauchfuss, *Organometallics*, **1984**, *3*, 1191.
9. M. C. Aragoni, M. Arca, F. Demartin, F. A. Demillanova, F. Isaia, V. Lippolis and G. Verani, *Inorg. Chim. Acta*, **2005**, *358*, 213.
10. Z. Weng, W. K. Leong, J. J. Vittal, J. Jagadese and L. Y. Goh, *Organometallics*, **2003**, *22*, 1645.
11. V. G. Albano, M. C. Aragoni, M. Arca, C. Castellari, F. Demartin, F. A. Devillanova, F. Isaia, V. Lippolis, L. Loddo and G. Verani, *Chem. Commun.*, **2002**, 1170.
12. W. E. Van Zyl, R. J. Staples and J. P. Fackler, *Inorg. Chem. Commun*, **1998**, *1*, 51.
13. D. Fenske, A. Rothenberger and M. Shafaei-Fallah, *Z. Anorg. Allg. Chem.*, **2004**, *630*, 943.
14. M. Shafaei-Fallah, C. E. Anson, D. Fenske and A. Rothenberger, *Dalton Trans.*, **2005**, 2300, and references therein.
15. I. P. Gray, A. M. Z. Slawin and J. D. Woollins, *Dalton Trans.*, **2005**, 2188.
16. Q. Chang, Y. Wang, X.-H. Li, Y.-L. Song, H.-G. Zheng, X.-Q. Xin, S. S. S. Raj and H.-K. Fun, *Wuji Huaxue Xuebao*, **2003**, *19*, 574.
17. H. P. S. Chauhan, N. M. Shaik and K. Kori, *Main Group Met. Chem.*, **2003**, *26*, 213.
18. J. Chen, S. Lu, Z. Huang, R. Yu and Q. Wu, *Chem. Eur. J.*, **2001**, *7*, 2002.
19. W. De Oliveira, J. L. Migot, M. B. Gomes de Lima, J. Sala-Pala, J. E. Guerchais and J. Y. Le Gall, *J. Organomet. Chem.*, **1985**, *284*, 313.
20. A. A. S. El-Khaldy, *Asian J. Chem.*, **2003**, *15*, 1561.

21. L. Y. Goh, Z. Weng, W. K. Leong, I. Haiduc, K. M. Lo and R. C. S. Wong, *J. Organomet. Chem.*, **2001**, *631*, 67.
22. A. V. Ivanov, A. V. Gerasimenko, O. N. Antzutkin and W. Forsling, *Inorg. Chim. Acta*, **2005**, *358*, 2585.
23. V. K. Jain and S. Chaudhury, *J. Organomet. Chem.*, **1994**, *468*, 279.
24. B.-J. Liaw, T. S. Lobana, Y.-W. Lin, J.-C. Wang and C. W. Liu, *Inorg. Chem.*, **2005**, *44*, 9921.
25. C. W. Liu, B.-J. Liaw and L.-S. Liou, *Inorg. Chem.Commun.*, **2004**, *7*, 868.
26. X. Liu, Q.-F. Zhang and W.-H. Leung, *J. Coord. Chem.*, **2005**, *58*, 1299.
27. R. Llusar, M. Sokolov and C. Vicent, *C. R. Chim.*, **2005**, *8*, 1815.
28. S. Lu, F. Sun, Y. Zhu, Y. Peng, Y. Liang, J. Li, Z. Huang, Q. Wu and C. Lu, *Huaxue Xuebao*, **2005**, *63*, 1979.
29. H. Ohta, M. Kita, H. Kanno and M. Kojima, *Inorg. Chim. Acta*, **2000**, *311*, 75.
30. R. J. Rao, G. Srivastava and R. C. Mehrotra, *Phosphorus, Sulfur Relat. Elem.*, **1985**, *25*, 183.
31. M. Rieckhoff, M. Noltemeyer, F. T. Edelmann, I. Haiduc and I. Silaghi-Dumitrescu, *J. Organomet. Chem.*, **1994**, *469*, C22.
32. Y. P. Singh and R. C. Mehrotra, *Polyhedron*, **1986**, *5*, 967.
33. Z. Travnicek, V. Machala, L. Szuecova, M. Malon and J. Marek, *Transition Met. Chem.*, **2004**, *29*, 352.
34. K.-H. Yih, G.-H. Lee, S.-L. Huang and Y. Wang, *J. Organomet. Chem.*, **2003**, *665*, 114.
35. I. Haiduc, L. Y. Goh, *Coord. Chem. Rev.*, **2002**, *224*, 151.
36. I. Haiduc, *Rev. Inorg. Chem.*, **1981**, *3*, 353.
37. I. Haiduc, D. B. Sowerby, S.-F. Lu, *Polyhedron*, **1995**, *14*, 3389, and references therein.
38. C. Silvestru, I. Haiduc, *Coord. Chem. Rev.*, **1996**, *147*, 117.
39. I. Haiduc, D.B. Sowerby, *Polyhedron*, **1996**, *15*, 2469.
40. I. Haiduc, *Coord. Chem. Rev.*, **1997**, *158*, 325.
41. H. P. S. Chauhan, N. M. Shaik and U. P. Singh, *Appl. Organometal. Chem.*, **2005**, *19*, 1132.
42. C. C. Lo, M. H. Ho, M. D. Hung, *J. Agric. Food Chem.*, **1996**, *44*, 2227.
43. B. C. Verma, D. K. Sharma, S. B. Kalia, S. Kumar, *Pollut. Res.*, **1997**, *16*, 19.

44. R. Ramesh, K. Natarajan, *Synth. React. Inorg. Met.-Org. Chem.*, **1996**, *26*, 1677.

45. J. Franekic, N. Bratulic, M. Pavlica, D. Papes, *Mutat. Res.*, **1994**, *325*, 65.

46. C. Safak, H. Erdogan, M. Ertan, N. Yulug, *J. Chem. Soc. Rak.*, **1990**, *12*, 296.

47. J. Aragones, C. Lopez-Rodriguez, A. Corbi. P. Gomez del Arco, M. Lopez-Cabrera, M. O. de Landazuri, J. M. Redondo, *J. Biol. Chem.*, **1996**, *271*, 10924.

48. B. E. Causton, F. J. Burka, N. H. Wilson, *Dent. Mater.*, **1993**, *9*, 209.

49. D. J. Johnson, D. G. Graham, V. Amarnath, K. Amarnath, W. M. Valentine, *Chem. Res. Toxicol.*, **1996**, *9*, 910.

50. W. Chen, M. Tian, *Chem. Abstr.*, **1989**, *111*, 7504.

51. Klaman, D., Ed., *Lubricant and Related Products*, Verlag Chemie, Weinheim, Germany, **1984**.

52. Y. Miyake, M. Harada, *Rev. Inorg. Chem.*, **1989**, *10*, 145.

53. Y.-A. Lee, J. E. McGarrah, R. J. Lachicotte, R. Eisenberg, *J. Am. Chem. Soc.*, **2002**, *124*, 10662.

54. W. E. Van Zyl, J. M. Lopez-de-Luzuriaga, A. A. Mohamed, R. J. Staples, J. P. Jr. Fackler, *Inorg. Chem.*, **2002**, *41*, 4579.

55. W. E. Van Zyl, J. M. Lopez-de-Luzuriaga, J. P. Jr. Fackler, *J. Mol. Struct.*, **2000**, *516*, 99.

56. P. A. Patnaik, *Comprehensive Guide to the Hazardous Properies of Chemical Substances*, Van Nostrand Reinhold: New York, **1992**, *Chapter 40* and references therein.

57. C. Byrom, M. A. Malik, P. O'Brien, A. J. P. White, D. J. Williams, *Polyhedron*, **2000**, *19*, 211.

58. C. J. Carmalt, J. D. Mileham, A. J. P. White, D. J. Williams, J. W. Steed, *Inorg. Chem.*, **2001**, *40*, 6035.

59. A. A. Eagle, L. J. Laughlin, C. G. Young, E. R. T. Tiekink, *J. Am. Chem. Soc.*, **1992**, *114*, 9195.

60. A. A. Eagle, S. Thomas, C. G. Young, In T*ransition Metal Sulfur Chemistry*; E. I. Stiefel, K. Mutsumoto, Eds., American Chemical Society: Washington, DC, **1996**, *Chapter 20*, p. 324.

61. W. T. Wiesler and M. H. Garuthers, *J. Org. Chem.*, **1996**, *61*, 4272.

62. L. Carius, *Ann.*, **1859**, *112*, 190.

63. J. H. Fletcher, J. C. Hamilton, I. Hechenbleikner, E. I. Hoegberg, B. J. Sertl and J.

T. Cassaday, *J. Am. Chem. Soc.*, **1950**, *72*, 2461.

64. J. R. Van Wazer, *Phosphorus and its compounds*, **1961**, *Volume II, chapter 19*, and references therein.
65. F. Jian, G. Zheng and H. Xiao, *Synth. React. Inorg. Met.-Org. Chem.*, **2004**, *34*, 1517.
66. M. Gianini, W. R. Caseri, V. Gramlich, U. W. Suter, *Inorg. Chim. Acta*, **2000**, *299*, 199.
67. J. A. Mccleverty, R. S. Z. Kowalski, N. A. Bailey, R. Mulvaney and D. A. O'Cleirigh, *Dalton Trans.*, **1983**, 627.
68. B. A. Khaskin, *Russ. Chem. Rev.*, **1984**, *53*, 768.
69. A. N. Shishkov, N. K. Nikolov, A. I. Busev, A. I. Nauch, Tr., Plovdivski, *Chem. Abstr.*, **1973**, *78*, 83952.
70. I. Cuadrado, M. Moran, *Transition Met. Chem.*, **1984**, *9*, 96.
71. M. Moran, I. Cuadrado, *J. Organomet. Chem.*, **1986**, *311*, 333.
72. F. T. Edelmann, M. R. Riecknoff, I. Haiduc, I. Silaghi-Dumitrescu, *J. Organomet. Chem.*, **1993**, *447*, 203.
73. S. Scheibye, B. S. Pedersen, S.-O. Lawesson, *Bull. Soc. Chim. Belg.*, **1978**, *87*, 229.
74. A. A. EL-Barbary, S. Scheibye, S.-O. Lawesson and H. Fritz, *Acta Chem. Scand. B*, **1980**, *34*, 597.
75. M. Jesberger, T. P. Davis, L. Barner, *Synthesis*, **2003**, *13*, 1929, and references therein.
76. M. P. Cava and M. I. Levinson, *Tetrahedron*, **1985**, *41*, 5061.
77. T. Ozturk, *Tetrahedron Lett.*, **1996**, *37*, 2821.
78. M. St. J. Foreman and J. D. Woollins, *Dalton Trans.*, **2000**, 1533.
79. K. Clausen, A. A. EL-Barbary, and S.-O. Lawesson, *Tetrahedron*, **1981**, *37*, 1019.
80. H. Davy, *Dalton Trans.*, **1982**, 457.
81. R. A. Cherkasov, G. A. Kutyrev, A. N. Pudovik, *Tetrahedron*, **1985**, *41*, 2567.
82. S. Scheibye, R. Shabana and S.-O. Lawesson, *Tetrahedron*, **1982**, *38*, 993.
83. P. Fay and H. P. Lankelma, *J. Am. Chem. Soc.*, **1952**, *74*, 4933.
84. H. Z. Lecher, R. A. Greenwood, K. C. Whitehouse and T. H. Chao, *J. Am. Chem. Soc.*, **1956**, *78*, 5018.
85. O. N. Grishina, N. A. Andreev and É. I. Babkina, *Zh. Obshch. Khim.*, **1977**, *47*, 72.

86. J. T. Shore, W. T. Pennington, M. C. Noble and A. W. Cordes, *Phosphorus and Sulfur*, **1988**, *39*, 153.

87. R. Kempe, J. Sieler, H. Beckmann and G. Ohms, *Z. Kristallographie*, **1992**, *202*, 159.

88. G. Grossmann, G. Ohms, K. Krüger and G. Jeschke, *Phosphorus, Sulfur and Silicon*, **1995**, *107*, 57.

89. I. P. Gray, A. M. Z. Slawin and J. D. Woollins, *Dalton Trans.*, **2004**, 2477, and references therein.

90. I. Haiduc, G. Meyei, R. Micu-Semeniuc, F. T. Edelmann and A. Fischer, *Z. Anorg. Allg. Chem.*, **2006**, *632*, 295.

91. I. P. Gray, H. L. Milton, A. M. Z. Slawin, J. D. Woollins, *Phosphorus, Sulfur Silicon Relat. Elem.*, **2004**, *179(4-5)*, 969.

92. H, Liu, H. Mao, C. Xu, H. Zhang, H. Hou, Q. Wu, Y. Zhu, B. Ye, L. Yuan, *Polyhedron*, **2004**, *23*, 1799

93. M. R. St. J. Foreman, A. M. Z. Slawin and J. D. Woollins, *Dalton Trans.*, **1996**, 3653.

94. I. P. Gray, H. L. Milton, A. M. Z. Slawin and J. D. Woollins, *Dalton Trans.*, **2003**, 3450.

95. I. P. Gray, A. M. Z. Slawin and J. D. Woollins, *New J. Chem.*, **2004**, *28*, 1383.

96. I. P. Gray, A. M. Z. Slawin and J. D. Woollins, *Z. Anorg. Allg. Chem.*, **2004**, *630*, 1851.

97. M. R. St. J. Foreman, A. M. Z. Slawin and J. D. Woollins, *Chem. Commun.*, **1997**, 1269.

98. B. McCulloch, D. L. Ward, J. D. Woollins and C. H. Brubaker, Jr., *Organometallics*, **1985**, *4*, 1425.

99. J. C. Fitzmaurice, D. J. Williams, P. T. Wood and J. D. Woollins, *Chem. Commun.*, **1988**, 741.

100. P. T. Wood and J. D. Woollins, *Chem. Commun.*, **1988**, 1190.

101. L. Horner, H. Hoffmann and P. Beck, *Chem. Ber.*, **1958**, *91*, 1583.

102. P. Bhattacharyya, A. M. Z. Slawin and J. D. Woollins, *Dalton Trans.*, **2001**, 300.

103. G. Grossmann, G. Ohms, K. Krüger, K. Karaghiosoff, K. Eckstein, J. Hahn, A. Hopp, O. L. Malkina, P. Hrobarik, *Z. Anorg. Allg. Chem.*, **2001**, *627*, 1269.

104. I. Baxter, A. F. Hill, J. M. Malget, A. J. P. White, D. J. Williams, *Chem. Commun.*,

1997, 2049.

105. P. Bhattacharyya, J. D. Woollins, *Tetrahedron Lett.*, **2001**, *42*, 5949.
106. J. Bethke, K. Karaghiosoff, L. A. Wessjohann, *Tetrahedron Lett.*, **2003**, *44*, 6911.
107. S. Knapp, E. Darout, *Org. Lett.*, **2005**, *7*, 203.
108. P. Bhattacharyya, A. M. Z. Slawin, J. D. Woollins, *Chem. Eur. J.*, **2002**, *8*, 2705.
109. P. Bhattacharyya, A. M. Z. Slawin, J. D. Woollins, *Angew. Chem. Int. Ed.*, **2000**, *39*, 1973.
110. I. P. Gray, P. Bhattacharyya, A. M. Z. Slawin, J. D. Woollins, *Chem. Eur. J.*, **2005**, *11*, 6221.
111. M. R. St. J. Foreman, A. M. Z. Slawin and J. D. Woollins, *Chem. Commun.*, **1997**, 855.
112. C. Q. Nguyen, A. Adeogun, M. Afzaal, M. A. Malik and P. O’Brien, *Chem. Commun.*, **2006**, 2182.
113. R. P. Davies and M. G. Martinelli, *Inorg. Chem.*, **2002**, *41*, 348.
114. R. P. Davies, M. G. Martinelli and A. J. P. White, *Chem. Commun.*, **2006**, 3240.
115. C. W. Liu, C. Hung, B. K. Santra, Y. Chu, J. Wang and Z. Lin, *Inorg. Chem.*, **2004**, *43*, 4306.
116. S. E. Kabir, N. Begum, Md. M. Hassan, Md. I. Hyder, H. Nur, D. W. Bennett, T. A. Siddiquee, D. T. Haworth, E. Rosenberg, *J. Organomet. Chem.*, **2004**, *689*, 1569.
117. A. P. Purdy, J. C. F. George and J. H. Callahan, *Inorg. Chem.*, **1991**, *30*, 2812 and references therein.
118. T. Tsuda, T. Hashimoto and T. Saegusa, *J. Am. Chem. Soc.*, **1972**, *94*, 658.
119. T. Greiser and E. Weiss, *Chem. Ber.*, **1976**, *109*, 3142.
120. D. Fenske, A. Rothenberger, *Inorg. Synth.*, **2006**, in press.
121. C. E. Anson, R. Langer, L. Ponikiewski, A. Rothenberger, *Inorg. Chim. Acta*, **2005**, *358*, 3967.
122. L. Ponikiewski, A. Rothenberger, *Inorg. Chim. Acta*, **2005**, *358*, 1322.
123. C. E. Anson, L. Ponikiewski, A. Rothenberger, *Inorg. Chim. Acta*, **2006**, *359*, 2263.
124. P. Kilian, A. M. Z. Slawin, J. D. Woollins, *Eur. J. Inorg. Chem.*, **1999**, 2327.
125. H. Masada, Y. Murotani, *Bull. Chem. Soc. Jpn.*, **1979**, *52*, 1213.
126. J. P. Lorand, *J. Am. Chem. Soc.*, **1974**, *96*, 2867.
127. T. Wen and C. E. McKenna, *Chem. Commun.*, **1991**, 1223.

128. R. G. Pearson, *J. Am. Chem. Soc.*, **1963**, *85*, 3533.

129. R. Köster, A. Sporzynski, W. Schüssler, D. Bläser and R. Boese, *Chem. Ber.*, **1994**, *127*, 1191.

130. G. A. Carriedo, V. Riera, M. L. Rodriguez and J. C. Jeffrey, *J. Organomet. Chem.*, **1986**, *314*, 139.

131. D. C. Cupertino, M. M. Harding and D. J. Cole-Hamilton, *J. Organomet. Chem.*, **1985**, *294*, C29.

132. D. Fenske, A. Rothenberger and M. Shafaei-Fallah, *Eur. J. Inorg. Chem.*, **2005**, 59.

133. D. Fenske, C. E. Anson, A. Eichhöfer, O. Fuhr, A. Ingendoh, C. Persau and C. Richert, *Angew. Chem., Int. Ed.*, **2005**, *44*, 5242.

134. Q. Gao, N. Guillou, M. Nogues, A. K. Cheetham and G. Ferey, *Chem. Mater.*, **1999**, *11*, 2937.

135. M. D. Santana, G. Garcia, A. A. Lozano, G. Lopez, J. Tudela, J. Perez, L. Garcia, L. Lezama and T. Rojo, *Chem. Eur. J.*, **2004**, *10*, 1738.

136. For a recent classification of H-bonds, see: *e.g.*, C. Giacovazzo, H. L. Monaco, G. Artioli, D. Viterbo, G. Ferraris, G. Gilli, G. Zanotti and M. Catti, in *Fundamentals of Crystallography*, ed. C. Giacovazzo, Oxford University Press, Oxford, 2nd ed., **2002**, p. 592.

137. H. E. Gottlieb, V. Kotlyar and A. Nudelman, *J. Org. Chem.*, **1997**, *62*, 7512.

138. L. Zhao, V. Niel, L. K. Thompson, Z. Xu, V. A. Milway, R. G. Harvey, D. O. Miller, C. Wilson, M. Leech, J. A. K. Howard and S. L. Heath, *Dalton Trans.*, **2004**, 1446.

139. D. Walther, S. Liesicke, L. Bottcher, R. Fischer, H. Gorls and G. Vaughan, *Inorg. Chem.*, **2003**, *42*, 625.

140. G. Psomas, A. J. Stemmler, C. Dendrinou-Samara, J. J. Bodwin, M. Schneider, M. Alexiou, J. W. Kampf, D. P. Kessissoglou and V. L. Pecoraro, *Inorg. Chem.*, **2001**, *40*, 1562.

141. M. Karakus, H. Yilmaz, Y. Ozcan and S. Ide, *Appl. Organomet. Chem.*, **2004**, *18*, 141.

142. T. Kimura, T. Murai, A. Miwa, D. Kurachi, H. Yoshikawa and S. Kato, *J. Org. Chem.*, **2005**, *70*, 5611.

143. T. Kimura and T. Murai, *J. Org. Chem.*, **2005**, *70*, 952.

144. J. G. Planas, F. Hampel and J. A. Gladysz, *Chem. Eur. J.*, **2005**, *11*,1402.

145. W. J. Parak, T. Pellegrino and C. Plank, *Nanotechnology*, **2005**, *16*, R9.

146. J. Janek, B. Mogwitz, G. Beck, M. Kreutzbruck, L. Kienle and C. Korte, *Prog. Solid State Chem.*, **2005**, *32*, 179.

147. M. J. Pilkington, A. M. Z. Slawin, D. J. Williams, P. T. Wood and J. D. Woollins, *Heteroat. Chem.*, **1990**, *1*, 351.

148. W. Kuchen and H. Hertel, *Angew. Chem. Int. Ed.*, **1969**, *8*, 89.

149. W. Kuchen and B. Knop, *Angew. Chem. Int. Ed.*, **1965**, *4*, 244.

150. R. P. Davies, M. G. Martinelli, A. E. H. Wheatley, A. J. P. White and D. J. Williams, *Eur. J. Inorg. Chem.*, **2003**, 3409.

151. R. P. Davies, C. V. Francis, A. P. S. Jurd, M. G. Martinelli, A. J. P. White and D. J. Williams, *Inorg. Chem.*, **2004**, *43*, 4802.

152. Bruker-Daltonik, Programs WinNMR and WinDaisy, Bremen, **1999**.

153. G. Hdgele, M. Engelhardt, W. Boenigk, Simulation und automatisierte Analyse von NMR-Spektren, VCH, Weinheim, **1987**.

154. M. J. Pilkington, A. M. Z. Slawin, D. J. Williams, J. D. Woollins, *Dalton Trans.*, **1992**, 2425.

155. C. Stoll, I.-P. Lorenz, H. Nöth, W. Ponikwar, *J. Organomet. Chem.*, **2000**, *602*, 24.

156. Z. Spichal, M. Necas, J. Pinkas, *Inorg. Chem.*, **2005**, *44*, 2074.

157. G. Gilli, in *Fundamentals of Crystallography* (Ed.: C. Giacovazzo), Oxford University Press, Oxford, **2002**, p. 590.

158. I. P. Parkin, M. J. Pilkington, A. M. Z. Slawin, D. J. Williams and J. D. Woollins, *Polyhedron*, **1990**, *9*, 987.

159. C. G. Lugmair, T. D. Tilley, A. L. Rheingold, *Chem. Mater.*, **1997**, *9*, 339.

160. K. C. K. Swamy, M. Veith, V. Huch, S. Mathur, *Inorg. Chem.*, **2003**, *42*, 5837.

161. R. Murugavel, S. Kuppuswamy, R. Boomishankar, A. Steiner, *Angew. Chem. Int. Ed.*, **2006**, *45*, 5536.

162. M. Westerhausen, M. W. Ossberger, A. Keilbach, C. Guckel, H. Piotrowski, M. Suter, H. Z. Nöth, *Z. Anorg. Allg. Chem.*, **2003**, *629*, 2398.

163. M. Pompetzki, M. Jansen, *Monatsh. Chem.*, **2002**, *133*, 975.

164. M. Pompetzki, R. E. Dinnebier, M. Jansen, *Solid State Sci.*, **2003**, *5*, 1439.

165. D. P. Elias, *Acta Cryst.*, **1957**, *10*, 600.

166. R. Shabana, F. H. Osman and S. S. Atrees, *Tetrahedron*, **1993**, *49*, 1271.

167. E. Fluck and H. Binder, *Angew. Chem. Int. Ed.*, **1967**, *6*, 260.

168. H. W. Roesky and M. Dietl, *Angew. Chem. Int. Ed.*, **1973**, *12*, 425.

169. M. St. J. Foreman, R. J. Mortimer, A. M. Z. Slawin and J. D. Woollins, *Dalton Trans.*, **1999**, 3419.

170. M. H. Chisholm, S. R. Drake, A. A. Naiini, W. E. Streib, *Polyhedron*, **1991**, *10*, 337.

171. L. M. Nguyen, M. E. Dellinger, J. T. Lee, R. A. Quinlan, A. L. Rheingold, R. D. Pike, *Inorg. Chim. Acta*, **2005**, *358*, 1331.

172. Stoe&Cie. GmbH, *Stoe IPDS Steuersoftware V 2.73*, Darmstadt **1996**.

173. G. M. Sheldrick, SHELXS-97, Program for Crystal Structure Solution, Göttingen, **1997**.

174. G. M. Sheldrick, SHELXL-97, Program for Crystal Structure Refinement, Göttingen, **1997**.

175. G. M. Sheldrick, SHELXP 5.05, Program for Molecular Graphics, Göttingen, **1994**.

8. Publication List

1. **Synthesis and crystal structures of octahedral metal complexes containing the new dianion $[PhP(Se,O)Se\text{-}Se(O,Se)PPh]^{2-}$**
   Weifeng Shi, Le Zhang, Maryam Shafaei-Fallah, Alexander Rothenberger, *Z. Anorg. Allg. Chem.*, **2007**, *633*, 440.

2. **Transformations of P-chalcogenide precursors with a hydrated metal salt**
   Weifeng Shi, Rebecca Kelting, Maryam Shafaei-Fallah, Alexander Rothenberger, *J. Organomet. Chem.*, **2007**, DOI: 10.1016/j.jorganchem.2006.11.009.

3. **Polymeric Organometallic Architectures of Novel P-Se Anions**
   Weifeng Shi, Maryam Shafaei-Fallah, Le Zhang, Christopher E. Anson, Eberhard Matern and Alexander Rothenberger, *Chem. Eur. J.*, **2007**, *13(2)*, 598.

4. **Metal thiophosphonates and related compounds: an emerging area of supramolecular coordination chemistry**
   Weifeng Shi, Maryam Shafaei-Fallah, Christopher E. Anson and Alexander Rothenberger, *Dalton Trans.*, **2006**, 3257.

5. **Polymeric arrangements of P-Se anions and a first insight into their reactivity**
   Weifeng Shi, Maryam Shafaei-Fallah, Christopher E. Anson and Alexander Rothenberger, *Dalton Trans.*, **2006**, 2979.

6. **Reactions of P/S-containing proligands with coinage metal salts: a new route to polynuclear complexes with unusual structural types**
   Weifeng Shi, Reinhart Ahlrichs, Christopher E. Anson, Alexander Rothenberger, Claudia Schrodt and Maryam Shafaei-Fallah, *Chem. Commun.*, **2005**, 5893.

7. **A Strategy for the build-up of transition-metal complexes containing tripodal $[ArPOS_2]^{2-}$ and $[ArPS_3]^{2-}$ ligands (Ar = 4-anisyl)**
   Weifeng Shi, Maryam Shafaei-Fallah, Christopher E. Anson and Alexander Rothenberger, *Dalton Trans.*, **2005**, 3909.

8. **Synthetic Applications of Lawesson's Reagent in Reactions with CuI Alkoxides**
   Weifeng Shi and Alexander Rothenberger, *Eur. J. Inorg. Chem.*, **2005**, 2935.

9. **Copper-mediated cleavage of disulfides by tertiary phosphines: A new route to As-S anions**
   Robert Langer, Weifeng Shi, Alexander Rothenberger, *Dalton Trans*., **2006**, 4435.

10. **Synthesen und Strukturen von Übergangsmetall-Komplexen mit Dithiophosphinato- und Trithiophophonato-Liganden**
    Maryam Shafaei-Fallah, Weifeng Shi, Dieter Fenske and Alexander Rothenberger, *Z. Anorg. Allg. Chem.*, **2006**, *632*, 1091.

11. **From neutral P-S precursors to oligo- and polymeric arrangements of P-S anions**
    Alexander Rothenberger, Maryam Shafaei-Fallah and Weifeng Shi, *Chem. Commun.*, **2007**, **DOI:** 10.1039/b617177j.

Acknowledgements:

It gives me great pleasure to thank the following people for their help and support to make it possible for me to accomplish this work.

Firstly, I acknowledge my sincere thanks and gratitude to Prof. Dr. D. Fenske for giving me this opportunity to come and start a research career in his group and for his constant encouragement and support throughout my doctorate studies.

A large debt of thanks is owed to Dr. A. Rothenberger, not only for this interesting topic, the fruitful discussions and innumerable valuable suggestions, but also for the help to this colorful life in Karlsruhe.

I extend my warm thanks to the following people, Dr. Ian Hewitt, Ms. A. Baust, Dr. L. Ponikiewski, Dr. I. Issac, Dr. M. Shafaei-Fallah, Dr. C. E. Anson, Priv.-Doz. Dr. U. Radius, Mr. K. Maisch, Dr. C. Persau, Dr. S. König, B. Bechlars, S. Dürr, T. Schaub, S. Wieber and other colleagues in this and other groups for their generous help and for this pleasure environment.

My big thanks to these people for their assistance and technical helps, Dr. E. Matern, Dr. W. Bensmann, Ms. H. Berberich, Ms. M. Stay, Mr. K. Keihauer, Mr. J. Treptow and Ms. G. Kuhne.

Finally, I would like to thank my wife, Xiaomei Hu for her entirely encouragement and to my family for their ever continuing support.

Curriculum vitae.

Personal Data:

Name: Weifeng Shi (施卫峰)
Data of birth: 01. Feb. 1977
Place of birth: Jiangsu, China
Nationality: Chinese

Education:

09/2005~02/2007	Ph.D. in Inorganic Chemistry, Institut für Anorganische Chemie, Universität Karlsruhe, Germany
09/2004~09/2005	Postdoctor, Institut für Anorganische Chemie, Universität Karlsruhe, Germany
09/1999~07/2004	Ph.D. in Organic Chemistry, College of Chemistry and Molecular Engineering, Peking University, P. R. China
09/1995~07/1999	B.S. in Chemistry, College of Chemistry and Molecular Engineering, Peking University, P. R. China
09/1992~07/1995	Liangfeng senior high school, Jiangsu province, China
09/1989~07/1992	Changyinsha Nongchang junior high school, Jiangsu province, China
09/1983~07/1989	Changyinsha Nongchang elementary school, Jiangsu province, China